

AD-A197 530

DTIC FILE COPY

2

NATURAL AND MIXED CONVECTION
ALONG SLENDER VERTICAL CYLINDERS
WITH NONUNIFORM HEATING

BY

JEFFREY JOHN HECKEL, 1957 -

A THESIS

DTIC
ELECTE
JUL 26 1988
S D

Presented to the Faculty of the Graduate School of the
UNIVERSITY OF MISSOURI - ROLLA
In Partial Fulfillment of the Requirements for the Degree

MASTER OF SCIENCE IN MECHANICAL ENGINEERING

May 15, 1988

Approved by

J. S. Acorn (Advisor) J. F. Acorn
A. K. Ryle

DISTRIBUTION STATEMENT A

Approved for public release
Distribution Unlimited

88 5 19 022

In memory of my father.

PUBLICATION THESIS OPTION

This paper has been prepared in the form of two papers for publication. Pages 12 through 37 have been prepared for possible publication in the Journal of Heat Transfer, and pages 38 through 99 have been prepared for possible publication in the International Journal of Heat and Mass Transfer. The balance of the thesis follows the standard thesis format.



Accession For	
NTIS CRA&I	<input checked="" type="checkbox"/>
DTIC TAB	<input type="checkbox"/>
Unannounced	<input type="checkbox"/>
Justification	
By <i>per ltr</i>	
On <i>10/10/71</i>	
Approved for release	
Date <i>10/10/71</i> of <i>10/10/71</i>	
<i>A-1</i>	

ABSTRACT

Lambda

This thesis presents an analytical study of laminar convective heat transfer along vertical slender cylinders. Chapter 2 covers the case of variable surface heating conditions of the form $q_{sub}(x) = Cx^n$ for natural convection. Results are presented for $Pr = 0.1, 0.7, 7$, and 100 and for $n = -0.5, -0.25, 0, 0.25$, and 0.5 . It is found that as the curvature parameter Λ increases the local heat transfer coefficient increases for the range of n investigated. The local wall shear stress decreases for a given location x with increasing curvature. It increases with increasing x for a constant radius cylinder with $n \geq 0$, but may decrease for $n < 0$. It is also found that a higher value of n or Prandtl number resulted in a lower wall velocity gradient, and a higher value for $Nu_x Gr_x^{1/5}$. However, as the curvature is increased, the effect of n and Pr on these values diminishes.

Chapter 3 covers the entire range of buoyancy-assisted, mixed convection along a vertical slender cylinder for the case of variable wall temperature distribution, of the form $T_w(x) - T_\infty = ax^n$. The buoyancy parameter δ is varied from zero for pure free convection to one for pure forced convection. Results are presented for $Pr = 0.1, 0.7, 7$, and 100 and for $n = -0.4, -0.2, 0, 0.2$ and 0.5 . It is found that for given values of Pr, n and δ , as the curvature parameter Λ increases both the local wall shear stress and the local heat transfer coefficient increase. Again higher values of n and Pr are found to lower the local wall shear stress and to raise the local Nusselt number, and the effect of n and Pr is found to lessen as the curvature parameter is increased. Average Nusselt numbers were calculated and correlation equations for the local and average Nusselt numbers are presented for both problems investigated.

(AW)

ACKNOWLEDGEMENTS

The author wishes to express his most sincere gratitude to his advisor, Professor T. S. Chen for his assistance and encouragement during his graduate study at the University. Dr. Chen proposed this thesis topic and made suggestions and recommendations throughout the course of study. He gave much of his valuable time to discuss problems as they arose. His patience and understanding are greatly appreciated. The author would also like to thank the other committee members, Professor B. F. Arnaly and Professor A. K. Rigler. Their comments and suggestions during the course of study are appreciated.

The author would like to extend his gratitude to the University, the Department of Mechanical and Aerospace Engineering, and the University Computer Center for providing the facilities to make this thesis possible.

Thanks are also in order to two fellow graduate students, Mr. H. R. Lee and Mr. K. C. Chiang, who listened to the author's analysis on many occasions and provided much useful feedback.

Finally, the author is indebted to his wife and daughter whose patience and understanding were truly remarkable. Without their support and ability to live through his many absences, this thesis would never have been completed. His most sincere thanks are extended for the encouragement and love they have provided.

TABLE OF CONTENTS

	Page
PUBLICATION THESIS OPTION	iii
ABSTRACT	iv
ACKNOWLEDGEMENTS	v
LIST OF ILLUSTRATIONS	vii
LIST OF TABLES	viii
I. INTRODUCTION	1
II. NATURAL CONVECTION ALONG A VERTICAL CYLINDER WITH VARIABLE SURFACE HEAT FLUX	11
III. MIXED CONVECTION ALONG A VERTICAL CYLINDER WITH VARIABLE WALL TEMPERATURE	38
IV. RECOMMENDATIONS FOR FURTHER STUDY	100
VITA	101
APPENDICES	
A. Transformation of the Governing System of Equations in Chapter 2	102
B. Method of Solution for the System of Equations in Chapter 2	110
C. Transformation of the Governing System of Equations for the Special Case of Natural Convection in Chapter 3	116
D. Transformation of the Governing System of Equations for Mixed Convection in Chapter 3	122
E. Solutions of the System of Equations (C-25)-(C-27) and (D-32)-(D-34) ..	130

LIST OF ILLUSTRATIONS

Figure		Page
CHAPTER 2 NATURAL CONVECTION ALONG A VERTICAL CYLINDER WITH VARIABLE SURFACE HEAT FLUX		
1.	$Nu_x/Nu_{x,p}$ vs. Λ_N^* , Uniform Surface Heat Flux ($n=0$)	36
2.	$Nu_x/Nu_{x,UHF}$ vs. n , Flat Plate ($\Lambda_N^* = 0$)	37
CHAPTER 3 MIXED CONVECTION ALONG A VERTICAL CYLINDER WITH VARIABLE SURFACE TEMPERATURE		
1.	$Nu_x/Nu_{x,p}$ vs. Λ_N for Pure Free Convection, UWT.	85
2.	$Nu_x/Nu_{x,UWT}$ vs. n for Pure Free Convection, Flat Plates.	86
3.	$Nu_x/Nu_{x,p}$ vs. Λ_F for Pure Forced Convection, UWT.	87
4.	$Nu_x/Nu_{x,UWT}$ vs. n for Pure Forced Convection, Flat Plates.	88
5.	$Nu_x/(Re_x^{1/2} + Gr_x^{1/4})$ vs. χ for Mixed Convection, $Pr=0.1$, UWT.	89
6.	$Nu_x/(Re_x^{1/2} + Gr_x^{1/4})$ vs. χ for Mixed Convection, $Pr=0.7$, UWT.	90
7.	$Nu_x/(Re_x^{1/2} + Gr_x^{1/4})$ vs. χ for Mixed Convection, $Pr=7$, UWT.	91
8.	$Nu_x/(Re_x^{1/2} + Gr_x^{1/4})$ vs. χ for Mixed Convection, $Pr=100$, UWT.	92
9.	$Nu_x/(Re_x^{1/2} + Gr_x^{1/4})$ vs. χ for Mixed Convection, $Pr=0.7$, $\Lambda=0$ (Flat Plate). ..	93
10.	$Nu_L/(Re_L^{1/2} + Gr_L^{1/4})$ vs. χ_L for Mixed Convection, $Pr=0.1$, UWT.	94
11.	$Nu_L/(Re_L^{1/2} + Gr_L^{1/4})$ vs. χ_L for Mixed Convection, $Pr=0.7$, UWT.	95
12.	$Nu_L/(Re_L^{1/2} + Gr_L^{1/4})$ vs. χ_L for Mixed Convection, $Pr=7$, UWT.	96
13.	$Nu_L/(Re_L^{1/2} + Gr_L^{1/4})$ vs. χ_L for Mixed Convection, $Pr=100$, UWT.	97
14.	$Nu_L/(Re_L^{1/2} + Gr_L^{1/4})$ vs. χ_L for Mixed Convection, $Pr=0.7$, $\Lambda=0$ (Flat Plate). ..	98
15.	Development of a Correlation Equation For Buoyancy-Assisting, Mixed Convection.	99

LIST OF TABLES

Table	Page
CHAPTER 2 NATURAL CONVECTION ALONG A VERTICAL CYLINDER WITH VARIABLE SURFACE HEAT FLUX	
1. The $Nu_x Gr_x^{1/5}$ results for Power Law Variation of the Surface Heat Flux.	32
2. The $Nu_x / Nu_{x,UHF}$ results for Power Law Variation of the Surface Heat Flux.	33
3. The $Nu_L Gr_L^{1/5}$ results for Power Law Variation of the Surface Heat Flux.	34
4. The $f'(\xi, 0)$ results for Power Law Variation of the Surface Heat Flux.	35
CHAPTER 3 MIXED CONVECTION ALONG A VERTICAL CYLINDER WITH VARIABLE SURFACE TEMPERATURE	
1. The $Nu_x Gr_x^{1/4}$ results for Power Law Variation of Surface Temperature, Free Convection.	66
2. The $Nu_x / Nu_{x,UWT}$ results for Power Law Variation of Surface Temperature, Free Convection.	67
3. The $Nu_L Gr_L^{1/4}$ results for Power Law Variation of Surface Temperature, Free Convection.	68
4. The $f'(\xi, 0)$ results for Power Law Variation of Surface Temperature, Free Convection.	69
5. The $Nu_x Re_x^{1/2}$ and $f'(\xi, 0)$ results for Power law Variation of Surface Temperature, Forced Convection.	70
6. The $Nu_x / Nu_{x,UWT}$ results for Power Law Variation of Surface Temperature, Forced Convection.	71
7. The $Nu_L Re_L^{1/2}$ results for Power Law Variation of Surface Temperature, Forced Convection.	72
8. The $Nu_x / (Re_x^{1/2} + Gr_x^{1/4})$ results for Power Law Variation of Surface Temperature, Mixed Convection, Along a Vertical Flat Plate ($\Lambda = 0, \Omega_0 = \infty$).	73
9. The $Nu_x / (Re_x^{1/2} + Gr_x^{1/4})$ results for Power Law Variation of Surface Temperature, Mixed Convection, $\Omega_0 = 0.02$	74
10. The $Nu_x / (Re_x^{1/2} + Gr_x^{1/4})$ results for Power Law Variation of Surface Temperature, Mixed Convection, $\Omega_0 = 0.1$	75
11. The $Nu_x / (Re_x^{1/2} + Gr_x^{1/4})$ results for Power Law Variation of Surface Temperature, Mixed Convection, $\Omega_0 = 0.5$	76
12. The $Nu_x / (Re_x^{1/2} + Gr_x^{1/4})$ results for Power Law Variation of Surface Temperature, Mixed Convection, $\Omega_0 = 1.0$	77

Table		Page
13.	The $Nu_x/(Re_x^{1/2} + Gr_x^{1/4})$ results for Power Law Variation of Surface Temperature, Mixed Convection, $\Omega_0 = 2.0$	78
14.	The $f'(\xi, 0)$ results for Power Law Variation of Surface Temperature, Mixed Convection, Along a Vertical Flat Plate ($\Lambda = 0$, $\Omega_0 = \infty$).....	79
15.	The $f'(\xi, 0)$ results for Power Law Variation of Surface Temperature, Mixed Convection, $\Omega_0 = 0.02$	80
16.	The $f'(\xi, 0)$ results for Power Law Variation of Surface Temperature, Mixed Convection, $\Omega_0 = 0.1$	81
17.	The $f'(\xi, 0)$ results for Power Law Variation of Surface Temperature, Mixed Convection, $\Omega_0 = 0.5$	82
18.	The $f'(\xi, 0)$ results for Power Law Variation of Surface Temperature, Mixed Convection, $\Omega_0 = 1.0$	83
19.	The $f'(\xi, 0)$ results for Power Law Variation of Surface Temperature, Mixed Convection, $\Omega_0 = 2.0$	84

I. INTRODUCTION

NOMENCLATURE

g	gravitational acceleration
Gr_x	local Grashof number, $g\beta[T_w(x) - T_\infty]x^3/\nu^2$
Gr_x^*	modified local Grashof number, $g\beta q_w(x)x^4/k\nu^2$
k	thermal conductivity of the fluid
m	exponent used in the mixed convection correlation
n	exponent in the power law variation of the surface temperature or surface heat flux
Pr	Prandtl number, ν/α
r	radial coordinate
r_o	radius of the cylinder
Re_x	Reynolds number based on x , $u_\infty x/\nu$
T	fluid temperature
u	axial velocity component
x	axial coordinate
α	thermal diffusivity
β	volumetric coefficient of thermal expansion
Λ_N	curvature parameter for natural convection with variable surface temperature, $(2x/r_o)Gr_x^{1/4}$
Λ_N^*	modified curvature parameter for natural convection with variable surface heat flux, $(2x/r_o)Gr_x^{*1/5}$
Λ_F	curvature parameter for pure forced convection, $(2x/r_o)Re_x^{1/2}$
Λ	curvature parameter for mixed convection with variable surface temperature, $(2x/r_o)(Re_x^{1/2} + Gr_x^{1/4})^{-1}$
Λ^*	curvature parameter for mixed convection with variable surface heat flux, $(2x/r_o)(Re_x^{1/2} + Gr_x^{*1/5})^{-1}$
ν	kinematic viscosity
χ	mixed convection parameter for variable surface temperature, $(1 + \Omega_x^{1/4})^{-1}$
χ^*	mixed convection parameter for variable surface heat flux, $(1 + \Omega_x^{*1/5})^{-1}$
Ω_x	buoyancy parameter for variable surface temperature, Gr_x/Re_x^2
Ω_x^*	buoyancy parameter for variable surface heat flux, Gr_x^*/Re_x^2

Subscripts

F	for the case of pure forced convection
N	for the case of pure natural convection
w	conditions at the wall
∞	condition at the free stream

INTRODUCTION

This thesis studies convective heat transfer along slender vertical cylinders. Chapter 2 presents an analysis of natural convection with a power law variation in surface heat flux of the form $q_w(x) = ax^n$. In Chapter 3 mixed convection covering the full range from pure free convection to pure forced convection for a power law variation in surface temperature of the form $T_w(x) - T_\infty = ax^n$ is studied.

In formulating the problem of free convection along slender vertical cylinders, the governing equations are written in their cylindrical coordinate form and then transformed into a dimensionless form. The boundary layers are nonsimilar due to the transverse surface curvature. As the radius r_0 approaches infinity, the equations reduce to those for a vertical plate, and the boundary layers become similar. The vertical plate problem has been studied extensively. The isothermal vertical flat plate was first analyzed by Ostrach [1]. Sparrow and Gregg [2] later studied the case of uniform surface heat flux. Subsequently many analytical studies using various solution methods were used to solve variations of the problem (see, e.g. Refs. [3 - 7]). These studies included cases of variable surface temperature distributions. The case of the power law temperature variation or a power law variation in surface heat flux lends itself to similarity solutions for the vertical flat plate. Results for these can be found in Sparrow and Gregg [5] for the power law variation in surface temperature and in Chen et al. [7] for both cases that include the local nonsimilarity solution for inclined plates.

The case of pure forced convection past a flat plate is the well known Blasius solution for the momentum equation and the Pohlhausen solution for the case of uniform wall temperature (UWT). The case of uniform surface heat flux (UHF) was solved numerically for the entire range of Prandtl numbers (Pr) by Churchill and Ozoe [8]. The solutions for both pure free convection and pure forced convection have been accurately correlated and should provide a basis for comparison for the limit of the vertical cylinder problem as $r_0 \rightarrow \infty$.

The case of pure forced convection past a vertical cylinder has been studied by various authors [9 - 14]. Seban and Bond [9] conducted an early study considering the UWT case for $Pr = 0.715$ and curvatures ($\Lambda_F \approx 2 \frac{x}{r_0} Re_x^{-1/2}$) up to 3.0 using a power series method of solution.

Chen and Mucoglu [13] first presented results for the case of UWT as part of the solution for mixed convection and then followed that with the case of UHF [14]. Their results covered curvatures up to $\Lambda_F = 8$ for $Pr = 0.7$ and 7, and they used the local nonsimilarity solution. Bui and Cebeci [12] analyzed the UWT case as part of their mixed convection study for $Pr = 0.1$, 1.0, and 10 for curvatures up to $\Lambda_F = 10$ using a central difference finite-difference method of solution. Lee et al. [10, 11] studied both the UWT and UHF cases as part of their mixed convection analysis for $Pr = 0.1$, 0.7, 7, and 100 for curvature parameter Λ_F up to 50 using a weighted finite-difference scheme. Lee et al. qualified the accuracy of their results for $\Lambda_F > 10$ due to the use of an insufficiently small step size in the radial direction.

More extensively researched has been the case of natural convection along a cylinder [10, 11, 15 – 22]. Elenbaas [15] used Langmuir's stagnant film model to evaluate the heat transfer coefficients for vertical cylinders under the UWT condition. Sparrow and Gregg [16] refined this method and reworked this problem using a power series solution and obtained results for $Pr = 0.72$ and 1 covering curvature parameter, $\Lambda_N = 2 \frac{X}{r_0} Gr_*^{1/4}$, up to about 1.5. Kuiken [18] also used a power series expansion and investigated power law variation in wall temperature and the UHF condition for $0.7 \leq Pr \leq 10$. Fujii and Uehara [20] also applied a power series solution to cylinders with variable wall temperature for Λ_N up to 2.73 and for $0.7 \leq Pr \leq 100$. To reduce the truncation errors of the power series solution and the local similarity solution, Minkowycz and Sparrow [21] employed the local nonsimilarity solution method and obtained results for $Pr = 0.733$ and $0 \leq \Lambda_N \leq 10$. Lee et al. [10, 11] solved the UWT and the UHF cases of natural convection along a vertical cylinder for $Pr = 0.1$, 0.7, 7, and 100 as part of their mixed convection study employing a finite-difference method designed to overcome the difficulties associated with increasing curvature. As a result, Lee et al. carried their results to $\Lambda_N = 50$. More recently, Lee et al. [17] used a modified method [23] to solve the variable wall temperature problem for natural convection along a vertical cylinder. They found that the results of [10] were incorrect for $\Lambda_N > 10$ due to an improper step size used in the radial direction.

The significant finding for pure forced or pure free convection along a vertical cylinder is that the nonsimilarity due to the surface curvature increases the heat transfer coefficient. The velocity gradient at the wall increases with increasing surface curvature for pure free convection under a power law variation in surface temperature or for pure forced convection, but decreases for the UHF case for free convection. Minkowycz and Sparrow [21] showed that the error caused by the power series solution increases with increasing curvature. Lee et al. [17] showed that the results provided by Fujii and Uehara [20] are valid only up to Λ_N of about 1.5. Lee et al. [10] demonstrated that the central difference scheme used by Bui and Cebeci [12] produces large errors as the curvature increases, but the results in [10, 11] are not accurate for $\Lambda > 10$ because they used too large a step size in the radial direction.

There have been relatively few studies on mixed convection along a vertical cylinder. The studies by Bui and Cebeci [12] and Chen and Mucoglu [13] are for the UWT case. They investigated the forced convection dominated regime in terms of the buoyancy force parameter $\Omega_x = Gr_x/Re_x^2$. Mucoglu and Chen also presented the UHF case with the modified buoyancy parameter $\Omega_x^* = Gr_x^*/Re_x^{5/2}$. Lee et al. [10] treated the UWT case for the entire regime using a new mixed convection parameter, $\chi = (1 + \Omega_x^{1/4})^{-1}$, which varies from zero for pure free convection to one for pure forced convection. In Lee et al. [11], the UHF case is presented for the entire regime using $\chi^* = (1 + \Omega_x^{*1/5})^{-1}$. The main difficulty addressed in these two studies has been the effect of curvature on the numerical solution. The results of Chen and Mucoglu [13, 14] for the forced-convection dominated solutions agree well with those of [10, 11] for curvature parameters $[\Lambda = 2\frac{x}{r_0}(Re_x^{1/2} + Gr_x^{1/4})^{-1} \text{ or } \Lambda^* = 2\frac{x}{r_0}(Re_x^{1/2} + Gr_x^{*1/5})^{-1}]$ from 0 to 8 for $Pr = 0.7$ and 7. The results of Bui and Cebeci for large curvature parameters were found to be inaccurate by Lee et al. [10] due to their use of a central difference finite-difference method of solution. Lee et al. [10, 11] used a weighted finite-difference scheme to correct this but failed to use the proper step size for large curvatures.

For comparison purposes the mixed convection solution for the vertical flat plate is needed. There are numerous studies of this flow geometry (see, e.g. Refs. [24 – 29]). These numerical results have been correlated by Chen et al. [24] and Churchill [30] using the simple form $Nu^m = Nu_F^m + Nu_N^m$ with $m = 3$, in which Nu_F is the Nusselt number for pure forced

convection and Nu_N is the Nusselt number for pure free convection. The correlation was also verified experimentally for the case of air [24].

To date no study has been done for the case of variable surface heat flux along a slender vertical cylinder for natural convection. This will be undertaken in Chapter 2. Similarly, the combined effects of buoyancy force and curvature in mixed convection with variable surface temperature along a slender vertical cylinder has not been solved. Furthermore, the results of Lee et al. [10] and Bui and Cebeci [12] for the UWT case are questionable for high values of the curvature parameter and need to be reassessed. This is the topic of Chapter 3.

REFERENCES

1. S. Ostrach, An analysis of laminar free-convection flow and heat transfer about a flat plate parallel to the direction of the generating body force, NACA , TN 2635 (1952).
2. E. M. Sparrow and J. L. Gregg, Laminar free convection from a vertical plate with uniform surface heat flux, Trans. ASME 78, 435-440 (1956).
3. M. Kelleher and K. T. Yang, A Gortler-type series for laminar free convection along a non-isothermal vertical plate, Q. J. Mech. and Appl. Math. 25, 447-457 (1972).
4. T. T. Kao, G. A. Domoto, and H. G. Elrod, Free convection along a nonisothermal vertical flat plate, J. Heat Transfer 99, 72-78 (1977).
5. E. M. Sparrow and J. L. Gregg, Similar solutions for free convection from a nonisothermal vertical plate, Trans. ASME 80, 379-386 (1958).
6. A. J. Ede, Advances in free convection, Adv. Heat Transfer 4, 1-64 (1967).
7. T. S. Chen, H. C. Tien, and B. F. Armaly, 1986, Natural convection on horizontal, inclined, and vertical plates with variable surface temperature or heat flux, Int. J. Heat Mass Transfer 29, 1465-1478 (1986).
8. S. W. Churchill and H. Ozoe, A correlation for laminar forced convection with uniform surface heating in flow over a plate and in developing and fully developed flow in a tube, J. Heat Transfer 95, 78-84 (1973).
9. R. A. Seban and R. Bond, Skin friction and heat-transfer characteristics of a laminar boundary layer on a cylinder in axial incompressible flow, J. Aero. Science 18, 671-675 (1951).
10. S. L. Lee, T. S. Chen, and B. F. Armaly, Mixed convection along isothermal vertical cylinders and needles, Proc. Eighth Int. Heat Transfer Conf. 3, 1425-1432 (1986).
11. S. L. Lee, T. S. Chen, and B. F. Armaly, Mixed convection along vertical cylinders and needles with uniform surface heat flux, J. Heat Transfer 109, 711-716 (1987).
12. M. N. Bui and T. Cebeci, Combined free and forced convection on vertical cylinders, J. Heat Transfer 107, 476-478 (1985).
13. T. S. Chen and A. Mucoglu, Buoyancy effects on forced convection along a vertical cylinder, J. Heat Transfer 97, 198-203 (1975).

14. A. Mucoglu and T. S. Chen, Buoyancy effects on forced convection along a vertical cylinder with uniform surface heat flux, J. Heat Transfer 98, 523-525 (1976).
15. W. Elenbaas, The dissipation of heat by free convection from vertical and horizontal cylinders, J. Appl. Physics 19, 1148-1154 (1948).
16. E. M. Sparrow and J. L. Gregg, Laminar-free-convection heat transfer from the outer surface of a vertical circular cylinder, Trans. ASME 78, 1823-1829 (1956).
17. H. R. Lee, T. S. Chen, and B. F. Armaly, Natural convection along vertical cylinders with variable surface temperature, J. Heat Transfer 110, 103-108 (1988).
18. H. K. Kuiken, Axisymmetric free convection boundary layer flow past slender bodies, Int. J. Heat Mass Transfer 15, 1141-1153 (1968).
19. K. T. Yang, Possible similarity solutions for laminar free convection on vertical plates and cylinders, J. Appl. Mech. 26, 230-236 (1960).
20. T. Fujii and H. Uehara, Laminar natural convective heat transfer from the outer surface of a vertical cylinder, Int. J. Heat Mass Transfer 13, 607-615 (1970).
21. W. J. Minkowycz and E. M. Sparrow, Local nonsimilar solutions for natural convection on a vertical cylinder, J. Heat Transfer 96, 178-183 (1974).
22. K. Millsaps and K. Pohlhausen, The laminar free convection heat transfer from the outer surface of a vertical circular cylinder, J. Aero. Science 25, 357-360 (1958).
23. S. L. Lee, T. S. Chen and B. F. Armaly, New finite difference solution methods for wave instability problems, Nume. Heat Transfer 10, 1-8 (1986).
24. T. S. Chen, B. F. Armaly and N. Ramachandran, Correlations for laminar mixed convection flows on vertical, inclined, and horizontal flat plates, J. Heat Transfer 108, 835-840 (1986).
25. N. Ramachandran, B. F. Armaly and T. S. Chen, Measurements and predictions of laminar mixed convection flow adjacent to a vertical surface, J. Heat Transfer 107, 636-641 (1985).
26. A. Mucoglu and T. S. Chen, Mixed convection on inclined surfaces, J. Heat Transfer 101, 422-426 (1979).
27. J. Gryzgoridis, Combined free and forced convection from an isothermal vertical plate, Int. J. Heat Mass Transfer 18, 911-916 (1975).

28. M. S. Raju, X. Q. Lin and C. K. Law, A formulation of combined forced and free convection past horizontal and vertical surfaces, Int. J. Heat Mass Transfer 17, 2215-2224 (1984).
29. J. R. Lloyd and E. M. Sparrow, Combined forced and free convection flow on vertical surfaces, Int. J. Heat Mass Transfer 13, 434-438 (1970).
30. S. W. Churchill, A comprehensive correlating equation for laminar assisting, forced and free convection, AIChE Journal 23, 10-16 (1977).

II. NATURAL CONVECTION ALONG A VERTICAL CYLINDER WITH VARIABLE SURFACE HEAT FLUX

NATURAL CONVECTION ALONG A VERTICAL CYLINDER WITH VARIABLE SURFACE HEAT FLUX

by

J. J. Heckel, T. S. Chen, and B. F. Armaly

Department of Mechanical and Aerospace Engineering

University of Missouri-Rolla, Rolla, MO 65401

ABSTRACT

Natural convection in laminar boundary layer flow along slender vertical cylinders is analyzed for the situation in which the surface heat flux $q_w(x)$ varies arbitrarily with the axial coordinate x . The governing boundary layer equations along with the boundary conditions are first cast into a dimensionless form by a nonsimilar transformation and the resulting system of equations is then solved by a weighted finite-difference method of solution in conjunction with the cubic spline interpolation. Sample calculations were performed for the case of power law variation in surface heat flux, $q_w(x) = ax^n$, for fluids with Prandtl numbers of 0.1, 0.7, 7, and 100 over a wide range of values for the curvature parameter $0 \leq \Lambda_N^* \leq 50$ or $0 \leq \xi \leq 5$. Results for the local and average Nusselt numbers as well as the local wall shear stress were obtained. It is found that the value of the radial coordinate η_∞ must be increased, as the curvature parameter is increased, to obtain valid results. Also the local Nusselt number is found to increase with increasing curvature, Prandtl number, and the exponent n . For any given location of x , the local wall shear stress was found to decrease with increasing curvature, increasing Prandtl number, and increasing n . Correlation equations for the local and average Nusselt numbers are presented.

NOMENCLATURE

f	reduced stream function, $(\psi/5\nu r_0)(Gr_x^*/5)^{1/5}$
g	$\partial f/\partial \eta$ or gravitational acceleration
Gr_x	local Grashof number, $g\beta[T_w(x) - T_\infty]x^3/\nu^2$
Gr_x^*	modified local Grashof number, $g\beta q_w(x)x^4/k\nu^2$
Gr_x^*, Gr_o^*	modified Grashof numbers defined, respectively, as $g\beta q_w(1)L^4/k\nu^2$ and $g\beta q_w(r_o)r_o^4/k\nu^2$
h	local heat transfer coefficient, $q_w/(T_w - T_\infty)$
\bar{h}	average heat transfer coefficient
k	thermal conductivity of the fluid
L	an arbitrary length of cylinder
n	exponent in the power law variation of heat flux
Nu_x	local Nusselt number, hx/k
\overline{Nu}_L	average Nusselt number, $\bar{h}L/k$
Pr	Prandtl number, ν/α
r	radial coordinate
r_o	radius of the cylinder
T	fluid temperature
u	axial velocity component
v	radial velocity component
x	axial coordinate
α	thermal diffusivity
β	volumetric coefficient of thermal expansion
γ	variable heat flux parameter, $(x/q_w)(dq_w/dx)$
η	pseudo-similarity variable, $[(r^2 - r_o^2)/2r_o x](Gr_x^*/5)^{1/5}$
θ	dimensionless temperature, $(T - T_\infty)(Gr_x^*/5)^{1/5}/[q_w(x)x/k]$
λ	curvature parameter, $(2x/r_o)(Gr_x^*/5)^{1/5}$
Λ_N	curvature parameter for variable surface temperature, $(2x/r_o)Gr_x^{1/4}$
Λ^*_N	modified curvature parameter, $(2x/r_o)Gr_x^{1/5}$

μ	dynamic viscosity
ν	kinematic viscosity
ξ	dimensionless axial coordinate, $(\Lambda^*_N/2)^{1/2}$
ρ	fluid density
τ_w	local wall shear stress
ϕ	normalized temperature profile, $\phi(\xi, \eta) = \theta(\xi, \eta)/\theta(\xi, 0)$
ψ	stream function
ω	relaxation factor

Subscripts

N	for the case of pure natural convection
o	quantities at $\xi - \Delta\xi$
p	for a flat plate
w	conditions at the wall
∞	condition at the free stream

INTRODUCTION

Heat transfer by natural convection along a vertical cylinder has been analyzed rather extensively. Elenbaas (1948) used Langmuir's stagnant film model to evaluate the heat transfer coefficients for vertical cylinders with uniform wall temperature (UWT). Sparrow and Gregg (1956) reworked this same problem using a power series expansion method for Prandtl numbers, Pr , of 0.72 and 1 for curvature parameter, $\Lambda_N = 2 \frac{x}{r_0} Gr_x^{-1/4}$, up to about 1.5. Kuiken (1968) also used a power series solution and investigated a power law variation in the wall temperature and the case of uniform surface heat flux (UHF) for $0.7 \leq Pr \leq 100$. The power series solution was also applied by Fujii and Uehara (1970) to cylinders with variable wall temperatures for Λ_N up to 2.73 and for $0.72 \leq Pr \leq 100$. To reduce truncation errors of the power series and the local similarity solutions, Minkowycz and Sparrow (1974) employed the local nonsimilarity method and obtained results for $Pr = 0.733$ and $0 \leq \Lambda_N \leq 10$.

Recently, Lee et al. (1986a, 1987) analyzed natural convection along slender vertical cylinders under UWT and UHF conditions as part of their mixed convection study by employing a weighted finite-difference method designed to overcome the numerical difficulties associated with increasing surface curvature. They presented results for $0.1 \leq Pr \leq 100$ that cover Λ_N up to 50 for the UWT case and $\Lambda_N^* = 2 \frac{x}{r_0} Gr_x^{*-1/5}$ up to 50 for the UHF case. More recently, Lee et al. (1988) analyzed natural convection along a vertical cylinder for the case of power law variation of wall temperature, $T_w(x) = T_\infty + ax^n$, and found that the results of Lee et al. (1986a) were not accurate for $\Lambda_N > 10$ because of the improper step sizes used in the radial direction. They presented results for $0.1 \leq Pr \leq 100$, covering Λ_N up to 50 and $n = -0.4, -0.2, 0, 0.2$, and 0.5 . Lee et al. (1987) attached a qualifying statement to their study of the UHF case as to the accuracy of their results for curvature parameters $\Lambda_N^* > 10$ and attributed this also to the use of improper step sizes in η . It appears that no experimental results for natural convection along vertical cylinders under nonuniform heating have been reported in the literature.

To date no analytical study seems to have been presented for the case of variable surface heat flux along a vertical slender cylinder and this has prompted the present study. Furthermore, since the results of Lee et al. (1987) are not correct for large values of Λ^*_N , they need to be reassessed.

ANALYSIS

Consider a semi-infinite, vertical cylinder with radius r_0 that is aligned in a quiescent ambient fluid at temperature T_∞ . The axial coordinate x is measured upward for $q_w > 0$ and downward for $q_w < 0$, while the radial coordinate r is measured from the axis of the cylinder. The surface of the cylinder is subjected to an arbitrary heat flux $q_w(x)$, and the gravitational acceleration g is acting downward. The fluid properties are assumed to be constant except for variations in density which induce the buoyancy force. By employing the laminar boundary layer assumptions and making use of the Boussinesq approximation the governing conservation equations for the problem under study can be written as:

Continuity:

$$\frac{\partial}{\partial x}(ru) + \frac{\partial}{\partial r}(rv) = 0 \quad (1)$$

Momentum:

$$u \frac{\partial u}{\partial x} + v \frac{\partial u}{\partial r} = \frac{\nu}{r} \frac{\partial}{\partial r} \left(r \frac{\partial u}{\partial r} \right) + g\beta(T - T_\infty) \quad (2)$$

Energy:

$$u \frac{\partial T}{\partial x} + v \frac{\partial T}{\partial r} = \frac{\alpha}{r} \frac{\partial}{\partial r} \left(r \frac{\partial T}{\partial r} \right) \quad (3)$$

In these equations u and v are the velocity components in the x and r directions respectively; T is the fluid temperature; and ν , β and α are, respectively, the kinematic viscosity, the volumetric coefficient of thermal expansion, and the thermal diffusivity of the fluid.

The boundary conditions are

$$u = v = 0, \quad \frac{\partial T}{\partial r} = \frac{-q_w(x)}{k} \quad \text{at } r = r_0 \quad (4a)$$

$$u \rightarrow 0, \quad T \rightarrow T_\infty \quad \text{as } r \rightarrow \infty \quad (4b)$$

$$u = 0, \quad T = T_\infty \quad \text{at } x = 0, \quad r \geq r_0 \quad (4c)$$

In writing the last boundary condition (4c) it is assumed that the flow and thermal boundary layer thicknesses are zero at the leading edge of the surface.

To proceed with the analysis, the conservation equations, along with the boundary conditions, are transformed into a dimensionless form by introducing the following dimensionless variables:

$$\eta = \frac{(r^2 - r_0^2)}{2r_0 x} (Gr_x^*/5)^{1/5}, \quad \lambda = \frac{2x}{r_0} (Gr_x^*/5)^{-1/5} \quad (5)$$

$$f(\lambda, \eta) = \psi(x, r) / [5vr_0(Gr_x^*/5)^{1/5}], \quad \theta(\lambda, \eta) = \frac{(T - T_\infty)(Gr_x^*/5)^{1/5}}{q_w(x) x/k} \quad (6)$$

where $Gr_x^* = g\beta q_w(x)x^4/k\nu^2$ is the modified Grashof number, η is the pseudo-similarity variable, $f(\lambda, \eta)$ is the reduced stream function, $\theta(\lambda, \eta)$ is the dimensionless temperature, λ is the curvature parameter, and $\psi(x, r)$ is the stream function that satisfies the continuity equation, with $u = (\epsilon \psi / \partial r)/r$ and $v = -(\partial \psi / \partial x)/r$.

The transformation yields

$$(1 + \eta\lambda)f''' + \lambda f'' + (\gamma + 4)\eta f'' - (2\gamma + 3)f'^2 + \theta = \lambda(\gamma - 1)\left(f' \frac{\partial f}{\partial \lambda} - f \frac{\partial f'}{\partial \lambda}\right) \quad (7)$$

$$(1 + \eta\lambda)\theta'' + \lambda\theta' + Pr(\gamma + 4)\eta\theta' - Pr(4\gamma + 1)f'\theta = \lambda(\gamma - 1)\left(\theta' \frac{\partial f}{\partial \lambda} - f' \frac{\partial \theta}{\partial \lambda}\right) \quad (8)$$

$$\begin{aligned} f(\lambda, 0) = f'(\lambda, 0) = 0, \quad \theta'(\lambda, 0) = -1 \\ f'(\lambda, \infty) = 0, \quad \theta(\lambda, \infty) = 0 \end{aligned} \quad (9)$$

where

$$\gamma = \frac{x}{q_w} \frac{dq_w}{dx} \quad (10)$$

and the primes denote partial differentiation with respect to η .

The system of equations (7)-(9) along with (10) represents the general form of the transformed boundary layer equations under arbitrary surface heat flux, $q_w(x)$. For the case of power law variation $q_w(x) = ax^n$, one has from equation (10) that

$$\gamma = n \quad (11)$$

For long slender cylinders, the curvature parameter $\lambda = 2(x/r_o)(Gr_x^*/5)^{-1/5}$ can be large. To lower the maximum value of calculations in the x or λ coordinate, one introduces a new $\xi(x)$ variable defined by

$$\xi = [(x/r_o)Gr_x^*]^{1/2} \quad (12)$$

such that $\lambda = C \xi^2$ with $C = 2 \cdot 5^{1/5}$.

Substituting equations (11) and (12) into equations (7)-(9) results in:

Momentum:

$$(1 + a_1\eta)f''' + a_1f'' + a_2ff'' + a_3f^2 + a_4\theta = a_5 \left(f' \frac{\partial f}{\partial \xi} - f \frac{\partial f'}{\partial \xi} \right) \quad (13)$$

Energy:

$$(1 + a_1\eta)\theta'' + a_1\theta' + Pr a_2f\theta' + Pr a_6f'\theta = Pr a_5 \left(\theta' \frac{\partial f}{\partial \xi} - f \frac{\partial \theta}{\partial \xi} \right) \quad (14)$$

Boundary Conditions :

$$\begin{aligned} f(\xi, 0) = f'(\xi, 0) = 0, \quad \theta'(\xi, 0) = -1 \\ f'(\xi, \infty) = \theta(\xi, \infty) = 0 \end{aligned} \quad (15)$$

where

$$\begin{aligned}
a_1 &= C\xi^2, & a_2 &= n+4, & a_3 &= -(2n+3) \\
a_4 &= 1, & a_5 &= \xi(n-1)/2, & a_6 &= -(4n+1)
\end{aligned}
\tag{16}$$

The proposed method of solution, developed by Lee et al.(1986b), requires boundary conditions in terms of f , f' and θ at $\eta = 0$. In equation (15) one has $\theta'(\lambda, 0) = -1$. This necessitates an additional transformation. Let

$$\phi(\xi, \eta) = \theta(\xi, \eta)/\theta(\xi, 0) \tag{17}$$

Applying equation (17) and the boundary condition $\theta'(\xi, 0) = -1$ to equations (13)-(15) results in:

$$(1 + a_1\eta)f'' + a_1f' + a_2ff'' + a_3f'^2 + a_7\phi = a_5 \left(f' \frac{\partial f}{\partial \xi} + f \frac{\partial f'}{\partial \xi} \right) \tag{18}$$

$$\begin{aligned}
&(1 + a_1\eta)\phi'' + a_1\phi' + a_2\text{Pr} f\phi' + a_6\text{Pr} f'\phi \\
&= \text{Pr} a_5 \left\{ \phi' \frac{\partial f}{\partial \xi} - f' \left(\phi'(\xi, 0) \left[\frac{\partial}{\partial \xi} \left(\frac{\phi}{\phi'(\xi, 0)} \right) \right] \right) \right\}
\end{aligned}
\tag{19}$$

$$\begin{aligned}
f(\xi, 0) = f'(\xi, 0) = 0 \quad \phi(\xi, 0) = 1 \\
f(\xi, \infty) = \phi(\xi, \infty) = 0
\end{aligned}
\tag{20}$$

where a_1 through a_6 are as before and

$$a_7 = - \frac{a_4}{\phi'(\xi, 0)} \tag{21}$$

The details of this derivation are given in Appendix A. The boundary conditions are now in the proper form to be used in the finite difference solution method described in Appendix B.

The physical quantities of interest are the local Nusselt number Nu_x , the average Nusselt number \overline{Nu}_L , the local wall shear stress τ_w , the axial velocity distribution u , and the temperature profile $\phi(\xi, \eta)$. The local Nusselt number is defined by

$$Nu_x = \frac{hx}{k} = \frac{q_w}{T_w - T_\infty} \frac{x}{k} \quad (22)$$

which can be expressed in the form

$$Nu_x (Gr_x^*/5)^{-1/5} = -\phi'(\xi, 0) \quad (23)$$

The average Nusselt number is defined by $\overline{Nu}_L = \bar{h}L/k$ where the average heat transfer coefficient, \bar{h} , is obtained from

$$\bar{h} = \frac{1}{L} \int_0^L h dx \quad (24)$$

This leads to

$$\overline{Nu}_L (Gr_L^*/5)^{-1/5} = -\frac{10}{1-n} \xi_L^N \int_0^{\xi_L} \xi^M \phi'(\xi, 0) d\xi \quad (25)$$

where $\xi_L = \xi$ at $x = L$, $M = (7 + 3n)/(1 - n)$, and $N = (8 + 2n)/(n - 1)$

Next, from the definition of local wall shear stress $\tau_w = \mu(\partial u/\partial r)_{r=r_0}$ one obtains

$$\tau_w = 5 \frac{\mu v}{x^2} (Gr_x^*/5)^{3/5} f'(\xi, 0) \quad (26)$$

The axial velocity distribution can be written as

$$\frac{ux}{v} = 5 (Gr_x^*/5)^{2/5} f(\xi, \eta) \quad (27)$$

and the temperature profile is given by equation (17).

METHOD OF SOLUTION

Equations (18)-(20) constitute a system of nonlinear partial differential equations in the (ξ, η) coordinates with parameters Pr and n . The method described in Lee et al. (1986b) is

employed to solve this system of equations. The first step is to convert the terms involving $\partial/\partial\xi$ in the following manner.

$$\frac{\partial H}{\partial \xi} = \frac{p}{\Delta \xi} (H - H_o) - q \left(\frac{\partial H}{\partial \xi} \right)_o = \frac{p}{\Delta \xi} (H - \bar{H}_o) \quad (28)$$

where H is a function of (ξ, η) , $\bar{H}_o = H_o + (q/p)\Delta\xi(\partial H/\partial\xi)_o$, and the subscript "o" denotes quantities at $\xi - \Delta\xi$. The values for p and q are $p=1$ and $q=0$ at $\xi=0$ and $\xi=\Delta\xi$, and $p=2$ and $q=1$ thereafter for $\xi \geq 2\Delta\xi$.

The f and ϕ equations are then linearized by using the simple technique for the product of two arbitrary functions F and G , defined as

$$FG = \tilde{F}G + \tilde{G}F - \tilde{F}\tilde{G} \quad (29)$$

where \tilde{F} and \tilde{G} indicate values to be guessed. The quasi-linearized function FG expressed by equation (29) will provide quadratic and monotone convergence. By employing equation (28) for the terms $\frac{\partial f}{\partial \xi}$, $\frac{\partial f'}{\partial \xi}$, and $\phi'(\xi, 0) \left[\frac{\partial}{\partial \xi} \left(\frac{\phi}{\phi'(\xi, 0)} \right) \right]$ and applying (29) to the terms ff'' , f'^2 , $f\phi'$, and $f'\phi$, one obtains

$$A_0 f''' + (a_1 + A_1) f'' + A_2 f' + A_3 f + A_4 \phi = A_5 \quad (30)$$

$$B_0 \phi'' + (a_1 + B_1) \phi' + B_2 \phi + B_3 f' + B_4 f = B_5 \quad (31)$$

where

$$\begin{aligned} A_0 &= 1 + a_1 \eta, & A_1 &= a^* \tilde{f} + d^* \tilde{f}_o, & A_2 &= 2b^* \tilde{f}' - d^* \tilde{f}_o' \\ A_3 &= a^* \tilde{f}'' , & A_4 &= a_7, & A_5 &= a^* \tilde{f} \tilde{f}'' + b^* \tilde{f}'^2 \end{aligned} \quad (32)$$

$$\begin{aligned} B_0 &= A_0, & B_1 &= \text{Pr } A_1, & B_2 &= \text{Pr } e^* \tilde{f}', & B_3 &= \text{Pr } (e^* \tilde{\phi} - d^* \tilde{\phi}_o) \\ B_4 &= \text{Pr } a^* \tilde{\phi}', & B_5 &= \text{Pr } (a^* \tilde{f} \tilde{\phi}' + e^* \tilde{f}' \tilde{\phi}) \end{aligned} \quad (33)$$

$$a^* = a_2 - d^*, \quad b^* = a_3 + d^*, \quad d^* = a_5 p / \Delta \xi, \quad c^* = a_6 + a_8 d^* \quad (34)$$

$$a_8 = \frac{\bar{\phi}'(\xi, 0)_o}{\tilde{\phi}'(\xi, 0)} \quad (35)$$

and the other variables are as previously defined.

The system of equations has now been reduced to a system of quasi-linear ordinary differential equations. By defining $g = f'$ and applying the weighting factors (see Lee et al., 1986b), one can write equations (30) and (31) in the finite-difference form as:

$$f_i - f_{i-1} - (\Delta\eta/2)(g_i + g_{i-1}) = 0 \quad (36)$$

$$A_0/(\Delta\eta)^2(\alpha_{-1}g_{i-1} + \alpha_0g_i + \alpha_{+1}g_{i+1}) + \Lambda_2g_i + \Lambda_3f_i + \Lambda_4\phi_i = \Lambda_5 \quad (37)$$

$$B_0/(\Delta\eta)^2(\beta_{-1}\phi_{i-1} + \beta_0\phi_i + \beta_{+1}\phi_{i+1}) + B_2\phi_i + B_3g_i + B_4f_i = B_5 \quad (38)$$

where $\Delta\eta$ is the step size in the η direction and the subscript "i" refers to values at the nodal point η_i .

In equations (37) and (38) the weighting factors are defined as:

$$\begin{aligned} \alpha_{-1} &= W_f(-z_{i-1/2}), & \alpha_{+1} &= W_f(z_{i+1/2}), & \alpha_0 &= -\alpha_{-1} - \alpha_{+1} \\ \beta_{-1} &= W_f(-z^*_{i-1/2}), & \beta_{+1} &= W_f(z^*_{i+1/2}), & \beta_0 &= -\beta_{-1} - \beta_{+1} \\ W_f(z) &= z/(1 - \exp(-z)), & z &= \Delta\eta(a_1 + \Lambda_1)/\Lambda_0, & z^* &= \Delta\eta(a_1 + B_1)/B_0 \end{aligned} \quad (39)$$

Equations (36)-(38) are applied to the interior points. On the boundaries, equation (20) is written as

$$\begin{aligned} f_1 &= g_1 = 0, & \phi_1 &= 1 \\ f_n - f_{n-1} - \frac{\Delta\eta}{2}(g_n + g_{n-1}) &= g_n = \phi_n = 0 \end{aligned} \quad (40)$$

where the subscript n is the number of nodes in the η direction.

Equations (36)-(40) constitute a system of algebraic equations that can be written in the matrix form as

$$[A][X] = [B] \quad (41)$$

where $[A]$ is a band matrix of order $3n$ and bandwidth seven. The array $[X]$ which contains the solution in the form $(f_1, g_1, \phi_1, f_2, g_2, \phi_2, \dots, f_n, g_n, \phi_n)^T$ is a column matrix of order $3n$. The matrix $[B]$ is a column matrix of order $3n$ which contains the right hand sides of equations (36)-(38) and (40). The matrix $[A]$ is approximately diagonally dominant and equation (41) can be solved by the Gaussian elimination technique with high accuracy.

To obtain values for f' and ϕ' , the results for f and ϕ along with the boundary conditions

$$f'''(\xi, 0) = -a_1 \tilde{f}''(\xi, 0) - a_4, \quad \phi''(\xi, 0) = -a_1 \tilde{\phi}'(\xi, 0), \quad f'''(\xi, \infty) = \phi''(\xi, \infty) = 0 \quad (42)$$

are used in a cubic spline interpolation routine (see, for example, Burden and Faires (1985)). As the solution converges, the boundary conditions become exact and the values for f' and ϕ' can be obtained with high accuracy.

Although equation (29) should provide quadratic monotone convergence, difficulties arose as the surface curvature was increased. This is due to the transformation to the ϕ variable with the resulting term in equation (35). Here the guess of $\phi'(\xi, 0)$ is needed and for high values of surface curvature simply updating $\phi'(\xi, 0)$ as the next guess may not be sufficient to obtain convergence of solutions. To improve convergence, attempts were made to improve the initial guesses of $f, f', f'', \phi,$ and ϕ' at each ξ value.

The present method of solution employs a quasi-linearization of the original nonlinear system of equations and requires initial guesses for $f, f', f'', \phi,$ and ϕ' . The flat plate solution (i.e., $\xi = 0$) for the uniform surface heat flux case (UHF) was obtained for $Pr = 0.7$ and these results were used as the initial guesses for all other combinations of Pr and n at $\xi = 0$. For $\xi = \Delta\xi$, initial guesses were taken to be the results at $\xi = 0$. At $\xi = 2\Delta\xi$, a linear extrapolation of the results at $\xi = 0$ and $\xi = \Delta\xi$ was used. For $\xi \geq 3\Delta\xi$ a three point inverse polynomial

extrapolation was used (see, for example, Traub (1964)). This approach was found to improve convergence of solutions up to 40% faster than simply using the previous node's values as the first guess.

To improve convergence of solutions, it was found that the η_∞ value needed to be taken larger as the value of the surface curvature parameter ξ was increased. The value of η_∞ was initially set to 10 for $Pr \geq 0.7$ and 15 for $Pr = 0.1$. It was increased by 5 when the value of f' or ϕ , at $\eta = 0.98\eta_\infty$ was greater than 0.001. Since $f'(\xi, \infty) = \phi(\xi, \infty) = 0$, the f' and ϕ values greater than 0.001 at $\eta = 0.98\eta_\infty$ indicate that the corresponding boundary layer thickness extends past η_∞ . To make this adjustment, all values of f and ϕ and their derivatives were set to zero for $\eta > \eta_\infty$ except the values for f were taken to be the value at the old η_∞ extended out to the new η_∞ . This adjustment introduced less than 1% difference in the values of the local Nusselt number when compared to a constant run at $\eta_\infty = 30$. This error was due primarily to η_∞ initially being less than 30 rather than to the adjustment itself.

The solution method is an iterative scheme and a solution was considered to be convergent when the calculated values for f , f' , and ϕ differed from the last guess of the respective values by less than 10^{-4} at all nodes (i.e., at all η values for a given ξ). When these criteria failed, new guesses for f , f' , and ϕ were found using a weighted average of the last guess and the resulting calculation. That is

$$\tilde{f}_{\text{new}} = \omega f + (1 - \omega)\tilde{f}_{\text{old}}, \quad \tilde{f}'_{\text{new}} = \omega f' + (1 - \omega)\tilde{f}'_{\text{old}}, \quad \tilde{\phi}_{\text{new}} = \omega \phi + (1 - \omega)\tilde{\phi}_{\text{old}} \quad (43)$$

in which ω is a relaxation factor. Generally $\omega = 1$ resulted in quick convergence. However, if η_∞ was too small or for some small values of Pr and n it was sometimes necessary to use under-relaxation and set $\omega = 0.5$ to facilitate convergence.

It was found that as ξ was increased, errors resulted due to an increase in the boundary layer thicknesses. By using a step size of $\Delta\eta = 0.01$ errors were reduced for $f''(\xi, 0)$ and $\phi'(\xi, 0)$ at high values of the curvature parameter ξ . It was also found that the solution was not sensitive to the step size in ξ and $\Delta\xi = 0.1$ was used.

RESULTS AND DISCUSSION

Typical numerical results for the case of power law variation of surface heat flux $q_w(x)$ were obtained for values of the exponent n of -0.5, -0.25, 0, 0.25, and 0.5 for Prandtl numbers of 0.1, 0.7, 7, and 100 over the range of $0 \leq \xi \leq 5$ (i.e., $0 \leq \Lambda_N^* \leq 50$). Representative values of n fall within the physical limits of realism, $-1 \leq n < 1$, for power law variation of the surface heat flux [see, for example, Gebhart (1971)].

Lee et al. (1987) qualified their results at high values of the surface curvature as a result of using an improper step size $\Delta\eta$, so it is worth noting how step size affects the local Nusselt number. For the UHF case with $\Lambda_N^* = 50$ and $Pr = 0.7$, the present calculation yields $Nu_x Gr_x^{*-1/5} = 16.6$ using $\Delta\eta = 0.036$ and $\eta_\infty = 7.24$. This compares to $Nu_x Gr_x^{*-1/5} = 6.43$ for $\Delta\eta = 0.01$ and $\eta_\infty = 45$. This trend is similar to what Lee et al. (1988) found for the UWT case. It was found that decreasing the step size or increasing η_∞ lowered the local Nusselt number. This finding explains why valid results were obtained at small values of the surface curvature where the range of η is small and errors appeared for large values of curvature where the range of η has increased. When that happens and the boundary conditions are imposed at a point that is actually within the boundary layer, the flow and thermal profiles are lowered thereby decreasing $f'(\xi, 0)$ and $\phi'(\xi, 0)$. As $\phi'(\xi, 0)$ becomes more negative the local Nusselt number increases.

With increasing η_∞ for increasing surface curvature it becomes necessary to determine the degree to which the boundary layer assumptions remain valid. For boundary layer theory to be valid $(r_s - r_o)/x$ is of the order of magnitude of the term $(Gr_x^*/5)^{-1/5}$ where $(r_s - r_o) = \delta$ is the thickness of the boundary layer. The equations for λ and η can be combined to give

$$Y \equiv \frac{\delta}{x} (Gr_x^*/5)^{1/5} = \frac{2}{\lambda} [(1 + \lambda\eta_\delta)^{1/2} - 1] \quad (44)$$

where Y is a measure of the boundary layer thickness.

Typically η_δ is defined as the value of η at $r = r_\delta (= r_o + \delta)$ where f' and ϕ are within 0.1% of their maximum value within the boundary layer. For $\lambda = 1$ this is typically about $\eta_\delta = 20$ and the right-hand side of equation (44) is about 7. If $[(r_s - r_o)/x](Gr_x^*/5)^{1/5}$ remains constant at

7 and λ increases to 50, η_δ will increase to about 620. This shows that the range of η_∞ can extend very large as the surface curvature increases and the boundary layer assumptions will remain valid. It also verifies the analysis presented in Lee et al. (1988) and Minkowycz and Sparrow (1974) for free convection under UWT, that the term that is a measure of the boundary layer thickness may actually decrease despite an increase in η_δ . This would happen in the example if η_δ is less than 620 but greater than 20.

An interesting finding is that a decrease in the step size $\Delta\eta$ (i.e., an increase in the number of nodes) has a large influence on reducing errors in the local Nusselt number at large values of the surface curvature. This is due to the effect of spreading the error imposed at the edge of the boundary layer among a greater number of nodes, thereby lessening its effect on the values of ϕ' at the wall. In actuality then, the error of Lee et al. (1987) arose from the use of η_∞ that was not sufficiently large. Since a decrease in the step size has an effect on the accuracy of the local Nusselt number at high surface curvatures, a small $\Delta\eta$ was used in conjunction with an increase in η_∞ as was explained in the method of solution.

Numerical results from the present analysis will now be presented. Attention is first turned to the local Nusselt number. For given values of Pr and n, as the surface curvature is increased the value of $Nu_x Gr_x^{*-1/5}$ is found to increase. This can be seen in Fig. 1 which is a plot of $(Nu_x/Nu_{x,p})_{UHF}$ vs. Λ_N^* for the UHF case, where $Nu_{x,p}$ is the local Nusselt number for a vertical flat plate. This plot demonstrates that the slope of such a normalized plot is greater for lower Prandtl numbers; that is, the relative effect of surface curvature on the Nusselt number is stronger for fluids with a smaller Prandtl number. It also shows a nearly linear relationship which is useful for correlations presented later. Table 1 presents the values used in plotting Fig. 1 prior to normalization. It should be noted from the table that as the curvature increases the effect of Prandtl number on the Nusselt number diminishes. This can be explained by noting that as the curvature increases the first two terms of the energy equation become dominant and the problem becomes essentially independent of Pr.

Figure 2 is a plot of $(Nu_x/Nu_{UHF})_p$ vs. n , demonstrating the effect of n on the local Nusselt number for the vertical flat plate. It shows that a lower value of n results in a lower value of $Nu_x Gr_x^{*-1/5}$. It also shows that for an increase in the Prandtl number there is a decrease in the deviation of the Nusselt number from the UHF case.

Table 2 shows the ratio of $Nu_x/Nu_{x,UHF}$ for various values of Λ^*_N . It can be seen from the table that as the curvature increases the effect of n on Nu_x decreases and the Nusselt number ratio approaches 1.0. This can be explained again by the dominance of the first two terms in the governing equations for large values of the curvature, which essentially makes the system of equations independent of n . Table 3 lists the average Nusselt number results $Nu_L Gr_L^{*-1/5}$. For given values of Pr and n , the average Nusselt number is seen to increase as the surface curvature increases.

The $f'(\xi, 0)$ results are shown in Table 4. It can be seen that the value of $f'(\xi, 0)$ decreases as the surface curvature parameter increases. However, a decrease in $f'(\xi, 0)$ does not necessarily mean that the local wall shear stress τ_w decreases as x increases along a constant radius cylinder. Equation [26] can be rewritten as

$$\tau_w \propto \xi^{[(4+6n)/(1-n)]} f'(\xi, 0), \quad -1 \leq n < 1 \quad (45)$$

For $n \geq 0$, the power to which ξ is raised will cause τ_w to increase despite a decrease in $f'(\xi, 0)$. As n decreases, the exponent of ξ in equation (45) decreases until at $n = -2/3$ it will be 0 and the ξ term will have no effect on τ_w . Since $f'(\xi, 0)$ decreases with an increase in the surface curvature, there will be some value of n in the range $-2/3 \leq n < 0$ where τ_w will decrease with increasing x for a constant radius cylinder. Therefore, when n is negative it is possible for τ_w to decrease with increasing x . This is particularly true for low Prandtl numbers for which $f'(\xi, 0)$ decreases at a greater rate.

The observation that $f'(\xi, 0)$ decreases with increasing ξ agrees with results reported by Kuiken (1968). It is interesting to note that this trend is opposite to that for pure forced convection or for pure natural convection under the power law variation of temperature. To understand why this occurs physically, one should consider an increase in the surface curvature

parameter to imply a decrease in the radius of the cylinder at a given x location. For constant x , $T_w(x)$ is constant, and the driving force for pure free convection under the variable wall temperature condition is constant. For constant x and u_∞ the driving force for pure forced convection is constant. In these cases, as r_0 decreases the velocity near the wall increases and $f'(\xi, 0)$ increases. However for the variable heat flux case, at a constant x location, $q_w(x)$ is constant. When q_w is constant, as r_0 decreases, $T_w - T_\infty$ must decrease which will in turn decrease the magnitude of the velocity profile and $f'(\xi, 0)$. This explains why $f'(\xi, 0)$ increases for the cases of pure forced convection and for natural convection under the power law variation of surface temperature, but decreases for natural convection under the power law variation of surface heat flux.

It is recognized that there are some irregularities in the values of $f'(\xi, 0)$ in Table 4 that occur for higher Prandtl numbers. This is due to a failure to increase η_∞ appropriately in the numerical computations. Although this caused little effect in the local Nusselt number results due to the small step size used, it was found that the velocity profile, and hence the value of $f'(\xi, 0)$, were more sensitive to the choice of η_∞ . This is only logical since f' starts at zero at the wall, increases, and then returns to zero in the free stream. If η_∞ is chosen to be too small, the maximum velocity within the boundary layer will be lower than it should be. Because the momentum boundary layer is thicker than the thermal boundary layer for high Pr , errors in $f'(\xi, 0)$ will result if η_∞ is large enough for the latter, but too small for the former. This does point out the need to revise the criterion for increasing η_∞ to properly account for the boundary layer thickness in numerical calculations.

For practical applications, the local and average Nusselt number results from the present calculations in the ranges of $0 \leq \Lambda^*_N \leq 50$, $-0.5 \leq n \leq 0.5$, and $0.1 \leq Pr \leq 100$ can be correlated in the following form

$$Nu_x Gr_x^{*-1/5} = \alpha(Pr)[\Lambda(\Lambda) + f_1(Pr)\Lambda](1 + VW) \quad (46)$$

where

$$\alpha(Pr) = Pr^{2/5}(4 + 9Pr^{1/2} + 10Pr)^{-1/5} \quad (47)$$

$$\Lambda(\Lambda) = 1 + 0.09\Lambda^{1/2} \quad (48)$$

$$f_1(\text{Pr}) = (0.032 + 0.176\text{Pr}^{-0.384}) \quad (49)$$

$$V = \{[0.328 + 0.343\exp(-2.12\text{Pr}^{1/5})] - 0.195n\}n \quad (50)$$

$$W = \exp[-(0.0265 + 0.0907\text{Pr}^{-0.444})\Lambda^{0.8}] \quad (51)$$

and

$$\text{Nu}_L \text{Gr}_L^{*-1/5} = \frac{5}{4}\alpha(\text{Pr})[B(\Lambda) + f_2(\text{Pr})\Lambda](1 + \bar{V}) \quad (52)$$

where

$$B(\Lambda) = 1 + 0.08\Lambda^{1/2} \quad (53)$$

$$f_2(\text{Pr}) = (0.026 + 0.14\text{Pr}^{-0.39}) \quad (54)$$

$$\bar{V} = (4vw - n\bar{w})/(4 + n\bar{w}) \quad (55)$$

$$\bar{W} = \exp(-0.5\Lambda^{0.6}) \quad (56)$$

For notational convenience, Λ in the above equations stands for $\Lambda = \Lambda_N^* = 2\frac{x}{r_0}\text{Gr}_x^{*-1/5}$. In equations (52) - (56) Λ is calculated at $x = L$.

It is interesting to note that for the UHF case the terms V and \bar{V} in equations (46) and (52) become zero and drop out of the equations. It is also interesting to note that for the flat plate solution, i.e., $\Lambda = 0$, the terms $[A(\Lambda) + f_1(\text{Pr})\Lambda]$ and $[B(\Lambda) + f_2(\text{Pr})\Lambda]$ both become one. Therefore, for the flat plate solution under UHF, $\text{Nu}_x \text{Gr}_x^{*-1/5} = \alpha(\text{Pr})$, where $\alpha(\text{Pr})$ is taken from Fujii and Fujii (1976). The maximum error in the correlations for the local and average Nusselt numbers is less than 5% for the UHF case and less than 8.3% for the variable heat flux solution.

CONCLUSION

In this paper, the problem of natural convection in laminar boundary layer flow along slender vertical cylinders has been investigated. A finite difference method in conjunction with a cubic spline interpolation scheme is used in the numerical calculations to remove the difficulties associated with the "stiffness" of the governing equations for high values of the curvature parameter. Additionally, a smaller radial step size and a larger value of η_∞ were used to correct reported errors in the Nusselt number at high values of the curvature parameter. The major findings from these results can be summarized as follows:

(1) Errors in the thermal and velocity profiles result if the magnitude of η_∞ is insufficient. The calculated values of the local Nusselt number will be too large and those of $f''(\xi, 0)$ will be too small. These errors can be reduced by decreasing the radial step size $\Delta\eta$ or by increasing η_∞ . A decrease in the radial step size is more effective at reducing errors for the local Nusselt number but it does not correct the entire velocity and thermal profiles.

(2) For the power law variation in surface heat flux, the local surface heat transfer rate increases with increasing value of the exponent n . It also increases with increasing curvature and increasing value of Pr . However, as the curvature increases the effects of n and Prandtl number on the Nusselt number diminish.

(3) The behavior of the average Nusselt number is similar to that for the local Nusselt number for UHF. The effect of n and Pr on the average Nusselt number decreases as the curvature increases.

(4) The value of $f''(\xi, 0)$ decreases with increasing curvature, decreases with increasing n , and decreases with increasing Prandtl number. The local wall shear stress τ_w , however, increases as x increases for a constant radius cylinder with $n \geq 0$. It may decrease with increasing curvature for $n < 0$.

REFERENCES

- Burden, R. L., and Faires, J. D., 1985, Numerical Analysis, 3rd ed., Prindle, Weber and Schmidt Publishers, Boston, MA, pp. 117-129.
- Elenbaas, W., 1948, "The Dissipation of Heat by Free Convection From Vertical and Horizontal Cylinders," Journal of Applied Physics, Vol. 19, pp. 1148-1154.
- Fujii, T. and Fujii, M., 1976, "The Dependence of Local Nusselt Number in the Case of Free Convection Along a Vertical Surface With Uniform Heat Flux," International Journal of Heat and Mass Transfer, Vol. 19, pp. 121-122.
- Fujii, T. and Uehara, H., 1970, "Laminar Natural Convective Heat Transfer from the Outer Surface of a Vertical Cylinder," International Journal of Heat and Mass Transfer, Vol. 13, pp. 607-615.
- Gebhart, B., 1971, Heat Transfer, second edition, McGraw-Hill, New York, NY, pp. 340.
- Kuiken, H. K., 1968, "Axisymmetric Free Convection Boundary Layer Flow Past Slender Bodies," International Journal of Heat and Mass Transfer, Vol. 11, pp. 1141-1153.
- Lee, H. R., Chen, T.S., and Armaly, B. F., 1988, "Natural Convection Along Vertical Cylinders With Variable Surface Temperature," ASME Journal of Heat Transfer, Vol. 110, pp. 103-108.
- Lee, S. L., Chen, T. S., and Armaly, B. F., 1986a, "Mixed Convection Along Isothermal Vertical Cylinders and Needles," Proceedings of the Eighth International Heat Transfer Conference, Vol. 3, pp. 1425-1432.
- Lee, S. L., Chen, T. S., and Armaly, B. F., 1986b, "New Finite Difference Solution Methods for Wave Instability Problems," Numerical Heat Transfer, Vol. 10, pp 1-8.
- Lee, S. L., Chen, T. S., and Armaly, B. F., 1987, "Mixed Convection Along Vertical Cylinders and Needles With Uniform Surface Heat Flux," ASME Journal of Heat Transfer, Vol. 109, pp. 711-716.
- Minkowycz, W. J. and Sparrow, E. M., 1974, "Local Nonsimilar Solutions for Natural Convection on a Vertical Cylinder," ASME Journal of Heat Transfer, Vol. 96, pp. 178-183.
- Sparrow, E. M. and Gregg, J. L., 1956, "Laminar-Free-Convection Heat Transfer From the Outer Surface of a Vertical Circular Cylinder," Transactions ASME, Vol. 78, pp. 1823-1829.
- Traub, Joe F., 1964, Iterative Methods for the Solutions of Equations, Prentice Hall, Inc., Englewood Cliffs, N.J., pp. 213-214.

Table 1. The $Nu_{Gr} \star^{-1/5}$ results for Power Law Variation of the Surface Heat Flux.

ξ	$Pr = 0.1$			$Pr = 0.7$			$Pr = 7$			$Pr = 100$		
	n			n			n			n		
	-0.5	0	0.5	-0.5	0	0.5	-0.5	0	0.5	-0.5	0	0.5
0	0.1937	0.2634	0.3052	0.3673	0.4834	0.5517	0.6791	0.8699	0.9817	1.2264	1.5560	1.7489
0.5	0.2579	0.3416	0.3881	0.4338	0.5640	0.6375	0.7497	0.9533	1.0701	1.2967	1.6385	1.8361
1.0	0.4370	0.5448	0.5992	0.6228	0.7820	0.8669	0.9472	1.1809	1.3094	1.4994	1.8736	2.0844
1.5	0.7520	0.8691	0.9233	0.9108	1.1013	1.1997	1.2504	1.5135	1.6482	1.8158	2.2352	2.4639
2.0	1.2436	1.3243	1.3661	1.2859	1.5052	1.6143	1.6306	1.9828	2.1434	2.2212	2.6904	2.9403
2.5	1.8517	1.8971	1.9252	1.7690	2.0068	2.1158	2.1091	2.4967	2.6805	2.6882	3.2133	3.4882
3.0	2.5546	2.5789	2.5966	2.4354	2.6321	2.7241	2.6564	3.0592	3.2664	3.3141	3.8831	4.1922
3.5	3.3546	3.3666	3.3769	3.2846	3.3915	3.4561	3.2483	3.6970	3.9225	3.9592	4.6065	4.9329
4.0	4.2554	4.2626	4.2691	4.2249	4.2757	4.3173	3.9665	4.4554	4.6793	4.7318	5.4551	5.7807
4.5	5.2719	5.2756	5.2791	5.2532	5.2828	5.3094	4.9552	5.3785	5.5723	5.5524	6.3389	6.7196
5.0	6.4191	6.4224	6.4252	6.4093	6.4271	6.4447	6.2231	6.4791	6.6276	6.4725	7.3556	7.7619

Table 2. The $Nu_x/Nu_{x,CHF}$ results for Power Law Variation of the Surface Heat Flux.

ξ	Pr = 0.1			Pr = 0.7			Pr = 7			Pr = 100		
	n			n			n			n		
	-0.5	0.25	0.5	-0.5	0.25	0.5	-0.5	0.25	0.5	-0.5	0.25	0.5
0	0.7353	1.0872	1.1584	0.7597	1.0778	1.1412	0.7806	1.0707	1.1285	0.7882	1.0682	1.1240
0.5	0.7551	1.0758	1.1361	0.7692	1.0923	1.1303	0.7864	1.0678	1.1226	0.7914	1.0664	1.1206
1.0	0.8021	1.0562	1.0998	0.7964	1.0607	1.1085	0.8021	1.0604	1.1088	0.8003	1.0622	1.1125
1.5	0.8652	1.0352	1.0623	0.8270	1.0504	1.0893	0.8262	1.0471	1.0890	0.8124	1.0568	1.1023
2.0	0.9391	1.0174	1.0316	0.8543	1.0411	1.0725	0.8224	1.0443	1.0810	0.8256	1.0519	1.0929
2.5	0.9761	1.0080	1.0148	0.8815	1.0307	1.0543	0.8448	1.0414	1.0736	0.8535	1.0479	1.0856
3.0	0.9905	1.0036	1.0069	0.9253	1.0195	1.0350	0.8683	1.0383	1.0677	0.8535	1.0432	1.0796
3.5	0.9964	1.0016	1.0031	0.9685	1.0102	1.0190	0.8786	1.0345	1.0610	0.8595	1.0405	1.0709
4.0	0.9983	1.0008	1.0015	0.9881	1.0051	1.0097	0.8903	1.0285	1.0503	0.8674	1.0341	1.0597
4.5	0.9993	1.0003	1.0007	0.9944	1.0026	1.0050	0.9213	1.0200	1.0360	0.8759	1.0292	1.0601
5.0	0.9995	1.0002	1.0004	0.9972	1.0014	1.0027	0.9605	1.0124	1.0229	0.8799	1.0320	1.0552

Table 3. The $Nu_L Gr_L^{*1/5}$ results for Power Law Variation of the Surface Heat Flux.

ξ_L	Pr = 0.1			Pr = 0.7			Pr = 7			Pr = 100		
	n			n			n			n		
	-0.5	0	0.5	-0.5	0	0.5	-0.5	0	0.5	-0.5	0	0.5
0	0.3818	0.4543	0.4678	0.7239	0.8338	0.8457	1.339	1.500	1.505	2.417	2.6814	2.6810
0.5	0.4710	0.5637	0.6039	0.8162	0.9466	0.9983	1.436	1.617	1.683	2.515	2.801	2.896
1.0	0.7218	0.8494	0.8805	1.081	1.252	1.288	1.714	1.936	1.966	2.797	3.125	3.154
1.5	1.141	1.297	1.328	1.490	1.706	1.753	2.140	2.403	2.439	3.244	3.634	3.678
2.0	1.794	1.926	1.940	2.026	2.279	2.334	2.691	3.063	3.123	3.828	4.286	4.347
2.5	2.649	2.724	2.715	2.688	2.979	3.032	3.366	3.816	3.890	4.516	5.042	5.120
3.0	3.654	3.677	3.645	3.544	3.833	3.870	4.157	4.634	4.718	5.335	5.961	6.054
3.5	4.796	4.778	4.727	4.646	4.868	4.874	5.035	5.538	5.635	6.305	7.011	7.137
4.0	6.075	6.027	5.961	5.953	6.077	6.054	6.008	6.569	6.677	7.373	8.163	8.293
4.5	7.499	7.430	7.355	7.409	7.459	7.414	7.198	7.786	7.887	8.562	9.431	9.609
5.0	9.080	9.000	8.924	9.015	9.018	8.963	8.696	9.226	9.308	9.859	10.850	11.046

Table 4. The $f''(\xi, 0)$ results for Power Law Variation of the Surface Heat Flux.

ξ	$Pr = 0.1$				$Pr = 0.7$				$Pr = 7$				$Pr = 100$			
	n				n				n				n			
	-0.5	0	0.5		-0.5	0	0.5		-0.5	0	0.5		-0.5	0	0.5	
0	2.3303	1.6380	1.3490		1.1450	.82119	.68338		.48311	.35101	.29396		.17507	.12768	.10720	
0.5	2.0150	1.4198	1.1750		1.0730	.76919	.64097		.46844	.34040	.28527		.17202	.12546	.10538	
1.0	1.6152	1.1557	0.9659		0.9513	.69076	.57706		.43973	.31947	.26803		.16492	.12036	.10124	
1.5	1.3210	0.9638	0.8169		0.8731	.64439	.53802		.41807	.29835	.24687		.15714	.11483	.09672	
2.0	1.0204	0.7884	0.6867		0.8252	.60494	.50589		.39810	.30110	.25149		.15012	.10969	.09245	
2.5	0.7548	0.6216	0.5584		0.7437	.53913	.45839		.38654	.29778	.24910		.14260	.10369	.08749	
3.0	0.5245	0.4676	0.4364		0.5739	.44098	.39028		.38189	.28608	.23981		.14589	.10132	.08597	
3.5	0.3642	0.3471	0.3344		0.3864	.33966	.31562		.36026	.26358	.22336		.13914	.10132	.08597	
4.0	0.2683	0.2626	0.2576		0.2734	.26021	.25019		.30948	.23025	.20054		.14346	.10406	.08563	
4.5	0.2063	0.2041	0.2020		0.2081	.20323	.19897		.23993	.19260	.17413		.14305	.10225	.08680	
5.0	0.1637	0.1627	0.1618		0.1644	.16237	.16048		.17725	.15837	.14845		.14317	.10149	.08713	

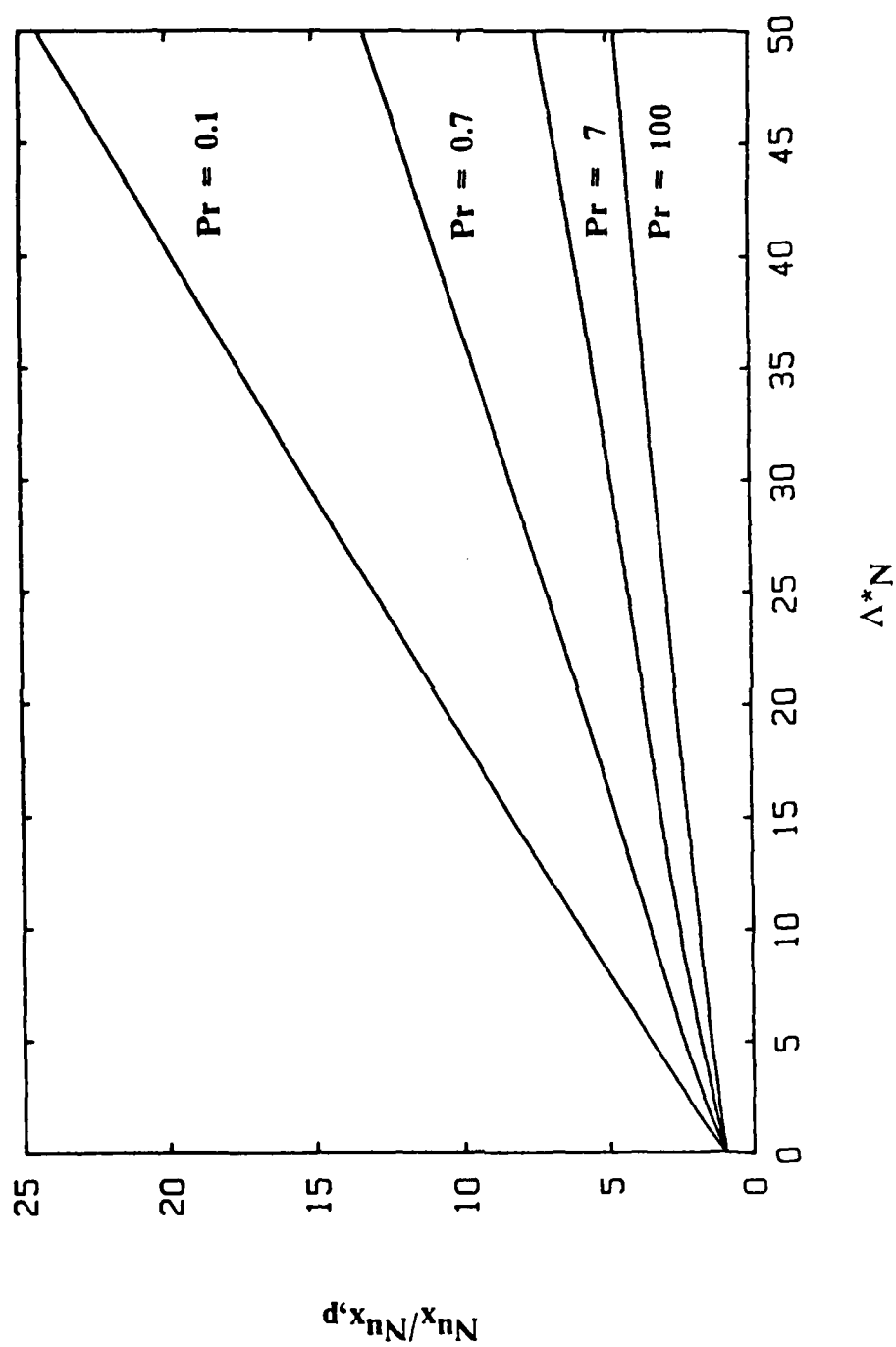


Figure 1. $Nu_x/Nu_{x,p}$ vs. Λ^*_N , Uniform Surface Heat Flux ($n=0$).

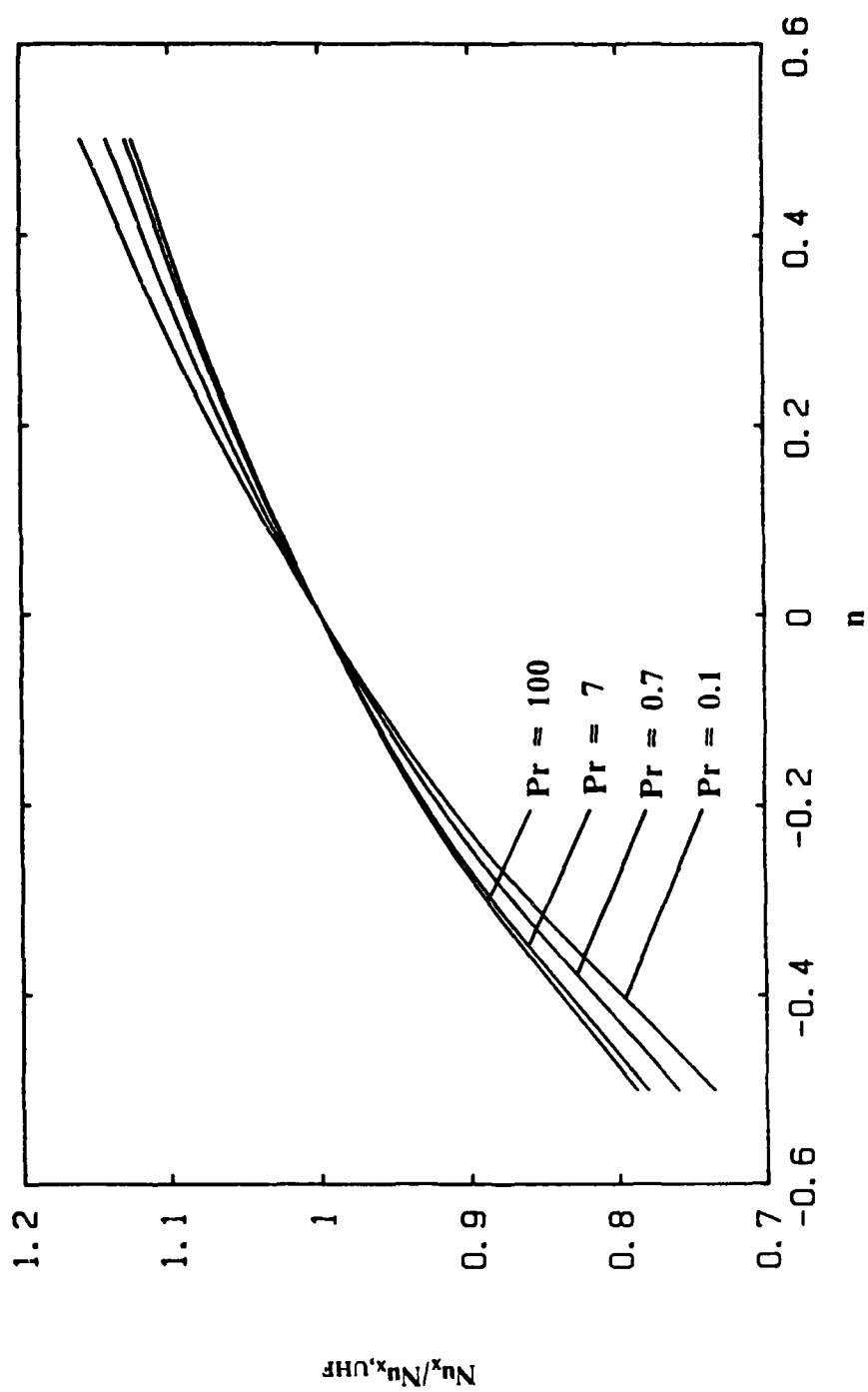


Figure 2. $Nu_x / Nu_{x,UHF}$ vs. n , Flat Plate ($\Lambda_N^* = 0$).

III. MIXED CONVECTION ALONG A VERTICAL CYLINDER WITH VARIABLE WALL TEMPERATURE

MIXED CONVECTION ALONG A VERTICAL CYLINDER WITH VARIABLE SURFACE TEMPERATURE

by

J. J. Heckel, T. S. Chen, and B. F. Armaly

Department of Mechanical and Aerospace Engineering

University of Missouri-Rolla, Rolla, MO 65401

ABSTRACT

Mixed convection in laminar boundary layer flow along slender vertical cylinders is analyzed for the situation in which the surface temperature $T_w(x)$ varies arbitrarily with the axial coordinate x . It covers the entire mixed convection regime from pure free convection ($\chi = 0$) to pure forced convection ($\chi = 1$), where $\chi = [1 + (Gr_x/Re_x^2)^{1/4}]^{-1}$ is the mixed convection parameter. The governing boundary layer equations along with the boundary conditions are first cast into a dimensionless form by a nonsimilar transformation and the resulting system of equations is then solved by a weighted finite-difference method of solution in conjunction with cubic spline interpolation. Sample calculations were performed for the case of power law variation in surface temperature, $T_w(x) - T_\infty = ax^n$, for fluids with Prandtl numbers of 0.1, 0.7, 7, and 100 over a wide range of values for the surface curvature parameter $0 \leq \Lambda \leq 50$ (or $0 \leq \xi \leq 5$). Local and average Nusselt numbers as well as the local wall shear stress are presented. It is found that the local Nusselt number in the form $Nu_x/(Re_x^{1/2} + Gr_x^{1/4})$ increases with increasing surface curvature, Prandtl number, and the exponent n . For low values of constant curvature Λ , the local Nusselt number initially decreases and then increases as χ goes from 0 to 1. As curvature increases a linear relationship is found to exist between the Nusselt number and the mixed convection parameter, particularly for low Prandtl numbers. The velocity gradient at the wall is found to increase with increasing curvature, decreasing Prandtl number, and decreasing n . Correlation equations for the local and average Nusselt numbers are also presented.

NOMENCLATURE

C_{f_x}	local skin friction coefficient, $2\tau_w/\rho u_\infty^2$
C_{f_L}	average skin friction coefficient, $(2/\rho u_\infty^2 L) \int_0^L \tau_w dx$
f	reduced stream function, $(\psi/\nu r_0)(Re_x^{1/2} + Gr_x^{1/4})^{-1}$
g	$\partial f/\partial \eta$ or gravitational acceleration
Gr_x	local Grashof number, $g\beta[T_w(x) - T_\infty]x^3/\nu^2$
Gr_x^*	modified local Grashof number, $g\beta q_w(x)x^4/k\nu^2$
Gr_L, Gr_0	Grashof numbers defined, respectively, as $g\beta[T_w(L) - T_\infty]L^3/\nu^2$ and $g\beta[T_w(r_0) - T_\infty]r_0^3/\nu^2$
h	local heat transfer coefficient, $q_w/(T_w - T_\infty)$
\bar{h}	average heat transfer coefficient
k	thermal conductivity of the fluid
L	an arbitrary length of cylinder
m	exponent used in the mixed convection correlation
n	exponent in the power law variation of the surface temperature or surface heat flux
Nu_x	local Nusselt number, hx/k
\overline{Nu}_L	average Nusselt number, $\bar{h}L/k$
Pr	Prandtl number, ν/α
r	radial coordinate
r_0	radius of the cylinder
Re_x	Reynolds number based on x , $u_\infty x/\nu$
Re_L, Re_0	Reynolds number based on L and r_0 , respectively, as $u_\infty L/\nu$ and $u_\infty r_0/\nu$
T	fluid temperature
u	axial velocity component
v	radial velocity component
x	axial coordinate
y	transverse coordinate
z	dimensionless axial coordinate, x/r_0
α	thermal diffusivity

β	volumetric coefficient of thermal expansion
γ	variable temperature parameter, $[x/(T_w - T_\infty)][d(T_w - T_\infty)/dx]$
η	pseudo-similarity variable, $[(r^2 - r_o^2)/2r_o x](Re_x^{1/2} + Gr_x^{1/4})$
θ	dimensionless temperature, $(T - T_\infty)/(T_w(x) - T_\infty)$
Λ_N	curvature parameter for natural convection with variable surface temperature, $(2x/r_o)Gr_x^{-1/4}$
Λ_N^*	modified curvature parameter for natural convection with variable surface heat flux, $(2x/r_o)Gr_x^{*-1/5}$
Λ_F	curvature parameter for pure forced convection, $(2x/r_o)Re_x^{-1/2}$
Λ	curvature parameter for mixed convection with variable surface temperature, $(2x/r_o)(Re_x^{1/2} + Gr_x^{1/4})^{-1}$
Λ^*	curvature parameter for mixed convection with variable surface heat flux, $(2x/r_o)(Re_x^{1/2} + Gr_x^{*1/5})^{-1}$
μ	dynamic viscosity
ν	kinematic viscosity
ξ	dimensionless axial coordinate, $[\Lambda/(2\chi)]^{1/2}$ or $[x/(r_o Re_o)]^{1/4}$
ρ	fluid density
τ_w	local wall shear stress
ψ	stream function
χ	mixed convection parameter for variable surface temperature, $(1 + \Omega_x^{1/4})^{-1}$
χ^*	mixed convection parameter for variable surface heat flux, $(1 + \Omega_x^{*1/5})^{-1}$
Ω_x	buoyancy parameter for variable surface temperature, Gr_x/Re_x^2
Ω_x^*	buoyancy parameter for variable surface heat flux, $Gr_x^*/Re_x^{5/2}$
Ω_o	modified buoyancy parameter, $[Gr_o/Re_o^{(1-n)}]^{1/4}$
ω	relaxation factor

Subscripts

F	for the case of pure forced convection
N	for the case of pure natural convection
o	quantities at $\xi = \Delta\xi$
p	for a flat plate

w conditions at the wall
 ∞ condition at the free stream

INTRODUCTION

There have been relatively few studies on mixed convection along a vertical cylinder. Chen and Mucoglu [1, 2] were the first to analyze the effects of buoyancy forces on forced convection along vertical cylinders for the case of uniform wall temperature (UWT) and uniform surface heat flux (UHF). They used the local nonsimilarity method of solution to obtain heat transfer results that cover the surface curvature parameter, $\Lambda_F = 2 \frac{x}{r_0} \text{Re}_x^{-1/2}$, from 0 to 8 for Prandtl numbers of 0.7 and 7. Bui and Cebeci [3] analyzed the UWT case for $\text{Pr} = 0.1, 1.0$, and 10 for curvatures up to $\Lambda_F = 10$ using a central difference finite-difference method of solution. The studies by Chen and Mucoglu [1] and by Bui and Cebeci for the UWT case used a mixed convection parameter $\Omega_x = \text{Gr}_x / \text{Re}_x^2$ which varies from zero for pure forced convection to infinity for pure free convection. Mucoglu and Chen [2] presented the UHF case with a mixed convection parameter $\Omega_x^* = \text{Gr}_x^* / \text{Re}_x^{5/2}$. Lee et al. [4] treated the UWT case for slender cylinders using a new mixed convection parameter $\chi = (1 + \Omega_x^{1/4})^{-1}$ which varies from zero for pure free convection to one for pure forced convection. In Lee et al. [5] the UHF case is presented using $\chi^* = (1 + \Omega_x^{*1/5})^{-1}$ which also varies from zero for pure free convection to one for pure forced convection. The main difficulty encountered in these studies has been the numerical solutions for large surface curvatures. The results of Chen and Mucoglu [1, 2] agree well with those of Lee et al. [4, 5] up to surface curvatures $\Lambda = 2 \frac{x}{r_0} (\text{Re}_x^{1/2} + \text{Gr}_x^{1/4})^{-1}$ for UWT or $\Lambda^* = 2 \frac{x}{r_0} (\text{Re}_x^{1/2} + \text{Gr}_x^{*1/5})^{-1}$ for UHF of 8 for $\text{Pr} = 0.7$ and 7.0. The results of Bui and Cebeci are about 36 percent higher for large values of the surface curvature and Lee et al. [4] attributed this to the latter's use of a central difference finite-difference method of solution which has difficulty handling the boundary layer equations as they become "stiff" with increasing curvature. Lee et al. [4, 5] advocates the use of a weighted difference finite-difference method [6] along with a cubic spline interpolation method [7] to overcome these difficulties associated with high values of curvature or Prandtl number.

Another advantage of the method used by Lee et al. [4, 5] was that it was applied to the full range of mixed convection to include pure free convection. The case of natural convection along a vertical cylinder has been extensively studied [8 – 13]. Elenbaas [8] used Langmuir's stagnant film model to evaluate the heat transfer coefficients for vertical cylinders under UWT

conditons. Sparrow and Gregg [9] reworked this same problem using a power series solution for $Pr = 0.72$ and 1 covering surface curvatures ($\Lambda_N = 2\frac{x}{r_0}Gr_x^{-1/4}$) of about 1.5. Kuiken [10] also applied the power series expansion method to investigate some nonuniform wall temperature conditions and obtained results for $0.7 \leq Pr \leq 10$. Similarly, Fujii and Uehara [11] treated the case of variable wall temperature and obtained results, again by the power series solution, for $0.72 \leq Pr \leq 100$ covering Λ_N from 0 to 2.73. To overcome truncation errors of the power series and the local similarity solution, Minkowycz and Sparrow [12] employed the local nonsimilarity method of solution and obtained results for $Pr = 0.733$ covering $0 \leq \Lambda_N \leq 10$. Lee et al. [4, 5] examined both the UWT and UHF cases of natural convection along a vertical cylinder as part of their mixed convection study and employed a modified finite-difference method designed to overcome the difficulties associated with increasing curvature. As a result, they were able to obtain results up to $\Lambda_N = 50$ for $0.1 \leq Pr \leq 100$. Very recently, Lee et al. [13] treated the variable wall temperature problem for natural convection along a vertical cylinder. They found that the results of [4] were inaccurate for $\Lambda_N > 10$ because an improper step size was used in the radial direction.

The significant finding for pure forced or pure free convection under a variation in surface temperature along a vertical cylinder is that as the surface curvature increases at a given x location both the heat transfer coefficient and the skin friction increase. For the UHF case of natural convection, as the surface curvature at a given x location increases, the heat transfer coefficient also increases, but the local wall shear stress decreases. Minkowycz and Sparrow [12] showed that the error caused by the power series solution increases with increasing curvature. Results by Lee et al. [13] showed that the results of Fujii and Uehara [11] are valid only for Λ_N up to about 1.5. Lee et al. [4] demonstrated that the central difference scheme used by Bui and Cebeci [3] produces large errors as the curvature increases, but the results of [4, 5] for $\Lambda > 10$ are not accurate because they used too large a step size in the radial direction.

For comparison purposes, results for mixed convection along a vertical flat plate are needed. There are numerous studies on mixed convection along a vertical flat plate (see, for example, [14] – [19]). The Nusselt number results for this flow geometry have been correlated by Churchill [20] using the simple form $Nu^m = Nu_F^m + Nu_N^m$, with $m = 3$, where Nu_F is the

Nusselt number for pure forced convection and Nu_N is the Nusselt number for pure free convection. Chen et al. [14] have carried out extensive correlations for mixed convection along vertical, inclined, and horizontal flat plates and verified them with experimental data for air.

From the past studies, it is clear that results for mixed convection under UWT conditions at high values of curvature need to be reassessed. In addition, the combined effects of variable surface temperature and curvature on the flow and heat transfer for mixed convection along slender vertical cylinders have not been studied for the entire mixed convection regime. This has motivated the present study. It is noted that free convection along slender vertical cylinders has been analyzed for the case of power law variation in the wall temperature. Details of this analysis can be found in [13] and for completeness its highlights are also given in Appendix C. Some results for this problem were obtained and will be discussed later. An analysis of the mixed convection problem under a power law variation in the wall temperature follows.

ANALYSIS

Consider a semi-infinite, vertical cylinder with radius r_0 that is aligned parallel to a uniform, laminar free stream with velocity u_∞ and temperature T_∞ . The axial coordinate x is measured in the direction of the forced flow and the radial coordinate r is measured from the axis of the cylinder. The surface of the cylinder is subjected to an arbitrary variation in temperature $T_w(x)$, and the gravitational acceleration g is acting downward. Fluid properties are assumed to be constant except for variations in density which induce the buoyancy force. By employing the laminar boundary layer assumptions and making use of the Boussinesq approximation, the governing conservation equations can be written as:

Continuity:

$$\frac{\partial}{\partial x}(ru) + \frac{\partial}{\partial r}(rv) = 0 \quad (1)$$

Momentum:

$$u \frac{\partial u}{\partial x} + v \frac{\partial u}{\partial r} = \frac{\nu}{r} \frac{\partial}{\partial r} \left(r \frac{\partial u}{\partial r} \right) \pm g\beta(T - T_\infty) \quad (2)$$

Energy:

$$u \frac{\partial T}{\partial x} + v \frac{\partial T}{\partial r} = \frac{\alpha}{r} \frac{\partial}{\partial r} \left(r \frac{\partial T}{\partial r} \right) \quad (3)$$

The positive sign in equation (2) applies to upward forced flow and the negative sign to downward forced flow. In these equations, u and v are the velocity components in the x and r directions, respectively; T is the fluid temperature; and ν , β and α are, respectively, the kinematic viscosity, the volumetric coefficient of thermal expansion, and the thermal diffusivity of the fluid.

The boundary conditions are

$$u = v = 0, \quad T = T_w(x) \quad \text{at } r = r_o \quad (4)$$

$$u \rightarrow 0, \quad T \rightarrow T_\infty \quad \text{As } r \rightarrow \infty \quad (5)$$

$$u = 0, \quad T = T_\infty \quad \text{At } x = 0, r \geq r_o \quad (6)$$

In writing equation (6) it is assumed that the flow and thermal boundary layer thicknesses are zero at the leading edge of the cylinder surface.

The conservation equations and the boundary conditions, are then transformed into a dimensionless form by introducing the following dimensionless variables:

$$\eta = \frac{[r^2 - r_o^2]}{2r_o x} (\text{Re}_x^{1/2} + \text{Gr}_x^{1/4}), \quad z = \frac{x}{r_o} \quad (7)$$

$$f(z, \eta) = \psi(x, r) / [\nu r_o (\text{Re}_x^{1/2} + \text{Gr}_x^{1/4})], \quad \theta(z, \eta) = (T - T_\infty) / [T_w(x) - T_\infty] \quad (8)$$

$$\Omega_x = \frac{\text{Gr}_x}{\text{Re}_x^2}, \quad \chi = (1 + \Omega_x^{1/4})^{-1} \quad (9)$$

where $\text{Gr}_x = g\beta[T_w(x) - T_\infty]x^3/\nu^2$ is the local Grashof number, $\text{Re}_x = u_\infty x/\nu$ is the local Reynolds number, η is the pseudo-similarity variable, z is the dimensionless axial coordinate, $f(z, \eta)$ is the reduced stream function, $\theta(z, \eta)$ is the dimensionless temperature, $\psi(x, r)$ is the

stream function that satisfies the continuity equation, with $u = (\partial\psi/\partial r)/r$ and $v = -(\partial\psi/\partial x)/r$, Ω_x is the buoyancy parameter which varies from zero for pure forced convection to infinity for pure free convection, and χ is the mixed convection parameter which varies from zero for pure free convection to one for pure forced convection.

The transformation yields:

$$(1 + \eta\Lambda)f''' + \Lambda f'' + \frac{1}{4}(2 + (1 - \chi)(\gamma + 1))ff'' - \frac{1}{2}(1 - \chi)(\gamma + 1)f'^2 \pm (1 - \chi)^4\theta = -z\left(f'\frac{\partial f}{\partial z} - f\frac{\partial f'}{\partial z}\right) \quad (10)$$

$$(1 + \eta\Lambda)\theta'' + \Lambda\theta' + \frac{Pr}{4}(2 + (1 - \chi)(\gamma + 1))f\theta' - Pr\gamma f'\theta = -Prz\left(\theta'\frac{\partial f}{\partial z} - f\frac{\partial \theta}{\partial z}\right) \quad (11)$$

$$\begin{aligned} f(z, 0) = f'(z, 0) = 0, \quad \theta(z, 0) = 1 \\ f'(z, \infty) = \chi^2, \quad \theta(z, \infty) = 0 \end{aligned} \quad (12)$$

where

$$\Lambda = 2\frac{x}{r_0}(\text{Re}_x^{1/2} + \text{Gr}_x^{1/4})^{-1} \quad (13)$$

is the mixed convection curvature parameter and

$$\gamma = \frac{x}{T_w(x) - T_\infty} \frac{d}{dx} [T_w(x) - T_\infty] \quad (14)$$

The primes in equations (10)-(12) denote partial differentiation with respect to η , and the plus and minus signs in front of the term $(1 - \chi)^4\theta$ in equation (10) now represent buoyancy assisting flow and buoyancy opposing flow, respectively.

The system of equations (10)-(12) represents the general form of the transformed boundary layer equations for variable wall temperature $T_w(x)$ along vertical cylinders in mixed convection. For the case of power law wall temperature distribution, $T_w(x) = T_\infty + ax^n$, one has from equation (14) that

$$\gamma = n \quad (15)$$

Equations (10)-(12) contain three x -dependent parameters, $z(x)$, $\Lambda(x)$, and $\chi(x)$. These parameters can be related to a single x -dependent parameter $\xi(x)$ defined by

$$\xi = \left(\frac{z}{\text{Re}_0} \right)^{1/4}, \quad z = x/r_0 \quad (16)$$

Thus,

$$\Lambda = 2 \xi^2 \chi, \quad \chi = (1 + \Omega_0 \xi^{(1+n)})^{-1} \quad (17)$$

where

$$\Omega_0 = [\text{Gr}_0/\text{Re}_0^{1-n}]^{1/4} \quad (18)$$

with $\text{Gr}_0 = \text{Gr}_x$ and $\text{Re}_0 = \text{Re}_x$ for $x = r_0$. Also, the right-hand sides of equations (10) and (11) become, respectively

$$-\frac{1}{4}\xi \left(f' \frac{\partial f}{\partial \xi} - f \frac{\partial f'}{\partial \xi} \right), \quad -\frac{\text{Pr}}{4}\xi \left(\theta' \frac{\partial f}{\partial \xi} - f \frac{\partial \theta}{\partial \xi} \right) \quad (19)$$

Rewriting equations (10)-(12) one has

Momentum:

$$(1 + a_1 \eta) f''' + a_1 f'' + a_2 f f' + a_3 f'^2 + a_4 \theta = a_5 \left(f' \frac{\partial f}{\partial \xi} - f \frac{\partial f'}{\partial \xi} \right) \quad (20)$$

Energy:

$$(1 + a_1 \eta) \theta'' + a_1 \theta' + \text{Pr } a_2 f \theta' + \text{Pr } a_6 f' \theta = \text{Pr } a_5 \left(\theta' \frac{\partial f}{\partial \xi} - f \frac{\partial \theta}{\partial \xi} \right) \quad (21)$$

Boundary Conditions :

$$\begin{aligned} f(\xi, 0) = f'(\xi, 0) = 0, \quad \theta(\xi, 0) = 1 \\ f'(\xi, \infty) = a_7, \quad \theta(\xi, \infty) = 0 \end{aligned} \quad (22)$$

where

$$\begin{aligned} a_1 &= \Lambda, & a_2 &= \frac{1}{4}(2 + (1 - \chi)(n + 1)), & a_3 &= \frac{1}{2}(\chi - 1)(n + 1) \\ a_4 &= \pm (1 - \chi)^4, & a_5 &= -\xi/4, & a_6 &= -n, & a_7 &= \chi^2 \end{aligned} \quad (23)$$

With Λ and χ related to ξ , the functions f and θ in equation (20)-(22) are functions of (ξ, η) and depend on three constant parameters n , Pr , and Ω_0 . These equations are now in the form that can be solved by the method proposed by Lee et al. [6]. See Appendix E for the solution method as applied to equations (20)-(22). For the purpose of comparisons, the problem of mixed convection along a vertical flat plate with a power law variation in the wall temperature is also solved. The governing equations and boundary conditions have exactly the same form as equations (20)-(23) with the exceptions that for this case

$$\begin{aligned} \eta &= \left(\frac{y}{x}\right)(Re_x^{1/2} + Gr_x^{1/4}) \\ \xi &= \chi, & \Lambda &= 0, & a_5 &= (1 + n)(1 - \chi)\chi/4 \end{aligned} \quad (24)$$

It should be noted that this problem must be solved numerically from $\xi = 1$ to $\xi = 0$.

The physical quantities of interest include the local and average Nusselt numbers, the local and average friction factors, the axial velocity distribution, and the temperature profile. The local Nusselt number and the local friction factor can be expressed as

$$Nu_x / (Re_x^{1/2} + Gr_x^{1/4}) = -\theta'(\xi, 0) \quad (25)$$

$$C_{fx} = \frac{2\tau_w}{\rho u_\infty^2} = 2\chi^{-3}\Gamma'(\xi, 0)Re_x^{-1/2} \quad (26)$$

The average Nusselt number and the average friction factor can be expressed as

$$\overline{Nu}_L / (Re_L^{1/2} + Gr_L^{1/4}) = -4\chi_L \xi_L^{-2} \int_0^{\xi_L} \frac{\theta'(\xi, 0)}{\chi} \xi d\xi \quad (27)$$

$$C_{fL} Re_L^{1/2} = 8\xi_L^{-2} \int_0^{\xi_L} \chi^{-3}\Gamma'(\xi, 0)\xi d\xi \quad (28)$$

where $\xi_L = \xi$ at $x = L$, and $\chi_L = \chi$ at $x = L$. The axial velocity distribution can be written as

$$\frac{u}{u_\infty} = \frac{f'(\xi, \eta)}{\chi^2} \quad (29)$$

and the temperature profile is given by $\theta(\xi, \eta) = (T - T_\infty)/(T_w - T_\infty)$.

METHOD OF SOLUTION

Equations (20)-(22) constitute a system of coupled nonlinear partial differential equations in the (ξ, η) coordinates with parameters Pr, n, Ω_0 . The solution method described in [6] was employed to solve this system of equations.

The first step is to convert the terms involving $\partial/\partial\xi$ in the following manner.

$$\frac{\partial H}{\partial \xi} = \frac{p}{\Delta \xi} (H - H_0) - q \left(\frac{\partial H}{\partial \xi} \right)_0 = \frac{p}{\Delta \xi} (H - \bar{H}_0) \quad (30)$$

where H is a function of (ξ, η) , $\bar{H}_0 = H_0 + (q/p)\Delta\xi(\partial H/\partial\xi)_0$, and the subscript "o" denotes quantities at $\xi - \Delta\xi$. The values for p and q are $p=1$ and $q=0$ at $\xi=0$ and $\xi=\Delta\xi$, and $p=2$ and $q=1$ thereafter for $\xi \geq 2\Delta\xi$. The f and θ equations are then linearized by using the simple technique for the product of two arbitrary functions F and G , defined as

$$FG = \tilde{F}G + \tilde{G}F - \tilde{F}\tilde{G} \quad (31)$$

where \tilde{F} and \tilde{G} indicate the values to be guessed. The quasi-linearized function FG expressed by equation (31) will provide quadratic and monotone convergence. By employing equation (30) for the terms $\frac{\partial f}{\partial \xi}$, $\frac{\partial f'}{\partial \xi}$ and $\frac{\partial \theta}{\partial \xi}$ and applying equation (31) to the terms ff' , f^2 , $f\theta'$ and $f\theta$ one obtains

$$A_0 f''' + (a_1 + A_1) f'' + A_2 f' + A_3 f + A_4 \theta = A_5 \quad (32)$$

$$B_0 \theta'' + (a_1 + B_1) \theta' + B_2 \theta + B_3 f' + B_4 f = B_5 \quad (33)$$

where

$$\begin{aligned}
A_0 &= 1 + a_1 \eta, & A_1 &= a^* \tilde{f} + d^* \tilde{f}_0, & A_2 &= 2b^* \tilde{f}' - d^* \tilde{f}_0' \\
A_3 &= a^* \tilde{f}'', & A_4 &= a_4, & A_5 &= a^* \tilde{f} \tilde{f}'' + b^* \tilde{f}'^2
\end{aligned} \tag{34}$$

$$\begin{aligned}
B_0 &= A_0, & B_1 &= \text{Pr } A_1, & B_2 &= \text{Pr } e^* \tilde{f}', & B_3 &= \text{Pr } (e^* \tilde{\theta} - d^* \tilde{\theta}_0) \\
B_4 &= \text{Pr } a^* \tilde{\theta}', & B_5 &= \text{Pr } (a^* \tilde{f} \tilde{\theta}' + e^* \tilde{f}' \tilde{\theta})
\end{aligned} \tag{35}$$

$$a^* = a_2 - d^*, \quad b^* = a_3 + d^*, \quad d^* = a_5 p / \Delta \xi, \quad e^* = a_6 + d^* \tag{36}$$

The coefficients a_i through a_6 and the functions \tilde{f}_0 , \tilde{f}_0' , and $\tilde{\theta}_0$ are as previously defined.

The f and θ equations have now been reduced to a system of quasi-linear ordinary differential equations. By defining $g = f'$ and applying the weighting factors (see Lee et al. [6]), one can write equations (32) and (33) in the finite difference form as:

$$f_i - f_{i-1} - (\Delta \eta / 2)(g_i + g_{i-1}) = 0 \tag{37}$$

$$A_0 / (\Delta \eta)^2 (\alpha_{-1} g_{i-1} + \alpha_0 g_i + \alpha_{+1} g_{i+1}) + A_2 g_i + A_3 f_i + A_4 \theta_i = A_5 \tag{38}$$

$$B_0 / (\Delta \eta)^2 (\beta_{-1} \theta_{i-1} + \beta_0 \theta_i + \beta_{+1} \theta_{i+1}) + B_2 \theta_i + B_3 g_i + B_4 f_i = B_5 \tag{39}$$

where $\Delta \eta$ is the step size in the η direction and the subscript "i" refers to values at the nodal point η_i .

In equations (38) and (39) the weighting factors are defined as:

$$\begin{aligned}
\alpha_{-1} &= W_f(-z_{i-1/2}), & \alpha_{+1} &= W_f(z_{i+1/2}), & \alpha_0 &= -\alpha_{-1} - \alpha_{+1} \\
\beta_{-1} &= W_\theta(-z^*_{i-1/2}), & \beta_{+1} &= W_\theta(z^*_{i+1/2}), & \beta_0 &= -\beta_{-1} - \beta_{+1} \\
W_f(z) &= z / [1 - \exp(-z)], & z &= \Delta \eta (a_1 + A_1) / A_0, & z^* &= \Delta \eta (a_1 + B_1) / B_0
\end{aligned} \tag{40}$$

Equations (37)-(40) are applied to the interior points. On the boundaries, equation (22) applies such that

$$\begin{aligned} f_1 = g_1 = 0, \quad \theta_1 = 1 \\ f_n - f_{n-1} - \frac{\Delta\eta}{2}(g_n + g_{n-1}) = \theta_n = 0, \quad g_n = a_7 \end{aligned} \quad (41)$$

where the subscript n is the number of nodes in the η direction and $a_7 = \chi^2$ for mixed convection.

Equations (37)-(41) constitute a system of algebraic equations that can be written in the matrix form

$$[A][X] = [B] \quad (42)$$

where $[A]$ is a band matrix of order $3n$ and bandwidth seven. The array $[X]$ which contains the solution in the form $(f_1, g_1, \theta_1, f_2, g_2, \theta_2, \dots, f_n, g_n, \theta_n)^T$ is a column matrix of order $3n$. The matrix $[B]$ is a column matrix of order $3n$ which contains the right hand sides of equations (37)-(39) and (41). The matrix $[A]$ is approximately diagonally dominant and equation (42) can be solved by the Gaussian elimination technique with high accuracy.

To obtain values for f'' and θ' , the results for f and θ along with the boundary conditions

$$f'''(\xi, 0) = -a_1 \tilde{f}''(\xi, 0) - a_4, \quad \theta''(\xi, 0) = -a_1 \tilde{\theta}'(\xi, 0), \quad f'''(\xi, \infty) = \theta''(\xi, \infty) = 0 \quad (43)$$

are used in a cubic spline interpolation routine (see, for example, Burden and Faires [7]). As the solution converges, the boundary conditions become exact and the values for f'' and θ' can be obtained with high accuracy.

The present method of solution employs a quasi-linearization of the original nonlinear system of equations and requires initial guesses for f , f' , f'' , θ , and θ' . The flat plate solution (i.e., $\xi = 0$) for the uniform wall temperature case (UWT) for $Pr = 0.7$ was obtained and these results were used as the initial guesses for all other combinations of Pr , n , and Ω_0 at $\xi = 0$. For $\xi \geq \Delta\xi$, good convergence was obtained by simply letting the solution at the previous node be the guesses for the next node.

The solution method is an iterative scheme. A solution was considered to be convergent when the calculated values for f , f' , and θ differed from the last guess of the respective values by less than 10^{-4} at all nodes. When these criteria failed to be met, new guesses for f , f' , and θ were found using a weighted average of the last guess and the resulting calculation. That is

$$\tilde{f}_{\text{new}} = \omega f + (1 - \omega)\tilde{f}_{\text{old}}, \quad \tilde{f}'_{\text{new}} = \omega f' + (1 - \omega)\tilde{f}'_{\text{old}}, \quad \tilde{\theta}_{\text{new}} = \omega \theta + (1 - \omega)\tilde{\theta}_{\text{old}} \quad (44)$$

Generally $\omega = 1$ resulted in quick convergence. However, for $\Omega_0 = 2$ it was often necessary to use under-relaxation with $\omega = 0.5$ to facilitate convergence.

It was found that numerical results depended upon the choice of η_∞ . As ξ was increased, it was necessary to increase η_∞ . The value of η_∞ was initially set to 15 and was increased by 5 when the value of $|f' - a_7|$ or θ was greater than 0.001 at $\eta = 0.98\eta_\infty$. Since $f(\xi, \infty) - a_7 = \theta(\xi, \infty) = 0$, the $|f' - a_7|$ and θ values greater than 0.001 at $\eta = 0.98\eta_\infty$ indicate that the corresponding boundary layer thickness extends past η_∞ . To make this adjustment for free convection, all values of f and θ and their derivatives were set to zero for $\eta > \eta_\infty$ except the values for f were taken to be the value at the old η_∞ extended out to the new η_∞ .

The adjustment for mixed convection is slightly more complicated. Again all values were set to zero except the values for \tilde{f} , \tilde{f}' , $\left(\frac{\partial f}{\partial \xi}\right)_{oi}$, $\left(\frac{\partial f'}{\partial \xi}\right)_{oi}$, \tilde{f}_o and \tilde{f}'_o . They were adjusted as follows.

$$\begin{aligned} \tilde{f}_i &= \tilde{f}_{i-1} + \Delta\eta \tilde{f}'_{i-1}, & \tilde{f}'_i &= \tilde{f}'_{i-1}, & \left(\frac{\partial f}{\partial \xi}\right)_{oi} &= (\tilde{f}_i - f_{oi})/\Delta\xi \\ \left(\frac{\partial f'}{\partial \xi}\right)_{oi} &= -2\chi_0^3 \Omega_0 (n+1) \xi_o^n, & \tilde{f}_{oi} &= f_{oi} + \frac{q}{p} \Delta\xi \left(\frac{\partial f}{\partial \xi}\right)_{oi}, & \tilde{f}'_{oi} &= f'_{oi} + \frac{q}{p} \Delta\xi \left(\frac{\partial f'}{\partial \xi}\right)_{oi} \end{aligned} \quad (45)$$

This adjustment introduced less than 1.0 % difference in the local Nusselt number for $Pr = 0.7$ as compared to a constant run at $\eta = 30$. This error was due primarily to η_∞ being less than 30 initially rather than to the adjustment itself.

It was found that as ξ was increased, errors resulted owing to the growing boundary layer thicknesses. By using $\Delta\eta = 0.01$ numerical errors were reduced for calculations at high values of

the curvature parameter ξ . It was found that the step size $\Delta\xi$ did not affect the solution appreciably and $\Delta\xi = 0.1$ was used.

RESULTS AND DISCUSSION

Numerical results were obtained for the case of buoyancy assisting flow. They cover Prandtl numbers of 0.1, 0.7, 7, and 100; values of Ω_0 of 0, 0.02, 0.1, 0.5, 1, 2 as well as the pure free convection case; for a power law temperature distribution of the form $T_w - T_\infty = ax^n$, with the exponent n varying in the range from $-0.4 \leq n \leq 0.5$ for mixed convection and $-0.5 \leq n \leq 0.5$ for pure free convection. These ranges are within the physical limits of n as determined in a manner outlined by Gebhart [21]. For pure forced convection the limits are $-0.5 \leq n$ and for pure free convection the physical limits are $-0.6 \leq n < 1.0$. The case of $\Omega_0 = 0$ corresponds to pure forced convection and $\Omega_0 = \infty$ corresponds to either $u_\infty = 0$ (pure free convection) or $r_0 = \infty$ (the flat plate solution in mixed convection). The solution method involves a system of simultaneous equations and the results depend heavily upon the choice of η_∞ . References [4] and [13] incompletely attributed the errors at high curvatures to a large step size in the radial direction. It was found that decreasing the step size does cause a corresponding decrease and a better accuracy in the local Nusselt number at high curvatures, but that the velocity profile, for pure free convection in particular, was more dependent on the choice of η_∞ .

First, the results for pure free convection will be presented. The results of Lee et al. [13] for the UWT case were recalculated using a smaller step size of $\Delta\eta^* = 0.01$ and a variable η_∞^* which was allowed to increase to 45. The radial coordinate η^* used in [13] is related to η by $\eta^* = \eta/\sqrt{2}$. As an example, for $Pr = 0.7$, present calculations for $\Lambda_N = 50$ using $\Delta\eta_\infty^* = 0.035$ and $\eta_\infty^* = 7.071$ as was done in [4] yield the result $Nu_x Gr_x^{-1/4} = 16.1$, whereas calculations using $\Delta\eta^* = 0.0125$ and $\eta_\infty^* = 30$, as was done in [13], gives $Nu_x Gr_x^{-1/4} = 6.93$. For $\Delta\eta^* = 0.01$ and $\eta_\infty^* = 45$, the present calculation gives $Nu_x Gr_x^{-1/4} = 6.46$. This is only 7.3 % lower than the result of [13], and further reductions in $\Delta\eta^*$ or increases in η_∞^* did not appreciably change the local Nusselt number. This led to the choice of $\Delta\eta^* = 0.01$ and a variable η_∞^* up to 45.

The $Nu_x Gr_x^{-1/4}$ results are listed in Table 1. It demonstrates that the local Nusselt number increases with increasing curvature and increasing Prandtl number for all n values investigated. It also shows that as the curvature increases the effect of Pr decreases and the value of the local Nusselt number converges to an asymptotic value. Table 2 shows the $Nu_x/Nu_{x,UWT}$ values as a function of the curvature. These values approach one as the curvature increases, independent of n for all Prandtl numbers. This is anticipated because as the curvature increases the first two terms in the energy equation become dominant and the equation becomes independent of both Pr and n . The average Nusselt number results, $Nu_L Gr_L^{-1/4}$, are shown in Table 3. They show trends similar to that for the local Nusselt number.

The effect of surface curvature on the local Nusselt number is illustrated in Fig. 1 for the UWT case. It is seen that as the curvature increases, the local Nusselt number increases at a faster relative rate for lower Prandtl numbers. Figure 2 illustrates the effect of the exponent n on the local Nusselt number for the flat plate. It is seen that the local Nusselt number increases with increasing n . It also shows a slight dependence on the Prandtl number such that the higher the Prandtl number the less is the deviation from the UWT case.

Results for $f''(\xi, 0)$ are given in Table 4. It is noted that the general trend is that $f''(\xi, 0)$ increases with increasing curvature, as noted by Minkowycz and Sparrow [12]. Exceptions to this may be found at high curvatures and may be due to numerical errors. It decreases with increasing n and increasing Prandtl number as noted by Chen et al. [22] for the vertical plate. The relationship between $f''(\xi, 0)$ and n is opposite to that for the local Nusselt number. This can be explained by realizing that lower Prandtl numbers will result in larger velocity gradients at the wall whereas larger Prandtl numbers will yield a larger wall temperature gradient and therefore a larger Nusselt number.

Next, the results for pure forced convection will be presented. Results of Lee et al. [4] for the UWT case were found to be in error at high curvatures for the same reasons as mentioned in the case of pure free convection. As an example, results in [4] were obtained using $\Delta\eta = 0.05$ and $\eta_\infty = 10$. At $\Lambda_F = 50$ for $Pr = 0.7$ and $n = 0$, this gives $Nu_x Re_x^{-1/2} = 16.2$, which compares with $Nu_x Re_x^{-1/2} = 6.72$ for $\Delta\eta = 0.01$ and $\eta_\infty = 45$. Further decreases in $\Delta\eta$ and η_∞ did

not appreciably lower the value of $Nu_x Re_x^{-1/2}$, so the problem was run using $\Delta\eta = 0.01$ and η_∞ was varied up to 45.

With η_∞ increasing for increasing curvature, it is of interest to determine the degree to which the boundary layer assumptions remain valid. For the boundary layer theory to be valid, $(r_\delta - r_o)/x$ must be of the order of magnitude of the term $(Re_x^{1/2} + Gr_x^{1/4})^{-1}$ where $(r_\delta - r_o)$ is the thickness of the boundary layer. The equations for Λ and η can be combined to give

$$\frac{r_\delta - r_o}{x} (Re_x^{1/2} + Gr_x^{1/4}) = \frac{2}{\Lambda} [(1 + \Lambda \eta_\delta)^{1/2} - 1] \quad (46)$$

Typically, η_δ is defined as the value of η where f and ϕ are within 0.1% of their maximum value inside the boundary layer. For $\Lambda = 1$, η_δ is about 20 and the right-hand side of equation (46) is about 7. If $[(r_\delta - r_o)/x](Re_x^{1/2} + Gr_x^{1/4})$ remains constant and Λ increases to 50, η_δ will increase to about 620. These values show that the range of η_∞ can extend very large as the curvature increases and the boundary layer assumptions will remain valid. It also verifies the analysis presented in [13] and [12] that for free convection under the UWT condition, the term that is a measure of the boundary layer thickness may actually decrease despite an increase in η_δ . This would happen in the example if η_δ was less than 620 but greater than 20.

The $Nu_x Re_x^{-1/2}$ results for pure forced convection are listed in Table 5. The table shows that as the curvature increases the local Nusselt number increases for all Pr and n that were investigated. It also shows that as the curvature increases, the effect of Pr diminishes and the Nusselt number converges to an asymptotic value. Included in Table 5 are the $f'(\xi, 0)$ results. It should be noted that for pure forced convection the momentum equation is not coupled to the energy equation and thus $f'(\xi, 0)$ is independent of n and Pr . It is seen that as the curvature increases $f'(\xi, 0)$ increases, as has been noted in other studies (for example, Seban and Bond [23]). In Table 6 are listed the Nu_x/Nu_{UWT} results as a function of n . The effect of n is seen to diminish as the curvature increases. Results for the average Nusselt number follow the same trends as the local Nusselt number, as can be seen in Table 7.

Figure 3 is a plot of $Nu_x/Nu_{x,p}$ vs. Λ_F and shows that the local Nusselt number ratio increases faster with increasing curvature for lower Prandtl numbers and becomes nearly linear at higher curvatures. This trend is similar to that for natural convection. The effect of the exponent n on the flat plate is illustrated in Fig. 4. It shows that as n increases the local Nusselt number increases and that as Pr increases the deviation from the UWT becomes less.

Calculations for mixed convection were done using $\Delta\eta = 0.01$ and η_∞ was varied up to 45. The independent variable ξ was varied from 0 (corresponding to pure forced convection for the vertical flat plate, $\chi = 1$ and $\Lambda = 0$) to the point where either $\Lambda \geq 50$ or $\chi \leq 0.1$. Tables 8 through 13 present the results for $Nu_x/(Re_x^{1/2} + Gr_x^{1/4})$ and Tables 14 through 19 present the results for $f''(\xi, 0)$. Tables 8 and 14 present the special case of mixed convection for vertical plates ($\Lambda = 0$, $\Omega_o = \infty$). For mixed convection along vertical cylinders, although calculations were done using the parameter Ω_o to combine the curvature and buoyancy parameters in one independent variable ξ , results are more meaningful when presented in terms of the curvature parameter Λ and the mixed convection parameter χ . This is shown for the UWT case in Figs. 5 through 8 for the local Nusselt number. In these figures the solid lines represent the actual runs for given values of Ω_o while the dashed lines are found by interpolation of the computer output for the values of Λ presented. In all cases the curve for the flat plate ($\Lambda = 0$) is concave upward and as χ decreases from 1 to 0 along the constant curvature curve of $\Lambda = 0$, the value of $Nu_x/(Re_x^{1/2} + Gr_x^{1/4})$ decreases to a minimum in the vicinity of $\chi = 0.6$ then increases to its pure free convection value at $\chi = 0$. This is seen more clearly in Fig. 9 for the flat plate, which also demonstrates that for $n \neq 0$, the curves run essentially parallel to the UWT curve. Figures 5 through 8 clearly show that as the curvature increases for constant values of χ the local Nusselt number increases. The results shown in Tables 8 through 13 thus reflect the combined effects of Λ and χ on the Nusselt number. That is, if the Nu_x value initially decreases with increasing ξ , as it does for the higher values of Ω_o , then the effects of mixed convection are dominant. If it initially increases with increasing ξ , then the effects of curvature are dominant.

To observe the effect of Ω_o on the Nusselt number results, one refers to Figs. 5 through 8 and notices that when $\Omega_o \rightarrow \infty$ either the flat plate solution is approached or the pure free

convection case is approached. If the curves cut off at $\chi \leq 0.1$ were extended they would rise sharply to run between the curves for $\Omega_0 = 0.5$ and $\Omega_0 = \infty$, the pure free convection case.

The local Nusselt number results obtained at high curvatures in this study were much lower than those obtained by Lee et al. [4], as has already been pointed out. It was found that results for higher Prandtl numbers were affected less by a decrease in the step size and an increase η_∞ . This perhaps may be due to an insufficient value of η_∞ , but it is most likely due to the fact that for lower Prandtl numbers, the first two terms of the energy equation essentially dominate the equation, whereas for higher Prandtl numbers other terms in the energy equation remain significant. Lee et al. [4] made the statement that for $\Lambda > 4$ the solution for mixed convection was independent of χ , Pr and n . Although this is true as $\Lambda \rightarrow \infty$, and appears nearly true for the results of [4] it is not the case for the present results. For $\Lambda \leq 50$, the effect of varying Pr from 0.1 to 100 remains significant and the pure free convection result $Nu_x Gr_x^{-1/4}$ does not equal the pure forced convection result $Nu_x Re_x^{-1/2}$ which Lee's statement seems to imply. For low Prandtl numbers this is nearly the case but for higher Prandtl numbers this is not the case.

The average Nusselt number results were also obtained. Those for the UWT case are presented in Figs. 10 through 13 and those for the flat plate with nonuniform $T_w(x)$ are illustrated in Fig. 14. The trends of the curves are similar to those for the local Nusselt number. The value of $f'(\xi, 0)$, listed in Tables 14 through 19, in general decreases initially and then increases as ξ increases. This is similar to the results of the Nusselt number but the magnitude of the increase with increasing curvature is less pronounced for $f'(\xi, 0)$.

For practical purposes, correlation equations were developed for the local and average Nusselt numbers. For pure free convection, for $0.1 \leq Pr \leq 100$, $-0.5 \leq n \leq 0.5$, and $0 \leq \Lambda \leq 50$ ($\Lambda = \Lambda_N$), the correlation equation for the local Nusselt number is given by

$$Nu_x Gr_x^{-1/4} = \alpha_N(Pr)[\Lambda_N(\Lambda) + f_{1,N}(Pr)\Lambda](1 + V_N W_N) \quad (47)$$

where

$$\alpha_N(\text{Pr}) = 0.75\text{Pr}^{1/2}[2.5(1 + 2\text{Pr}^{1/2} + 2\text{Pr})]^{-1/4} \quad (48)$$

$$A_N(\Lambda) = 1.4^{(1-0.7\Lambda)} \quad (49)$$

$$f_{1,N}(\text{Pr}) = 0.045 + 0.27\text{Pr}^{-0.46} \quad (50)$$

$$V_N = \{[0.88 + 0.5 \exp(-2\text{Pr}^{1/4})] - 0.77n\}n \quad (51)$$

$$W_N = \exp\{-[0.07 + 7.5 \exp(-3.6\text{Pr}^{1/10})]\Lambda^{0.7}\} \quad (52)$$

The average Nusselt numbers are correlated by

$$\text{Nu}_L \text{Gr}_L^{-1/4} = \frac{4}{3} \alpha_N(\text{Pr}) [B_N(\Lambda) + f_{2,N}(\text{Pr})\Lambda] (1 + \bar{V}_N) \quad (53)$$

where

$$B_N(\Lambda) = 1.4^{(1-0.75\Lambda)} \quad (54)$$

$$f_{2,N}(\text{Pr}) = 0.03 + 0.21\text{Pr}^{-0.44} \quad (55)$$

$$\bar{V} = (3V_N W_N - n\bar{W}) / (3 + n\bar{W}) \quad (56)$$

$$\bar{W} = \exp(-0.11\Lambda^{1.2}) \quad (57)$$

In equations (53) - (57), Λ now stands for Λ_N with $x = L$.

For the case of pure forced convection, for $0.1 \leq \text{Pr} \leq 100$, $-0.4 \leq n \leq 0.5$, and $0 \leq \Lambda \leq 50$ ($\Lambda = \Lambda_F$), the correlation equations are

$$\text{Nu}_x \text{Re}_x^{-1/2} = \alpha_F(\text{Pr}) [\Lambda_F(\Lambda) + f_{1,F}(\text{Pr})\Lambda] (1 + V_F W_F) \quad (58)$$

where

$$\alpha_F(\text{Pr}) = 0.339\text{Pr}^{1/3}[1 + (0.0468/\text{Pr})^{2/3}]^{-1/4} \quad (59)$$

$$\Lambda_F(\Lambda) = (1 + 0.4\Lambda^{1/2}) \quad (60)$$

$$f_{1,F}(\text{Pr}) = (0.04 + 0.3\text{Pr}^{-0.45}) \quad (61)$$

$$V_F = \{[1.17 + 11\exp(-5.6\text{Pr}^{1/10})] - 0.92n\}n \quad (62)$$

$$W_F = \exp[-(0.07 + 0.3\text{Pr}^{-0.32})\Lambda^{3/5}] \quad (63)$$

and

$$\text{Nu}_L \text{Re}_L^{-1/2} = 2\alpha_F(\text{Pr})[\Lambda_F(\Lambda) + f_{2,F}(\text{Pr})\Lambda](1 + \bar{V}_F) \quad (64)$$

where

$$B_F(\Lambda) = (1 + 0.25\Lambda^{1/2}) \quad (65)$$

$$f_{2,F}(\text{Pr}) = (0.025 + 0.15\text{Pr}^{-0.45}) \quad (66)$$

$$\bar{V}_F = V_F \exp[-(0.06 + 0.17\text{Pr}^{-1/3})\Lambda^{0.65}] \quad (67)$$

In equations (64) - (67), Λ stands for Λ_F with $x = L$.

It should be noted that the form of these correlation equations is such that for the UWT case V_N , V_F , \bar{V}_N , \bar{V}_F are zero and the last terms in equations (47), (53), (58), and (64) can be omitted. Also the form of Λ_N , Λ_F , B_N and B_F are such that for $\Lambda = 0$ they become one and for the flat plate UWT case only α_N and α_F are needed. The expression for α_N is taken from Ede [24] and the expression for α_F is taken from Churchill and Ozoe [25]. The error in equations (47) and (53) is less than 8.5 % for the UWT case and less than 13.5 % for $-0.5 \leq n \leq 0.5$. The maximum error in equations (58) and (64) is about 9.2 % for the UWT case and about 14.5 % for $-0.4 \leq n \leq 0.5$.

Following Churchill [20], the correlation equation for Nusselt numbers in mixed convection is expressed by the form

$$\begin{aligned} \left(\frac{Nu}{Nu_F} \right)^m &= 1 + \left(\frac{Nu_N}{Nu_F} \right)^m \\ \left(\frac{Nu}{Nu_N} \right)^m &= 1 + \left(\frac{Nu_F}{Nu_N} \right)^m \end{aligned} \quad (68)$$

This form of correlation has been found to give an accuracy of about 5% for $0.1 \leq Pr \leq 100$ for flat plates with $m=3$ and was also verified experimentally for air in the UWT case [14, 15]. For the present study with a single mixed convection parameter χ , the corresponding correlation equation can be represented by

$$\frac{Nu_x}{(Re_x^{1/2} + Gr_x^{1/4})} = \left\{ \left[\chi \left(\frac{Nu_x}{Re_x^{1/2}} \right) \right]^m + \left[(1 - \chi) \left(\frac{Nu_x}{Gr_x^{1/4}} \right) \right]^m \right\}^{1/m} \quad (69)$$

This equation was found to be valid for the case of flow along a vertical cylinder with a power law variation in the surface temperature in the following manner. It was found that as Λ increases the corresponding value for m decreases to 1. This can be seen by observing the decrease in the concavity of the dashed lines in the Nusselt number figures as Λ increases. It is also seen that the concavity disappears more quickly for lower Prandtl numbers. The graphical technique of Churchill [20] was used to determine the relationship among m , Λ , and Pr for the UWT case. Figure 15 shows a sample graph for $Pr=0.7$. In this graph Nu_F is the Nusselt number as a function of $\Lambda_F = \Lambda$, Pr , and n for the pure forced convection case and Nu_N is the Nusselt number as a function of $\Lambda_N = \Lambda$, Pr , and n for the pure free convection case. That is, they are calculated from the endpoints of the curves in the Nusselt number figures at $\chi = 0$ and 1 for lines of constant Λ for given Pr and n . Reference lines for various values of m are plotted and points corresponding to various curvatures are marked with different symbols. For $Pr = 0.7$ it is seen that as the curvature increases from $\Lambda = 0$ to 50 the value of m decreases from about 3 to about 1. This was done for the other Prandtl numbers for the UWT case for both the local and average Nusselt numbers and the relationship

$$m = 1 + 2\exp[-(0.8 + 0.55\text{Pr}^{-0.34})\Lambda^{0.3}] \quad (70)$$

was developed. It was found that equation (69) was also valid for the flat plate for $-0.4 \leq n \leq 0.5$ with $m=3$ and the values of $\text{Nu}_x \text{Re}_x^{-1/2}$ and $\text{Nu}_x \text{Gr}_x^{-1/4}$ were those obtained for the given values of Pr and n , with $\Lambda = 0$. For $\Lambda > 0$, it was found that equation (70) could be used for $n > 0$ but was inconsistent for $n < 0$. However, a better relation for $n < 0$ could not be found. For the ranges of Pr , Λ , and $n \geq 0$ studied, equation (69) along with the m expression from equation (70) produce results valid to within about 9% when using computer output for Nu_F and Nu_N and to within about 14% when using equations (47) and (58). The corresponding correlation equation for the average Nusselt number, where Nu_x , Re_x , Gr_x , and χ are replaced, respectively, by $\overline{\text{Nu}}_L$, Re_L , Gr_L and χ_L , was also found to be valid with the same accuracy for $n \geq 0$. A reliable relationship for $n < 0$ was not obtained, but equations (69) and (70) usually will provide a satisfactory result for both the local and average Nusselt numbers.

These correlations presented are in a different form than those proposed by Lee et al. [4] and Lee et al. [13]. Their forms were derived based on the asymptotic solution as $\Lambda \rightarrow \infty$. As a result, they proposed a logarithmic correlation form for the cases of pure forced and pure free convection, which may be difficult for use in practice. The correlations in the present study are based on the flat plate solution and take advantage of the nearly linear relation between the Nusselt number and curvature as shown in Fig. 1 and 3

The correlation proposed in [4] for mixed convection is also based on the asymptotic solution as $\Lambda \rightarrow \infty$. The correlation presented here is based on the correlation for the vertical flat plate proposed by Churchill [20], which has been verified experimentally for air [15]. It also is based on the curvature parameter Λ , whereas in Ref. [4] Λ_N and Λ_F were used in the calculations of the normalized Nusselt number for mixed convection. As χ approaches 0 or 1, these calculations become unwieldy. Therefore, it is suggested that the Nusselt number calculations for the pure free or pure forced convection, which are used in the mixed convection calculations, be based on Λ .

CONCLUSIONS

Mixed convection along a vertical cylinder with a power law variation in the wall temperature is investigated for the entire regime ranging from pure free convection to pure forced convection. Results were presented for the local and average Nusselt numbers and values of $f''(\xi, 0)$ were tabulated. Correlation equations for the local and average Nusselt numbers are also presented. It is found that the local Nusselt number $Nu_x/(Re_x^{1/2} + Gr_x^{1/4})$ increases with increasing Prandtl number, increasing value of the exponent n , and increasing curvature for the entire mixed convection regime ranging from pure free convection ($\chi = 0$) to pure forced convection ($\chi = 1$). For the vertical flat plate, this quantity initially decreases as χ is decreased from 1 and then increases to the pure free convection value as χ approaches 0. However, this trend tends to become a linear relationship as the curvature increases; that is, the value of $Nu_x/(Re_x^{1/2} + Gr_x^{1/4})$ for constant curvature Λ will lie on a line with end points at $\chi = 0$ and $\chi = 1$ for that curvature. This trend is approached more rapidly for lower Prandtl numbers. The quantity $Nu_L/(Re_L^{1/2} + Gr_L^{1/4})$ follows a similar pattern as that for the local Nusselt number. The effects of both the Prandtl number and n on the Nusselt number diminish as the curvature increases, but remain significant for curvatures $\Lambda \leq 50$ when Prandtl numbers are large.

REFERENCES

1. T. S. Chen and A. Mucoglu, Buoyancy effects on forced convection along a vertical cylinder, J. Heat Transfer 97, 198-203 (1975).
2. A. Mucoglu and T. S. Chen, Buoyancy effects on forced convection along a vertical cylinder with uniform surface heat flux, J. Heat Transfer 98, 523-525 (1976).
3. M. N. Bui and T. Cebeci, Combined free and forced convection on vertical cylinders, J. Heat Transfer 107, 476-478 (1985).
4. S. L. Lee, T. S. Chen and B. F. Armaly, Mixed convection along isothermal vertical cylinders and needles, Proceedings of the Eighth International Heat Transfer Conference 3, 1425-1432 (1986).
5. S. L. Lee, T. S. Chen and B. F. Armaly, Mixed convection along vertical cylinders and needles with uniform surface heat flux, J. Heat Transfer 109, 711-716 (1987).
6. S. L. Lee, T. S. Chen and B. F. Armaly, New finite difference solution methods for wave instability problems, Nume. Heat Transfer 10, 1-8 (1986).
7. R. L. Burden and J. D. Faires, Numerical Analysis 3rd ed., Prindle, Weber and Schmidt, Boston, 117-129 (1985).
8. W. Elenbaas, The dissipation of heat by free convection from vertical and horizontal cylinders, J. Appl. Physics 19, 1148-1154 (1948).
9. E. M. Sparrow and J. L. Gregg, Laminar-free-convection heat transfer from the outer surface of a vertical circular cylinder, Trans. ASME 78, 1823-1829 (1956).
10. H. K. Kuiken, Axisymmetric free convection boundary layer flow past slender bodies, Int. J. Heat Mass Transfer 11, 1141-1153 (1968).
11. T. Fujii and H. Uehara, Laminar natural convective heat transfer from the outer surface of a vertical cylinder, Int. J. Heat Mass Transfer 13, 607-615 (1970).
12. W. J. Minkowycz and E. M. Sparrow, Local nonsimilar solutions for natural convection on a vertical cylinder, J. Heat Transfer 96, 178-183 (1974).
13. H. R. Lee, T. S. Chen B. F. and Armaly, Natural convection along vertical cylinders with variable surface temperature, J. Heat Transfer 110, 103-108 (1988).

14. T. S. Chen, B. F. Armaly, and N. Ramachandran, Correlations for laminar mixed convection flows on vertical, inclined, and horizontal flat plates, J. Heat Transfer 108, 835-840 (1986).
15. N. Ramachandran, B. F. Armaly T. S. and Chen, Measurements and predictions of laminar mixed convection flow adjacent to a vertical surface, J. Heat Transfer 107, 636-641 (1985).
16. A. Mucoglu and T. S. Chen, Mixed convection on inclined surfaces, J. Heat Transfer 101, 422-426 (1979).
17. J. Gryzagoridis, Combined free and forced convection from an isothermal vertical plate, Int. J. Heat Mass Transfer 18, 911-916 (1975).
18. M. S. Raju, X. Q. Lin and C. K. Law, A formulation of combined forced and free convection past horizontal and vertical surfaces, Int. J. Heat Mass Transfer 17, 2215-2224 (1984).
19. J. R. Lloyd and E. M. Sparrow, Combined forced and free convection flow on vertical surfaces, Int. J. Heat Mass Transfer 13, 434-438 (1970).
20. S. W. Churchill, A comprehensive correlating equation for laminar assisting, forced and free convection, AIChE Journal 23, 10-16 (1977).
21. B. Gebhart, Heat Transfer, 2d ed., McGraw-Hill, New York, 340 (1971).
22. T. S. Chen, H. C. Tien and B. F. Armaly, Natural convection on horizontal, inclined, and vertical plates with variable surface temperature or heat flux, Int. J. Heat Mass Transfer 29, 1465-1478 (1986).
23. R. A. Seban and R. Bond, Skin friction and heat-transfer characteristics of a laminar boundary layer on a cylinder in axial incompressible flow, J. Aero. Science 18, 671-675 (1951).
24. A. J. Ede, Advances in free convection, Advances in Heat Transfer 4, 1-64 (1967).
25. S. W. Churchill and H. Ozoe, Correlations for laminar forced convection in flow over an isothermal flat plate and in developing and fully developed flow in an isothermal tube, J. Heat Transfer 95, 416-419 (1973).

Table 1. The $Nu_x Gr_x^{-1/4}$ results for Power Law Variation of Surface Temperature, Free Convection.

ξ	Pr = 0.1			Pr = 0.7			Pr = 7			Pr = 100		
	n			n			n			n		
	-0.5	0	0.5	-0.5	0	0.5	-0.5	0	0.5	-0.5	0	0.5
0	0.0513	0.1638	0.2186	0.1093	0.3532	0.4598	0.2549	0.7455	0.9474	0.5494	1.5493	1.9522
0.5	0.1359	0.2616	0.3189	0.2040	0.4562	0.5659	0.3586	0.8541	1.0588	0.6554	1.6588	2.0642
1.0	0.3546	0.4946	0.5587	0.3867	0.7154	0.8351	0.6192	1.1376	1.3530	0.9413	1.9635	2.3786
1.5	0.7289	0.8522	0.9136	0.7674	1.0792	1.2144	0.9928	1.5516	1.7791	1.3585	2.4199	2.8536
2.0	1.2295	1.3238	1.3772	1.1688	1.5272	1.6813	1.4543	2.0646	2.2998	1.8697	2.9911	3.4517
2.5	1.8304	1.9017	1.9463	1.6780	2.0657	2.2310	1.9872	2.6642	2.9165	2.4521	3.6518	4.1470
3.0	2.5284	2.5822	2.6188	2.3316	2.7053	2.8706	2.5780	3.3369	3.6345	3.0900	4.3869	4.9245
3.5	3.3261	3.3666	3.3961	3.1353	3.4547	3.6095	3.2186	4.0860	4.4233	3.8597	5.1980	5.7828
4.0	4.2295	4.2594	4.2831	4.0762	4.3224	4.4598	3.9273	4.9187	5.2975	4.7248	6.2565	6.7352
4.5	5.2490	5.2714	5.2904	5.1394	5.3177	5.4353	4.7400	5.8295	6.2818	5.7093	7.2490	7.9254
5.0	6.4029	6.4200	6.4354	6.3251	6.4554	6.5547	5.7147	6.8771	7.3422	6.7810	8.5257	9.1301

Table 2. The $Nu_x/Nu_{x,UWT}$ results for Power Law Variation of Surface Temperature, Free Convection.

ξ	$Pr = 0.1$			$Pr = 0.7$			$Pr = 7$			$Pr = 100$		
	n			n			n			n		
	-0.5	0.2	0.5	-0.5	0.2	0.5	-0.5	0.2	0.5	-0.5	0.2	0.5
0	0.2777	1.1600	1.3435	0.3093	1.1413	1.3017	0.3420	1.1269	1.2707	0.3546	1.1219	1.2601
0.5	0.4984	1.1085	1.2314	0.4472	1.1128	1.2404	0.4198	1.1123	1.2396	0.3951	1.1146	1.2444
1.0	0.7080	1.0614	1.1312	0.6170	1.0784	1.1673	0.5493	1.0889	1.1893	0.4794	1.0992	1.2114
1.5	0.8543	1.0331	1.0720	0.7111	1.0587	1.1253	0.6399	1.0718	1.1466	0.5614	1.0841	1.1792
2.0	0.9285	1.0180	1.0403	0.7653	1.0474	1.1009	0.7044	1.0571	1.1139	0.6251	1.0723	1.1540
2.5	0.9625	1.0104	1.0235	0.8123	1.0377	1.0800	0.7459	1.0477	1.0947	0.6715	1.0637	1.1356
3.0	0.9791	1.0061	1.0141	0.8619	1.0284	1.0611	0.7726	1.0342	1.0892	0.7044	1.0576	1.1225
3.5	0.9880	1.0038	1.0081	0.9075	1.0204	1.0448	1.7877	1.0336	1.0826	0.7425	1.0530	1.1125
4.0	0.9930	1.0023	1.0055	0.9430	1.0142	1.0318	0.7984	1.0381	1.0770	0.7552	1.0460	1.0765
4.5	0.9958	1.0015	1.0036	0.9665	1.0096	1.0221	0.8131	1.0371	1.0776	0.7876	1.0441	1.0933
5.0	0.9973	1.0010	1.0024	0.9798	1.0065	1.0154	0.8310	1.0321	1.0676	0.7954	1.0396	1.0709

Table 3. The $Nu_L Gr_L^{-1/4}$ results for Power Law Variation of Surface Temperature, Free Convection.

ξ_L	Pr = 0.1				Pr = 0.7				Pr = 7				Pr = 100			
	n				n				n				n			
	-0.5	0	0.5		-0.5	0	0.5		-0.5	0	0.5		-0.5	0	0.5	
0	0.0723	0.2170	0.2499		0.1748	0.4710	0.5255		0.4079	0.9940	1.0827		0.8790	2.0657	2.2311	
0.5	0.1599	0.3150	0.3557		0.2726	0.5755	0.6408		0.5141	1.1038	1.2099		0.9870	2.1762	2.3724	
1.0	0.3817	0.5571	0.5960		0.5227	0.8442	0.9071		0.7875	1.3960	1.4949		1.2812	2.4857	2.6628	
1.5	0.7579	0.9232	0.9553		0.8733	1.2248	1.2946		1.1857	1.8273	1.9219		1.7224	2.9570	3.1435	
2.0	1.2748	1.4062	1.4246		1.3053	1.6954	1.7732		1.6807	2.3651	2.4662		2.2740	3.5542	3.7546	
2.5	1.9051	1.9982	2.0002		1.8244	2.2517	2.3343		2.2579	2.9923	3.0794		2.9116	4.2516	4.4686	
3.0	2.6375	2.6948	2.6796		2.4619	2.9040	2.9829		2.9053	3.7060	3.8128		3.6181	5.0316	5.2682	
3.5	3.4695	3.4948	3.4631		3.2377	3.6603	3.7273		3.6105	4.4885	4.6153		4.3947	5.8872	6.1481	
4.0	4.4027	4.4000	4.3540		4.1549	4.5282	4.5781		4.3738	5.3549	5.5110		5.2920	6.8923	7.1142	
4.5	5.4421	5.4163	5.3600		5.2072	5.5155	5.5475		5.2091	6.2954	6.5012		6.2924	7.9883	8.3064	
5.0	6.5964	6.5541	6.4943		6.3876	6.6318	6.6507		6.1450	7.3353	7.5804		7.3881	9.2037	9.5211	

Table 4. The $f''(\xi, 0)$ results for Power Law Variation of Surface Temperature, Free Convection.

ξ	Pr = 0.1			Pr = 0.7			Pr = 7			Pr = 100		
	n			n			n			n		
	-0.5	0	0.5	-0.5	0	0.5	-0.5	0	0.5	-0.5	0	0.5
0	1.1052	0.8559	0.7607	0.8559	0.6789	0.6009	0.5862	0.4508	0.3968	0.3339	0.2516	0.2204
0.5	1.1314	0.9066	0.7999	0.9048	0.7135	0.6288	0.6072	0.4666	0.4100	0.3396	0.2559	0.2240
1.0	1.3237	1.0415	0.9121	1.0004	0.8076	0.7073	0.6667	0.5088	0.4449	0.3560	0.2683	0.2344
1.5	1.5153	1.1964	1.0471	1.2231	0.9458	0.8227	0.7620	0.5744	0.4946	0.3813	0.2873	0.2504
2.0	1.6450	1.3278	1.1733	1.4572	1.1151	0.9628	0.8852	0.6576	0.5522	0.4128	0.3108	0.2702
2.5	1.7153	1.4204	1.2713	1.6574	1.2564	1.0843	1.0272	0.7520	0.6075	0.4481	0.3367	0.2919
3.0	1.7173	1.4645	1.3326	1.7630	1.3504	1.1804	1.1730	0.8509	0.6954	0.4838	0.3621	0.3135
3.5	1.6562	1.4656	1.3594	1.7520	1.3936	1.2435	1.3120	0.9483	0.7721	0.5444	0.3841	0.3330
4.0	1.5657	1.4400	1.3610	1.6538	1.3970	1.2768	1.4341	1.0491	0.8624	0.5809	0.4317	0.3492
4.5	1.4834	1.4057	1.3494	1.5378	1.3796	1.2896	1.5259	1.1216	0.9641	0.6478	0.4617	0.4003
5.0	1.4231	1.3738	1.3341	1.4524	1.3573	1.2917	1.5769	1.1747	1.0267	0.7117	0.5170	0.4245

Table 5. The $Nu_x Re_x^{-1/2}$ and $f''(\xi, 0)$ results for Power Law Variation of Surface Temperature, Forced Convection.

ξ	$Pr = 0.1$			$Pr = 0.7$			$Pr = 7$			$Pr = 100$			$f'(\xi, 0)$
	n			n			n			n			
	-0.4	0	0.5	-0.4	0	0.5	-0.4	0	0.5	-0.4	0	0.5	
0	0.0451	0.1404	0.2007	0.1021	0.2927	0.4059	0.2343	0.6459	0.8856	0.5736	1.5720	2.1522	0.3321
0.5	0.1602	0.2576	0.3234	0.2324	0.4338	0.5586	0.4041	0.8439	1.1082	0.8412	1.9146	2.5551	0.4797
1.0	0.4011	0.5136	0.5971	0.5195	0.7475	0.8971	0.7752	1.2679	1.5774	1.3918	2.5856	3.3285	0.8064
1.5	0.7925	0.8878	0.9718	0.8987	1.1690	1.3516	1.2564	1.8179	2.1799	2.0732	3.4029	4.2586	1.2387
2.0	1.3162	1.3890	1.4643	1.3571	1.6799	1.8955	1.8270	2.4664	2.8854	2.8583	4.3295	5.2890	1.7580
2.5	1.9398	1.9998	2.0667	1.8936	2.2680	2.5240	2.4802	3.2052	3.6852	3.7403	5.3587	6.4287	2.3579
3.0	2.6610	2.7132	2.7738	2.5400	2.9356	3.2307	3.2118	4.0289	4.5735	4.7133	6.4856	7.6681	3.0406
3.5	3.4801	3.5273	3.5831	3.3245	3.7077	4.0170	4.0214	4.9372	5.5499	5.7776	7.7113	9.0096	3.8166
4.0	4.3988	4.4424	4.4948	4.2399	4.5968	4.9062	4.9143	5.9143	6.6209	6.9426	9.0480	10.467	4.6973
4.5	5.4212	5.4624	5.5122	5.2726	5.6018	5.9097	5.8966	7.0314	7.7939	8.2173	10.506	12.054	5.6909
5.0	6.5550	6.5944	6.6423	6.4186	6.7249	7.0297	6.9732	8.2295	9.0748	9.6065	12.091	13.775	6.8044

Table 6. The $Nu_x/Nu_{x,Pr}$ results for Power Law Variation of Surface Temperature, Forced Convection.

ξ	Pr = 0.1			Pr = 0.7			Pr = 7			Pr = 100		
	n			n			n			n		
	-0.4	0.2	0.5	-0.4	0.2	0.5	-0.4	0.2	0.5	-0.4	0.2	0.5
0	0.3211	1.1990	1.4299	0.3488	1.1807	1.3868	0.3627	1.1734	1.3711	0.3649	1.1724	1.3691
0.5	0.6218	1.1150	1.2557	0.5357	1.1336	1.2876	0.4788	1.1456	1.3131	0.4394	1.1556	1.3345
1.0	0.7810	1.0748	1.1626	0.6951	1.0924	1.2001	0.6114	1.1129	1.2441	0.5383	1.1329	1.2873
1.5	0.8926	1.0415	1.0946	0.7688	1.0737	1.1562	0.6911	1.0918	1.1991	0.6092	1.1152	1.2500
2.0	0.9476	1.0230	1.0542	0.8078	1.0584	1.1283	0.7408	1.0782	1.1699	0.6602	1.1019	1.2216
2.5	0.9700	1.0139	1.0335	0.8349	1.0511	1.1129	0.7738	1.0689	1.1498	0.6980	1.0917	1.1997
3.0	0.9808	1.0091	1.0223	0.8652	1.0452	1.1005	0.7972	1.0622	1.1352	0.7267	1.0837	1.1823
3.5	0.9866	1.0064	1.0158	0.8966	1.0367	1.0834	0.8145	1.0571	1.1241	0.7492	1.0773	1.1684
4.0	0.9902	1.0048	1.0118	0.9224	1.0295	1.0673	0.8279	1.0531	1.1154	0.7673	1.0720	1.1568
4.5	0.9925	1.0037	1.0100	0.9412	1.0238	1.0550	0.8386	1.0499	1.1084	0.7822	1.0676	1.1473
5.0	0.9940	1.0029	1.0073	0.9545	1.0193	1.0453	0.8473	1.0473	1.1027	0.7945	1.0639	1.1393

Table 7. The $Nu_L Re_L^{-1/2}$ results for Power Law Variation of Surface Temperature, Forced Convection.

ξ_L	Pr = 0.1			Pr = 0.7			Pr = 7			Pr = 100		
	n			n			n			n		
	-0.4	0	0.5	-0.4	0	0.5	-0.4	0	0.5	-0.4	0	0.5
0	0.0901	0.2807	0.4014	0.2042	0.5854	0.8118	0.4686	1.2919	1.7713	1.1471	3.1440	4.3044
0.5	0.2124	0.4050	0.5305	0.3417	0.7339	0.9721	0.6476	1.5016	2.0071	1.4320	3.5120	4.7373
1.0	0.4809	0.6886	0.8326	0.6612	1.0804	1.3469	1.0600	1.9762	2.5356	2.0566	4.2873	5.6384
1.5	0.8757	1.0857	1.2446	1.0877	1.5521	1.8547	1.6091	2.6027	3.2257	2.8548	5.2506	6.7401
2.0	1.4184	1.6088	1.7679	1.6028	2.1243	2.4685	2.2597	3.3450	4.0381	3.7723	6.3480	7.9800
2.5	2.0824	2.2514	2.4042	2.1982	2.7839	3.1742	3.0006	4.1871	4.9549	4.7958	7.5580	9.3344
3.0	2.8536	3.0050	3.1500	2.8804	3.5252	3.9652	3.8258	5.1215	5.9681	5.9179	8.8731	10.796
3.5	4.7009	4.8275	4.9578	4.5837	5.2788	5.7954	5.7183	7.2537	8.2697	8.4453	11.808	14.031
4.0	5.7758	5.8935	6.0179	5.6185	6.3115	6.8492	6.7880	8.4539	9.5606	9.8559	13.435	15.815
4.5	5.7758	5.8935	6.0179	5.6185	6.3115	6.8492	6.7880	8.4539	9.5606	9.8559	13.435	15.815
5.0	6.9539	7.0646	7.1839	6.7725	7.4543	8.0063	7.9440	9.7478	10.950	11.371	15.177	17.719

Table 8. The $Nu_x/(Re_x^{1/2} + Gr_x^{1/4})$ results for Power Law Variation of Surface Temperature, Mixed Convection, Along a Vertical Flat Plate ($\Lambda = 0, \Omega_0 = \infty$).

ξ	$Pr = 0.1$			$Pr = 0.7$			$Pr = 7$			$Pr = 100$		
	n			n			n			n		
	-0.4	0	0.5	-0.4	0	0.5	-0.4	0	0.5	-0.4	0	0.5
0	0.0794	0.1634	0.2186	0.1849	0.3532	0.4598	0.4148	0.7455	0.9476	0.8797	1.5493	1.9540
0.1	0.0714	0.1483	0.1973	0.1666	0.3184	0.4145	0.3729	0.6716	0.8540	0.7905	1.3956	1.7608
0.2	0.0631	0.1342	0.1775	0.1480	0.2850	0.3711	0.3288	0.5998	0.7638	0.6943	1.2466	1.5768
0.3	0.0544	0.1214	0.1596	0.1290	0.2536	0.3309	0.2814	0.5314	0.6799	0.5886	1.1079	1.4112
0.4	0.0453	0.1104	0.1447	0.1093	0.2255	0.2962	0.2325	0.4713	0.6090	0.4835	0.9969	1.2890
0.5	0.0373	0.1019	0.1349	0.0901	0.2046	0.2728	0.1904	0.4304	0.5670	0.4061	0.9487	1.2583
0.6	0.0329	0.0982	0.1347	0.0767	0.1980	0.2703	0.1670	0.4255	0.5760	0.3806	0.9931	1.3526
0.7	0.0311	0.1022	0.1480	0.0739	0.2092	0.2956	0.1653	0.4592	0.6424	0.3973	1.1077	1.5514
0.8	0.0347	0.1165	0.1692	0.0763	0.2404	0.3404	0.1759	0.5315	0.7430	0.4307	1.2936	1.8064
0.9	0.0411	0.1297	0.1856	0.0923	0.2698	0.3752	0.2121	0.5956	0.8188	0.5209	1.4518	1.9930
1.0	0.0450	0.1404	0.2007	0.1021	0.2927	0.4059	0.2345	0.6422	0.8861	0.5767	1.5758	2.1579

Table 9. The $Nu_x/(Re_x^{1/2} + Gr_x^{1/4})$ results for Power Law Variation of Surface Temperature, Mixed Convection, $\Omega_0 = 0.02$.

ξ	$Pr = 0.1$			$Pr = 0.7$			$Pr = 7$			$Pr = 100$		
	n			n			n			n		
	-0.4	0	0.5	-0.4	0	0.5	-0.4	0	0.5	-0.4	0	0.5
0	0.0451	0.1400	0.2007	0.1021	0.2927	0.4059	0.2343	0.6459	0.8856	0.5736	1.5720	2.1522
0.5	0.1582	0.2526	0.3206	0.2206	0.4297	0.5548	0.3987	0.8358	1.1008	0.8303	1.8961	2.5380
1.0	0.3944	0.5036	0.5856	0.5050	0.7378	0.8795	0.7576	1.2453	1.5465	1.3588	2.5402	3.2633
1.5	0.7772	0.8646	0.9390	0.8757	1.1367	1.3046	1.2246	1.7658	2.1031	2.0198	3.3057	4.1040
2.0	1.2849	1.3424	1.3924	1.3187	1.6154	1.7961	1.7736	2.3720	2.7319	2.7749	4.1639	5.0079
2.5	1.8858	1.9172	1.9305	1.8342	2.1604	2.3396	2.3977	3.0533	3.4167	3.6164	5.1052	5.9609
3.0	2.5771	2.5796	2.5407	2.4557	2.7718	2.9256	3.0927	3.8016	4.1445	4.5392	6.1203	6.9499
3.5	3.3584	3.3253	3.2129	3.2085	3.4770	3.5571	3.8579	4.6143	4.9078	5.5433	7.2079	7.9691
4.0	4.2302	4.1516	3.9390	4.0812	4.2790	4.2508	4.6978	5.4950	5.7066	6.6378	8.3779	9.0255
4.5	5.1953	5.0587	4.7128	5.0582	5.1717	4.9982	5.6169	6.4459	6.5370	7.8290	9.6342	10.116
5.0	6.2593	6.0489	5.5302	6.1344	6.1526	5.7925	6.6178	7.4670	7.3926	9.1189	10.975	11.231

Table 10. The $Nu_s/(Re)^{1/2} + Gr_s^{1/4}$ results for Power Law Variation of Surface Temperature, Mixed Convection, $\Omega_0 = 0.1$.

ξ	$Pr = 0.1$			$Pr = 0.7$			$Pr = 7$			$Pr = 100$		
	-0.4	n	0.5	-0.4	n	0.5	-0.4	n	0.5	-0.4	n	0.5
0	0.0451	0.1404	0.2007	0.1021	0.2927	0.4059	0.2343	0.6459	0.8856	0.5736	1.5720	2.1522
0.5	0.1472	0.2460	0.3120	0.2160	0.4134	0.5403	0.3779	0.8045	1.0721	0.7886	1.8255	2.4720
1.0	0.3697	0.4690	0.5439	0.4688	0.6821	0.8157	0.6990	1.1548	1.4342	1.2511	2.3555	3.0261
1.5	0.7227	0.7842	0.8289	0.7974	1.0205	1.1436	1.1121	1.5828	1.8493	1.8324	2.9634	3.5994
2.0	1.1753	1.1869	1.1690	1.1812	1.4015	1.4787	1.5870	2.0584	2.2543	2.4823	3.6145	4.1336
2.5	1.6997	1.6510	1.5394	1.6271	1.8163	1.8085	2.1157	2.5687	2.6500	3.1914	4.2966	4.6249
3.0	2.2929	2.1646	1.9227	2.1734	2.2789	2.1367	2.6939	3.1063	3.0252	3.9550	5.0039	5.0751
3.5	2.9527	2.7200	2.3073	2.8259	2.8039	2.4802	3.3193	3.6661	3.3802	4.7712	5.7275	5.4914
4.0	3.6773	3.3117	2.6862	3.5620	3.3794	2.8294	3.9962	4.2453	3.7164	5.6492	6.4766	5.8795
4.5	4.4664	3.9361	3.0553	4.3650	3.9939	3.1764	4.7250	4.8482	4.0343	6.5900	7.2533	6.2409
5.0	5.3213	4.5907	3.4129	5.2307	4.6413	3.5170	5.5039	5.4683	4.3327	7.5889	8.0457	6.5714
6.0		5.9857	4.0903		6.0260	4.1710		6.7577	4.8854		9.6715	7.1582
7.0			4.7181			4.7844			5.3940			7.6741
8.0			5.3005			5.3573			5.8836			8.1444
9.0			5.8429			5.8933			6.3606			8.5853
10.0			6.3506			6.3964			6.8221			9.0065

Table 11. The $Nu_x/(Re_x^{1/2} + Gr_x^{1/4})$ results for Power Law Variation of Surface Temperature, Mixed Convection, $\Omega_0 = 0.5$.

ξ	$Pr = 0.1$			$Pr = 0.7$			$Pr = 7$			$Pr = 100$		
	-0.4	n	0.5	-0.4	n	0.5	-0.4	n	0.5	-0.4	n	0.5
0	0.0451	0.1404	0.2007	0.1021	0.2927	0.4059	0.2343	0.6459	0.8856	0.5736	1.5720	2.1522
0.5	0.1139	0.2072	0.2758	0.1657	0.3478	0.4760	0.2909	0.6784	0.9450	0.6068	1.5395	2.1789
1.0	0.2864	0.3514	0.4017	0.3408	0.5059	0.6045	0.5027	1.8519	1.0596	0.8855	1.7309	2.2289
1.5	0.5450	0.5537	0.5492	0.5574	0.6875	0.7359	0.7683	1.0652	1.1835	1.2534	1.9813	2.2772
2.0	0.8378	0.7804	0.7033	0.7979	0.8810	0.8745	1.0591	1.2915	1.3320	1.6482	2.2481	2.3793
2.5	1.1601	1.0154	0.8433	1.0902	1.0886	1.0133	1.3671	1.5231	1.4834	2.0450	2.5259	2.5084
3.0	1.5098	1.2540	0.9670	1.4403	1.3143	1.1430	1.6835	1.7515	1.6248	2.4679	2.7961	2.6461
3.5	1.8846	1.4942	1.0770	1.8251	1.5469	1.2592	2.0191	1.9791	1.7539	2.9010	3.0603	2.7843
4.0	2.2824	1.7351	1.1756	2.2324	1.7821	1.3630	2.3701	2.2080	1.8706	3.3432	3.3194	2.9166
4.5	2.7017	1.9760	1.2651	2.6588	2.0184	1.4565	2.7350	2.4360	1.9902	3.7962	3.5743	3.0409
5.0	3.1413	2.2165	1.3469	3.1036	2.2551	1.5414	3.1127	2.6615	2.0938	4.2585	3.8255	3.1563
6.0	4.0785	2.6958	1.4930	4.0480	2.7283	1.6911	3.9207	3.1109	2.2900	5.2134	4.3177	3.3627
7.0	5.0904	3.1721		5.0647	3.2001		4.8465	3.5376		6.2107	4.9720	
8.0	6.6779	3.6457		6.1556	3.6702		5.9062	3.9666		7.2549	5.2649	
9.0		4.1169			4.1386			4.4003			5.7223	
10.0		4.5862			4.6057			4.8381			6.1724	
11.0		5.0544			5.0720			5.2799			6.6377	
12.0		5.5220			5.5380			5.7253			7.1181	

Table 12. The $Nu_x/(Re_x^{1/2} + Gr_x^{1/4})$ results for Power Law Variation of Surface Temperature, Mixed Convection, $\Omega_0 = 1.0$.

ξ	$Pr = 0.1$			$Pr = 0.7$			$Pr = 7$			$Pr = 100$		
	n			n			n			n		
	-0.4	0	0.5	-0.4	0	0.5	-0.4	0	0.5	-0.4	0	0.5
0	0.0451	0.1404	0.2007	0.1021	0.2927	0.4059	0.2343	0.6459	0.8856	0.5736	1.5720	2.1522
0.5	0.0898	0.1779	0.2425	0.1285	0.2955	0.4167	0.3238	0.5756	0.8268	0.4480	1.2973	1.9033
1.0	0.2334	0.2874	0.3259	0.2736	0.4139	0.4952	0.3995	0.6972	0.8604	0.6727	1.3761	1.7584
1.5	0.4208	0.4321	0.4351	0.4367	0.5552	0.6154	0.6055	0.8699	1.0031	0.9642	1.5748	1.8598
2.0	0.6251	0.5788	0.5294	0.6103	0.6982	0.7273	0.8127	1.0387	1.1434	1.2492	1.7762	2.0153
2.5	0.8453	0.7239	0.6071	0.8062	0.8396	0.8198	1.0209	1.1983	1.2601	1.5271	1.9692	2.1598
3.0	1.0800	0.8670	0.6725	1.0277	0.9788	0.8965	1.2397	1.3629	1.3640	1.8036	2.1544	2.2838
3.5	1.3277	1.0081	0.7291	1.2706	1.1155	0.9613	1.4688	1.5170	1.4504	2.0812	2.3326	2.3893
4.0	1.5872	1.1474	0.7792	1.5307	1.2500	1.0175	1.7020	1.6749	1.5244	2.3612	2.5046	2.4798
4.5	1.8575	1.2850		1.8046	1.3825		1.9431	1.8280		2.6442	2.6711	
5.0	2.1377	1.4211		2.0897	1.5135		2.1915	1.9762		2.9303	2.8327	
6.0	2.7255	1.6893		2.6873	1.7715		2.6847	2.2475		3.5117	3.1430	
7.0	3.3470	1.9528		3.3162	2.0258		3.2094	2.5038		4.1040	3.4384	
8.0	4.0000	2.2124		3.9746	2.2771		3.7935	2.7508		4.7073	3.7213	
9.0	4.6837	2.4686		4.6621	2.5262		4.4432	2.9906		5.3477	3.9941	
10.0	5.3980			5.3794			5.1546			5.9990		
11.0	6.1437			6.1273			5.9173			6.6933		

Table 13. The $Nu_x/(Re_x^{1/2} + Gr_x^{1/4})$ results for Power Law Variation of Surface Temperature, Mixed Convection, $\Omega_0 = 2.0$.

ξ	$Pr = 0.1$			$Pr = 0.7$			$Pr = 7$			$Pr = 100$		
	n			n			n			n		
	-0.4	0	0.5	-0.4	0	0.5	-0.4	0	0.5	-0.4	0	0.5
0	0.0451	0.1404	0.2007	0.1021	0.2927	0.4059	0.2343	0.6459	0.8856	0.5736	1.5720	2.1522
0.5	0.0748	0.1520	0.2031	0.1306	0.2683	0.3518	0.2407	0.5219	0.6912	0.4554	1.1300	1.5918
1.0	0.1994	0.2508	0.2810	0.2286	0.3776	0.4580	0.3707	0.6604	0.8150	0.6218	1.2584	1.5837
1.5	0.3293	0.3313	0.3535	0.3447	0.4829	0.5575	0.5213	0.8024	0.9611	0.8373	1.4528	1.7944
2.0	0.4685	0.4173	0.4062	0.4646	0.5774	0.6277	0.6672	0.9235	1.0611	1.0374	1.6103	1.9435
2.5	0.6161	0.5000	0.4471	0.5935	0.6644	0.6804	0.8108	1.0326	1.1361	1.2245	1.7463	2.0492
3.0	0.7710	0.5803		0.7331	0.7462		0.9540	1.1342		1.4060	1.8694	
3.5	0.9323	0.6587		0.8836	0.8243		1.0974	1.2300		1.5857	1.9834	
4.0	1.0994	0.7356		1.0443	0.8996		1.2412	1.3227		1.7652	2.0908	
4.5	1.2717	0.8112		1.2141	0.9728		1.3854	1.4107		1.9454	2.1930	
5.0	1.4489			1.3917			1.5304			2.1264		
6.0	1.8165			1.7656			1.8251			2.4920		
7.0	2.1999			2.1580			2.1323			2.8623		
8.0	2.5976			2.5638			2.4602			3.2371		
9.0	3.0087			2.9810			2.8164			3.6160		
10.0	3.4324			3.4092			3.2057			3.9988		
11.0	3.8683			3.8485			3.6287			4.3851		
12.0	4.3162			4.2990			4.0823			4.7748		

Table 15. The $f''(\xi, 0)$ results for Power Law Variation of Surface Temperature, Mixed Convection, $\Omega_0 = 0.02$.

ξ	$Pr = 0.1$			$Pr = 0.7$			$Pr = 7$			$Pr = 100$		
	n			n			n			n		
	-0.4	0	0.5	-0.4	0	0.5	-0.4	0	0.5	-0.4	0	0.5
0	0.3321	0.3321	0.3321	0.3321	0.3321	0.3321	0.3321	0.3321	0.3321	0.3321	0.3321	0.3321
0.5	0.4647	0.4677	0.4704	0.4640	0.4664	0.4702	0.4640	0.4664	0.4702	0.4640	0.4664	0.4702
1.0	0.7603	0.7603	0.7600	0.7602	0.7618	0.7600	0.7602	0.7643	0.7600	0.7602	0.7643	0.7600
1.5	1.1486	1.1337	1.1117	1.1492	1.1362	1.1185	1.1555	1.1434	1.1185	1.1555	1.1434	1.1185
2.0	1.6073	1.5628	1.4905	1.6085	1.5687	1.5067	1.6239	1.5799	1.5067	1.6239	1.5799	1.5067
2.5	2.1290	2.0371	1.8770	2.1304	2.0455	1.9004	2.1571	2.0649	1.9039	2.1571	2.0649	1.9039
3.0	2.7148	2.5547	2.2629	2.7156	2.5606	2.2858	2.7483	2.5873	2.2933	2.7483	2.5873	2.2933
3.5	3.3736	3.1215	2.6478	3.3739	3.1239	2.6589	3.3972	3.1436	2.6667	3.3972	3.1436	2.6667
4.0	4.1134	3.7415	3.0297	4.1135	3.7423	3.0330	4.1223	3.7494	3.0354	4.1223	3.7494	3.0352
4.5	4.9382	4.4141	3.4018	4.9383	4.4144	3.4026	4.9410	4.4164	3.4028	4.9410	4.4164	3.4025
5.0	5.8508	5.1370	3.7567	5.8508	4.5455	3.7567	5.8515	5.1375	3.7562	5.8515	5.1375	3.7557

Table 16. The $f''(\xi, 0)$ results for Power Law Variation of Surface Temperature, Mixed Convection, $\Omega_0 = 0.1$.

ξ	Pr = 0.1			Pr = 0.7			Pr = 7			Pr = 100		
	n			n			n			n		
	-0.4	0	0.5	-0.4	0	0.5	-0.4	0	0.5	-0.4	0	0.5
0	0.3321	0.3321	0.3321	0.3321	0.3321	0.3321	0.3321	0.3321	0.3321	0.3321	0.3321	0.3321
0.5	0.4115	0.4207	0.4356	0.4085	0.4178	0.4348	0.4084	0.4178	0.4348	0.4084	0.4178	0.4348
1.0	0.6077	0.6064	0.6063	0.6071	0.6069	0.6063	0.6071	0.6101	0.6063	0.6070	0.6100	0.6063
1.5	0.8648	0.8150	0.7478	0.8651	0.8174	0.7534	0.8709	0.8237	0.7551	0.8708	0.8236	0.8755
2.0	1.1518	1.0186	0.8362	1.1526	1.0225	0.8441	1.1677	1.0348	0.8497	1.1676	1.0345	0.8489
2.5	1.4617	1.2111	0.8796	1.4624	1.2148	0.8853	1.4881	1.2348	0.8954	1.4878	1.2341	0.8931
3.0	1.7963	1.3959	0.8976	1.7966	1.3971	0.8967	1.8256	1.4222	0.9067	1.8252	1.4209	0.9009
3.5	2.1611	1.5784	0.9048	2.1612	1.5783	0.9005	2.1786	1.5954	0.9001	2.1780	1.5901	0.8883
4.0	2.5573	1.7579	0.9052	2.5574	1.7575	0.8997	2.5618	1.7590	0.8856	2.5609	1.7531	0.8646
4.5	2.9825	1.9309	0.9003	2.9826	1.9304	0.8942	2.9830	1.9259	0.8699	2.9818	1.9198	0.8366
5.0	3.4338	2.0945	0.8920	3.4339	2.0941	0.8857	3.4334	2.0878	0.8519	3.4319	2.0796	0.8031
6.0		2.3912	0.8735		2.3908	0.8669		2.3835	0.8182		2.3692	0.7322
7.0			0.8599			0.8533			0.7945			0.6697
8.0			0.8539			0.8474			0.7869			0.6222
9.0			0.8550			0.8487			0.7912			0.5901
10.0			0.8550			0.8487			0.7912			0.5901

Table 17. The $f'(\xi, 0)$ results for Power Law Variation of Surface Temperature, Mixed Convection, $\Omega_0 = 0.5$.

ξ	$Pr = 0.1$			$Pr = 0.7$			$Pr = 7$			$Pr = 100$		
	-0.4	n 0	0.5	-0.4	n 0	0.5	-0.4	n 0	0.5	-0.4	n 0	0.5
0	0.3321	0.3321	0.3321	0.3321	0.3321	0.3321	0.3321	0.3321	0.3321	0.3321	0.3321	0.3321
0.5	0.2615	0.2738	0.3045	0.2423	0.2578	0.2996	0.2396	0.2570	0.2993	0.2373	0.2563	0.2992
1.0	0.2752	0.2644	0.2592	0.2651	0.2575	0.2542	0.2552	0.2503	0.2482	0.2473	0.2447	0.2435
1.5	0.3415	0.3028	0.2730	0.3312	0.2866	0.2498	0.3136	0.2690	0.2215	0.2980	0.2519	0.1984
2.0	0.4107	0.3573	0.3528	0.4044	0.3344	0.3075	0.3848	0.2966	0.2383	0.3589	0.2622	0.1828
2.5	0.4783	0.4191	0.4621	0.4791	0.3967	0.4017	0.4600	0.3322	0.2782	0.4139	0.2774	0.1853
3.0	0.5444	0.4814	0.5746	0.5491	0.4612	0.4997	0.5234	0.3673	0.3252	0.4761	0.2910	0.1964
3.5	0.6087	0.5399	0.6798	0.6138	0.5213	0.5920	0.5850	0.4011	0.3719	0.5371	0.3037	0.2115
4.0	0.6704	0.5928	0.7743	0.6746	0.5756	0.6755	0.6464	0.4391	0.4152	0.5959	0.3158	0.2277
4.5	0.7291	0.6399	0.8578	0.7324	0.6240	0.7498	0.7069	0.4795	0.4618	0.6526	0.3277	0.2436
5.0	0.7849	0.6816	0.9309	0.7876	0.6670	0.8154	0.7679	0.5206	0.5066	0.7073	0.3395	0.2585
6.0	0.8888	0.7507	1.0511	0.8907	0.7385	0.9248	0.8887	0.6074	0.5865	0.8116	0.3632	0.2851
7.0	0.9843	0.8048		0.9858	0.7945		0.9949	0.6800		0.9104	0.3866	
8.0	1.0739	0.8474		1.0750	0.8387		1.0873	0.7398		1.0053	0.4093	
9.0		0.8814			0.8740			0.7889			0.4310	
10.0		0.9089			0.9025			0.8293			0.4510	
11.0		0.9313			0.9258			0.8625			0.4741	
12.0		0.9499			0.9451			0.8902			0.5004	

Table 18. The $f''(\xi, 0)$ results for Power Law Variation of Surface Temperature, Mixed Convection, $\Omega_0 = 1.0$.

ξ	$Pr = 0.1$			$Pr = 0.7$			$Pr = 7$			$Pr = 100$		
	-0.4	n	0.5	-0.4	n	0.5	-0.4	n	0.5	-0.4	n	0.5
0	0.3321	0.3321	0.3321	0.3321	0.3321	0.3321	0.3321	0.3321	0.3321	0.3321	0.3321	0.3321
0.5	0.2254	0.1980	0.2135	0.1933	0.1727	0.2048	0.1745	0.1653	0.2026	0.1570	0.1592	0.2008
1.0	0.2746	0.2364	0.2152	0.2394	0.2048	0.1879	0.1889	0.1653	0.1543	0.1447	0.1423	0.1266
1.5	0.3656	0.3562	0.3686	0.3261	0.3003	0.3003	0.2428	0.2173	0.2092	0.1731	0.1505	0.1344
2.0	0.4491	0.4786	0.5362	0.4188	0.4090	0.4334	0.2995	0.2742	0.2816	0.2055	0.1739	0.1619
2.5	0.5217	0.5910	0.6807	0.5068	0.5148	0.5508	0.3535	0.3271	0.3466	0.2365	0.1966	0.1898
3.0	0.5825	0.6907	0.7987	0.5806	0.6107	0.6498	0.4074	0.3815	0.4043	0.2660	0.2179	0.2141
3.5	0.6317	0.7779	0.8944	0.6387	0.6963	0.7299	0.4616	0.4315	0.4519	0.2939	0.2376	0.2344
4.0	0.6710	0.8537	0.9726	0.6828	0.7724	0.7953	0.5148	0.4851	0.4913	0.3206	0.2559	0.2512
4.5	0.7025	0.9193		0.7157	0.8398		0.5691	0.5370		0.3462	0.2729	
5.0	0.7283	0.9760		0.7408	0.8333		0.6524	0.5874		0.3708	0.2888	
6.0	0.7682	1.0671		0.7743	0.9976		0.7197	0.6719		0.4175	0.3176	
7.0	0.7987	1.1345		0.8051	1.0733		0.7927	0.7448		0.4611	0.3431	
8.0	0.8234	1.1842		0.8280	1.1312		0.8442	0.8085		0.5015	0.3656	
9.0	0.8442	1.2208		0.8477	1.1751		0.8773	0.8645		0.5472	0.3857	
10.0	0.8625			0.8652			0.8975			0.5855		
11.0	0.8791			0.8812			0.9104			0.6322		

Table 19. The $f''(\xi, 0)$ results for Power Law Variation of Surface Temperature, Mixed Convection, $\Omega_0 = 2.0$.

ξ	Pr = 0.1			Pr = 0.7			Pr = 7			Pr = 100		
	-0.4	n 0	0.5	-0.4	n 0	0.5	-0.4	n 0	0.5	-0.4	n 0	0.5
0	0.3321	0.3321	0.3321	0.3321	0.3321	0.3321	0.3321	0.3321	0.3321	0.3321	0.3321	0.3321
0.5	0.3457	0.2178	0.1619	0.2988	0.1836	0.3142	0.2338	0.1469	0.1265	0.1712	0.1152	0.1211
1.0	0.4758	0.4072	0.3579	0.4067	0.3277	0.2862	0.2806	0.2221	0.1955	0.1691	0.1319	0.1168
1.5	0.5925	0.5902	0.5848	0.5225	0.4713	0.4605	0.3473	0.3087	0.3007	0.1983	0.1729	0.1668
2.0	0.6856	0.7350	0.7478	0.6255	0.5891	0.5886	0.4095	0.3788	0.3777	0.2267	0.2058	0.2050
2.5	0.7592	0.8515	0.8627	0.7144	0.6896	0.6802	0.4675	0.4367	0.4334	0.2527	0.2319	0.2321
3.0	0.8162	0.9476		0.7882	0.7762		0.5223	0.4859		0.2766	0.2534	
3.5	0.8585	1.0284		0.8462	0.8513		0.5742	0.5292		0.2991	0.2715	
4.0	0.8882	1.0975		0.8889	0.9173		0.6235	0.5686		0.3204	0.2872	
4.5	0.9073	1.1573		0.9176	0.9759		0.6700	0.6036		0.3409	0.3010	
5.0	0.9180			0.9343			0.7135			0.3606		
6.0	0.9233			0.9425			0.7900			0.3985		
7.0	0.9178			0.9335			0.8505			0.4346		
8.0	0.9088			0.9200			0.8936			0.4694		
9.0	0.8989			0.9069			0.9194			0.5029		
10.0	0.8891			0.8950			0.9299			0.5355		
11.0	0.8797			0.8842			0.9283			0.5669		
12.0	0.8709			0.8744			0.9186			0.5973		

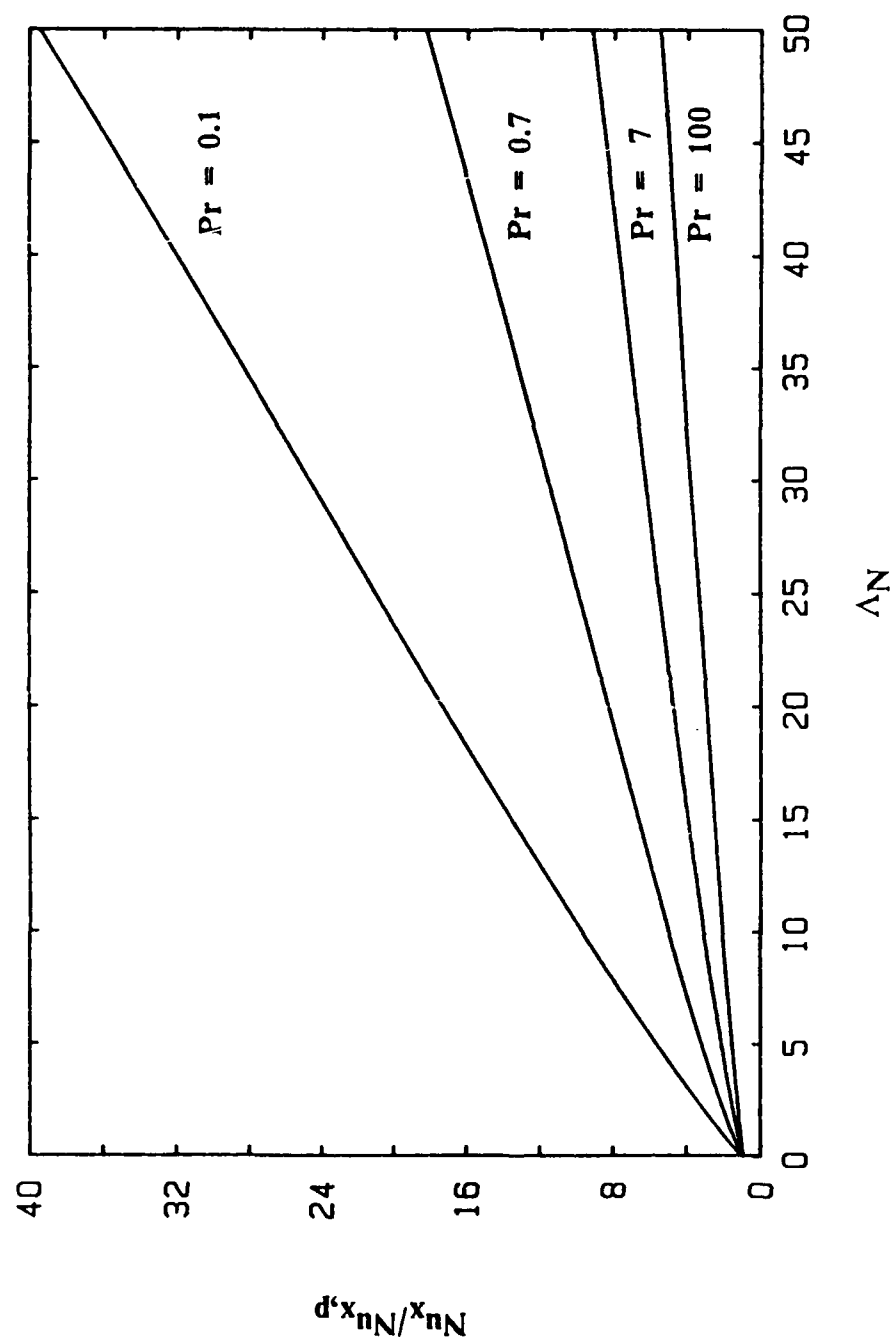


Figure 1. $Nu_x/Nu_{x,p}$ vs. Λ_N for Pure Free Convection, UWT.

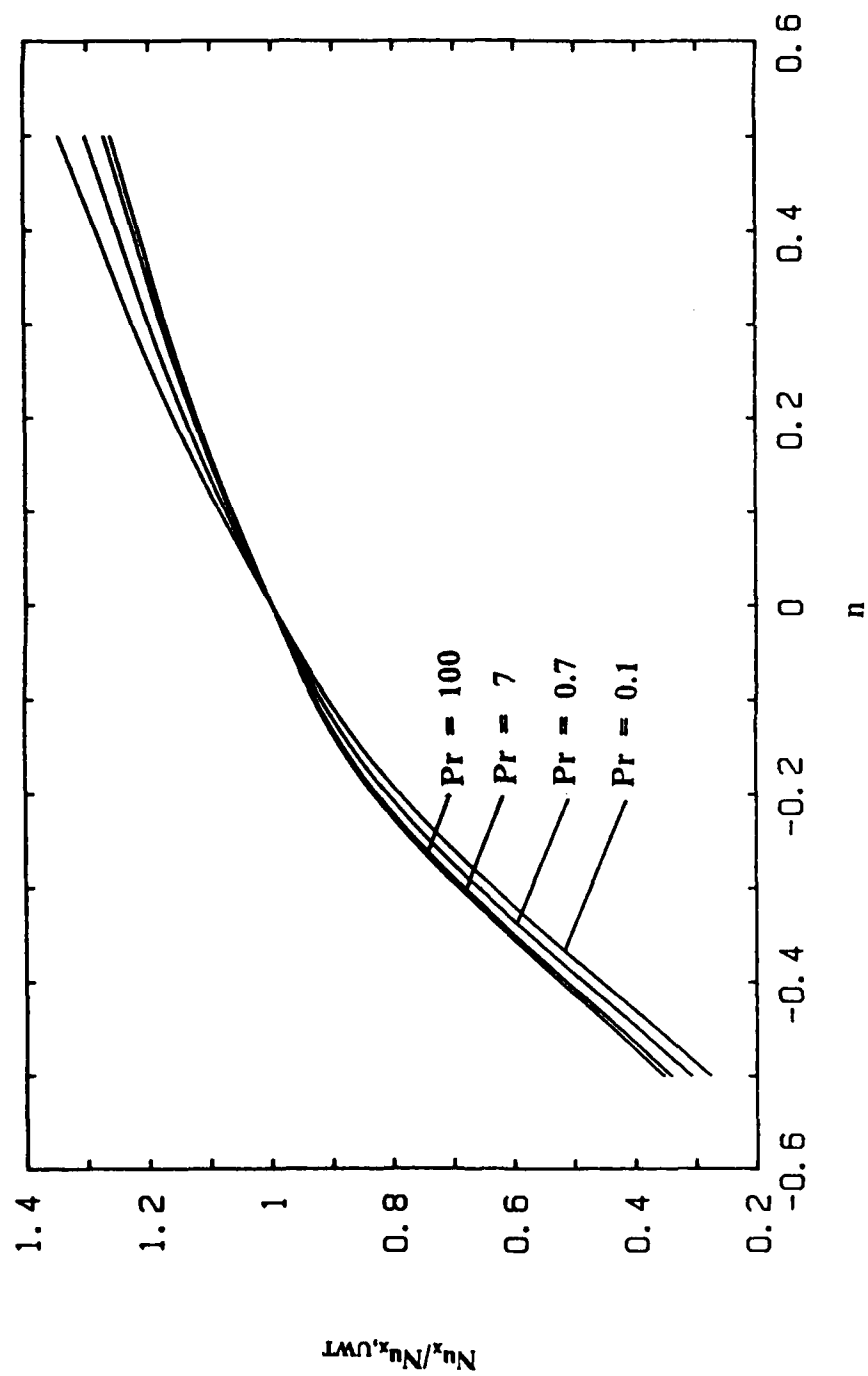


Figure 2. $Nu_x / Nu_{x,WT}$ vs. n for Pure Free Convection, Flat Plates.

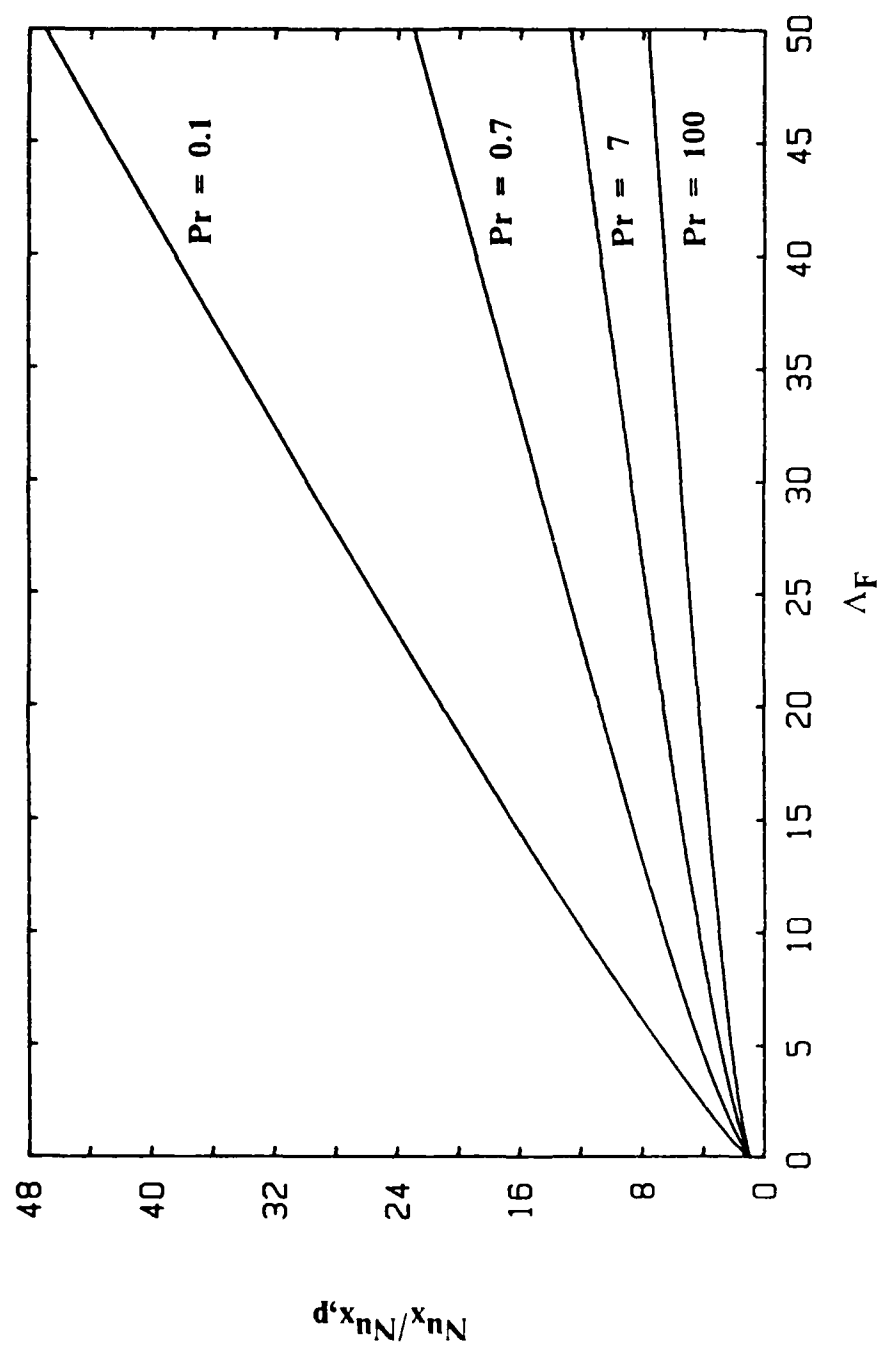


Figure 3. $Nu_x/Nu_{x,p}$ vs. Λ_F for Pure Forced Convection, UWT.

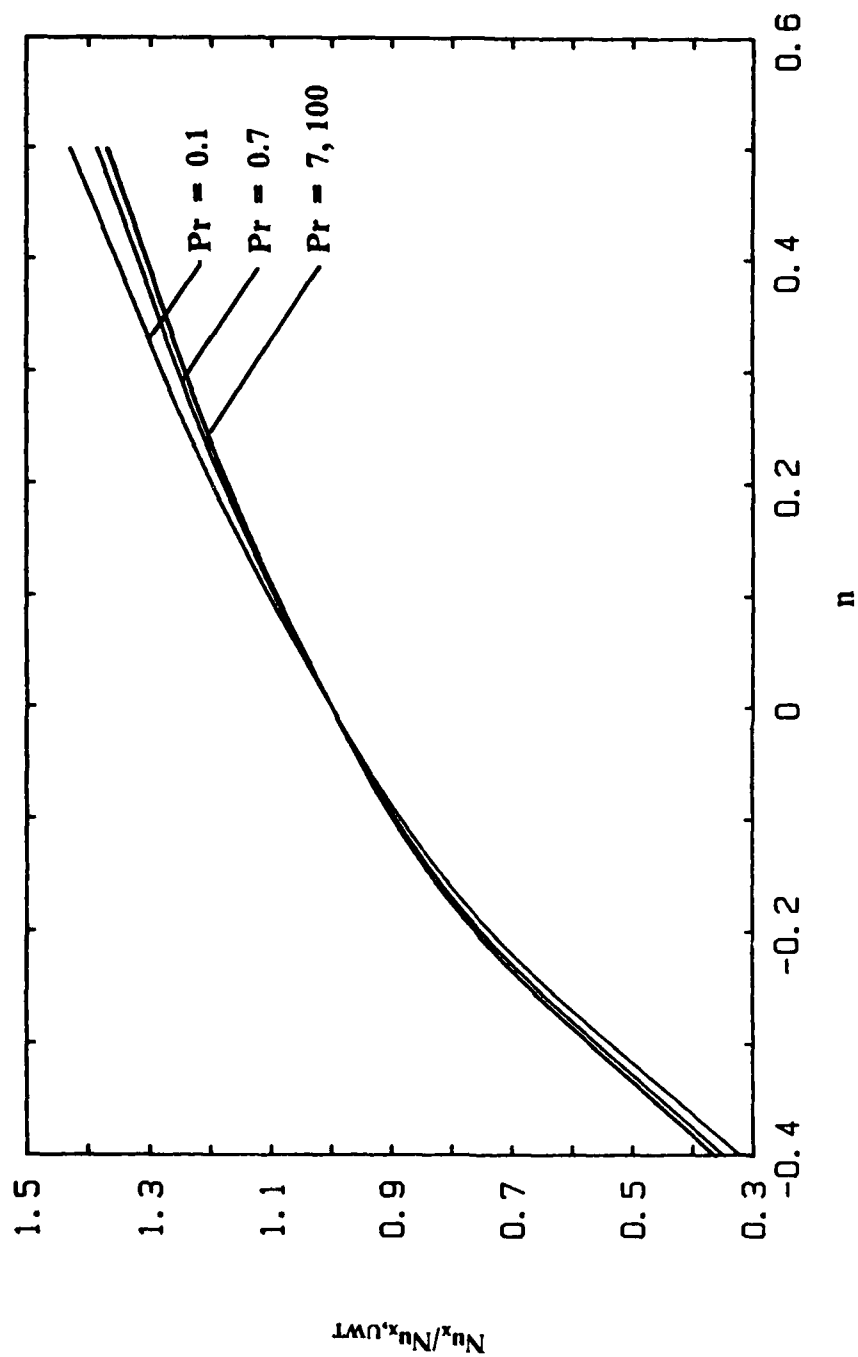


Figure 4. $Nu_x/Nu_{x,uWT}$ vs. n for Pure Forced Convection, Flat Plates.

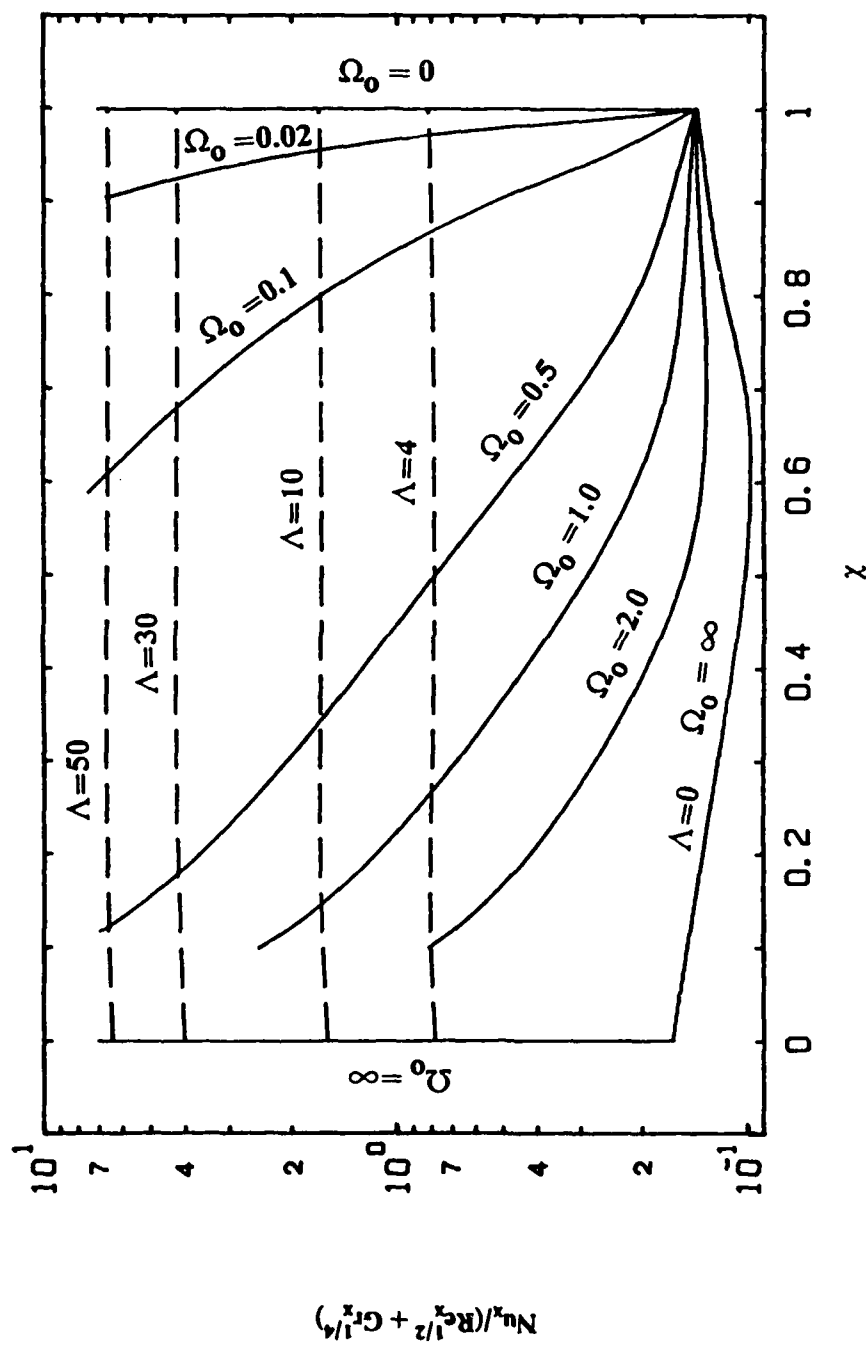


Figure 5. $Nu_x / (Re_x^{1/2} + Gr_x^{1/4})$ vs. χ for Mixed Convection, $Pr = 0.1$, UWT

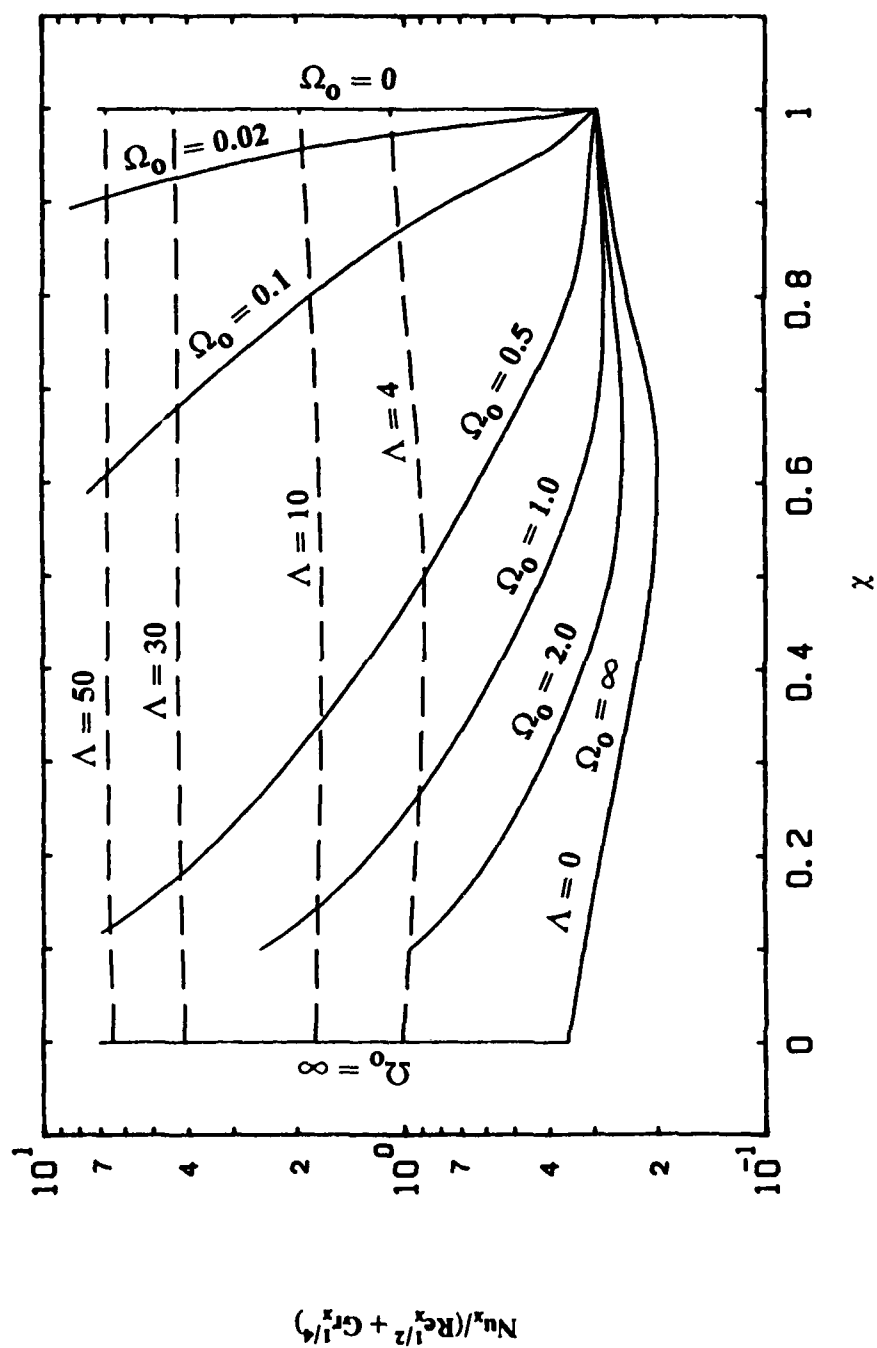


Figure 6. $Nu_x / (Re_x^{1/2} + Gr_x^{1/4})$ vs. χ for Mixed Convection, $Pr = 0.7$, UWT

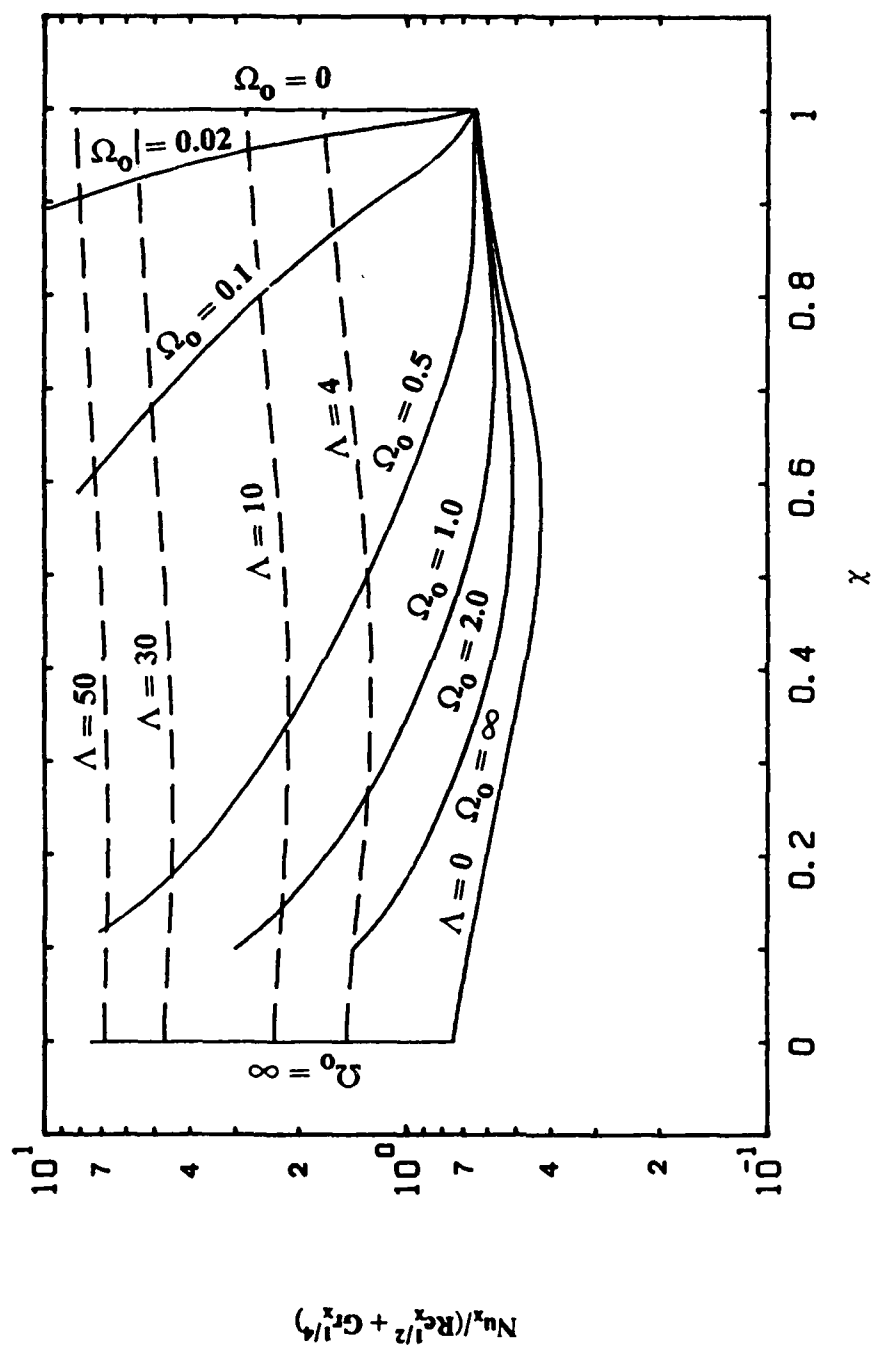


Figure 7. $Nu_x / (Re_x^{1/2} + Gr_x^{1/4})$ vs. χ for Mixed Convection, $Pr = 7$, UWT

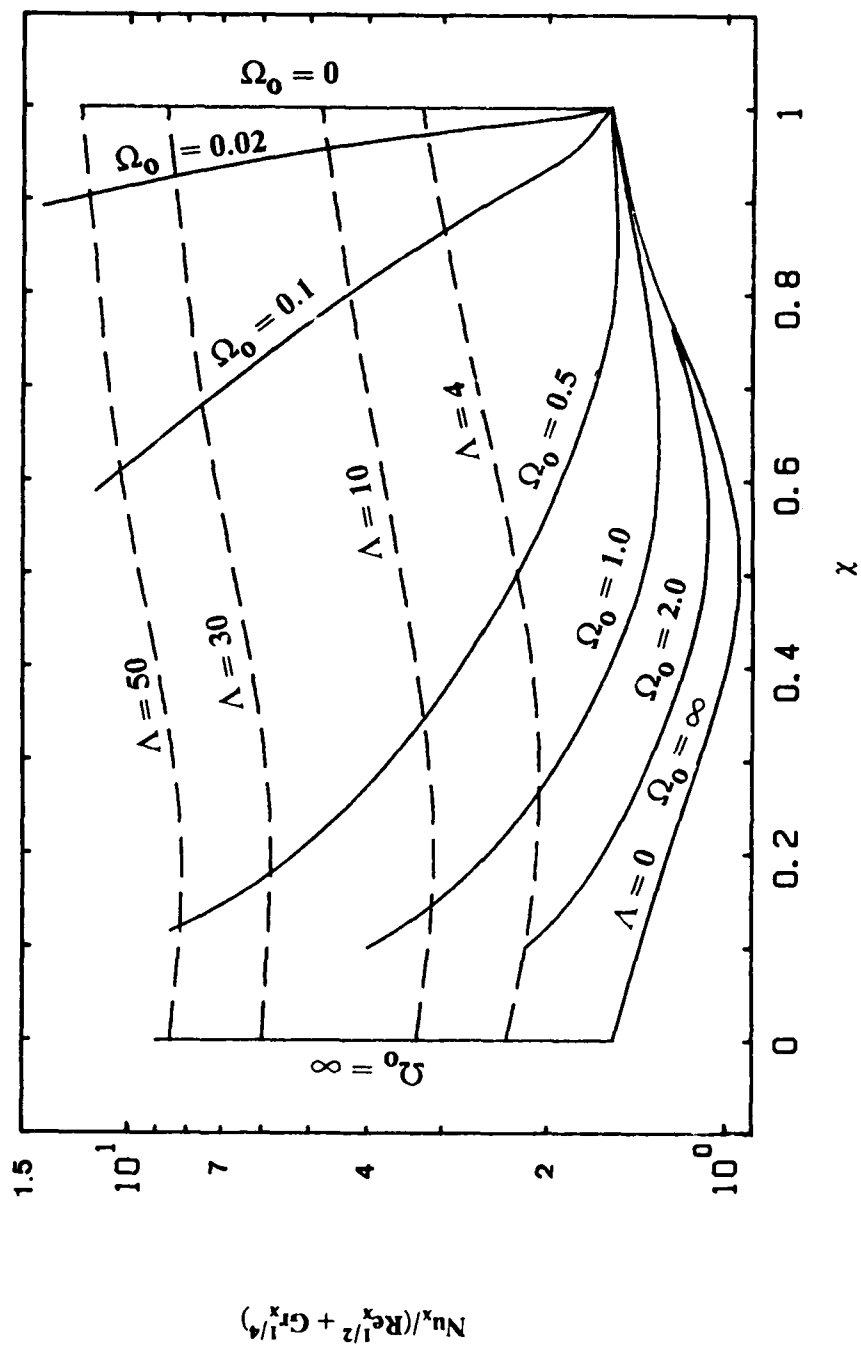


Figure 8. $Nu_x / (Re_x^{1/2} + Gr_x^{1/4})$ vs. x for Mixed Convection, $Pr = 100$, UWT

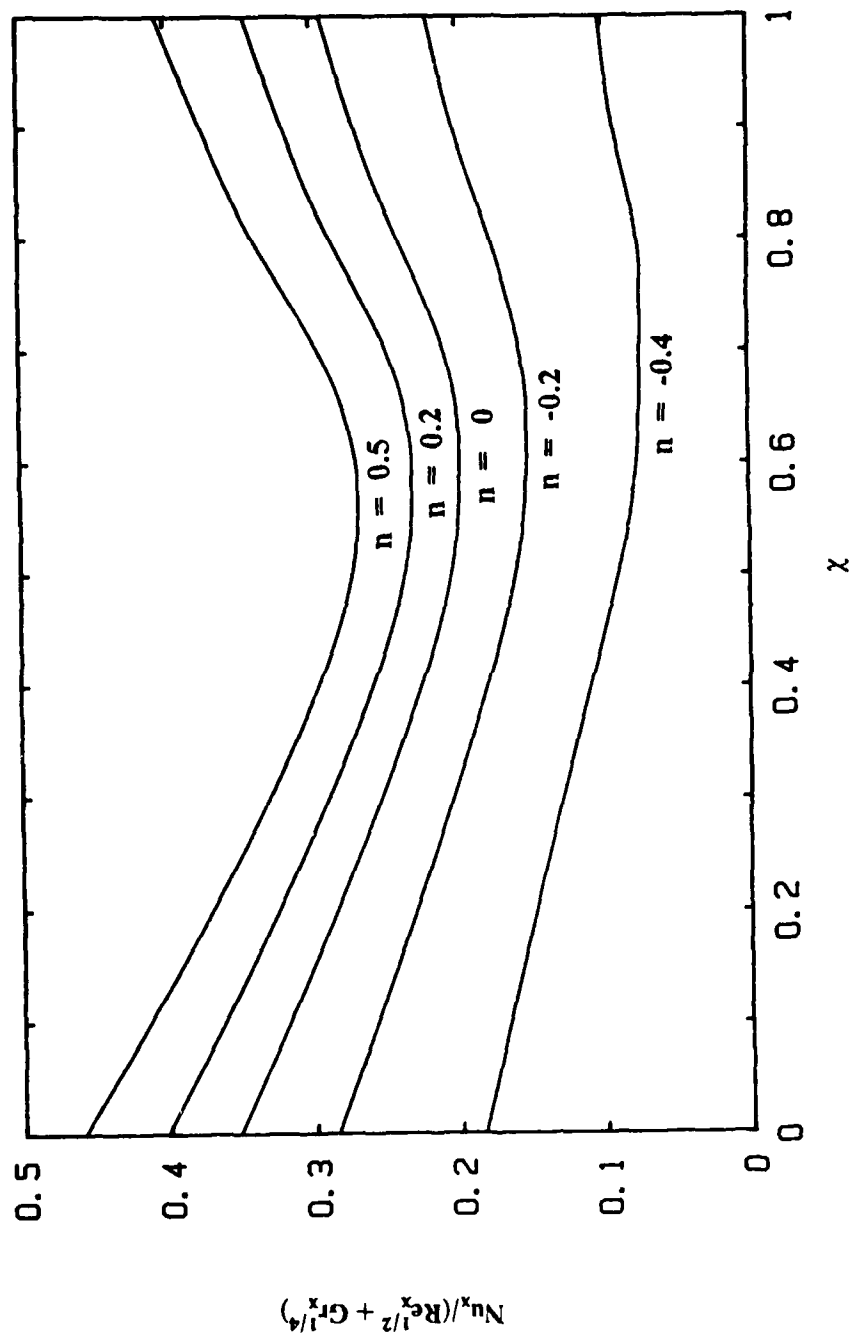


Figure 9. $Nu_x / (Re_x^{1/2} + Gr_x^{1/4})$ vs. x for Mixed Convection, $Pr = 0.7$, $\Lambda = 0$ (Flat Plate).

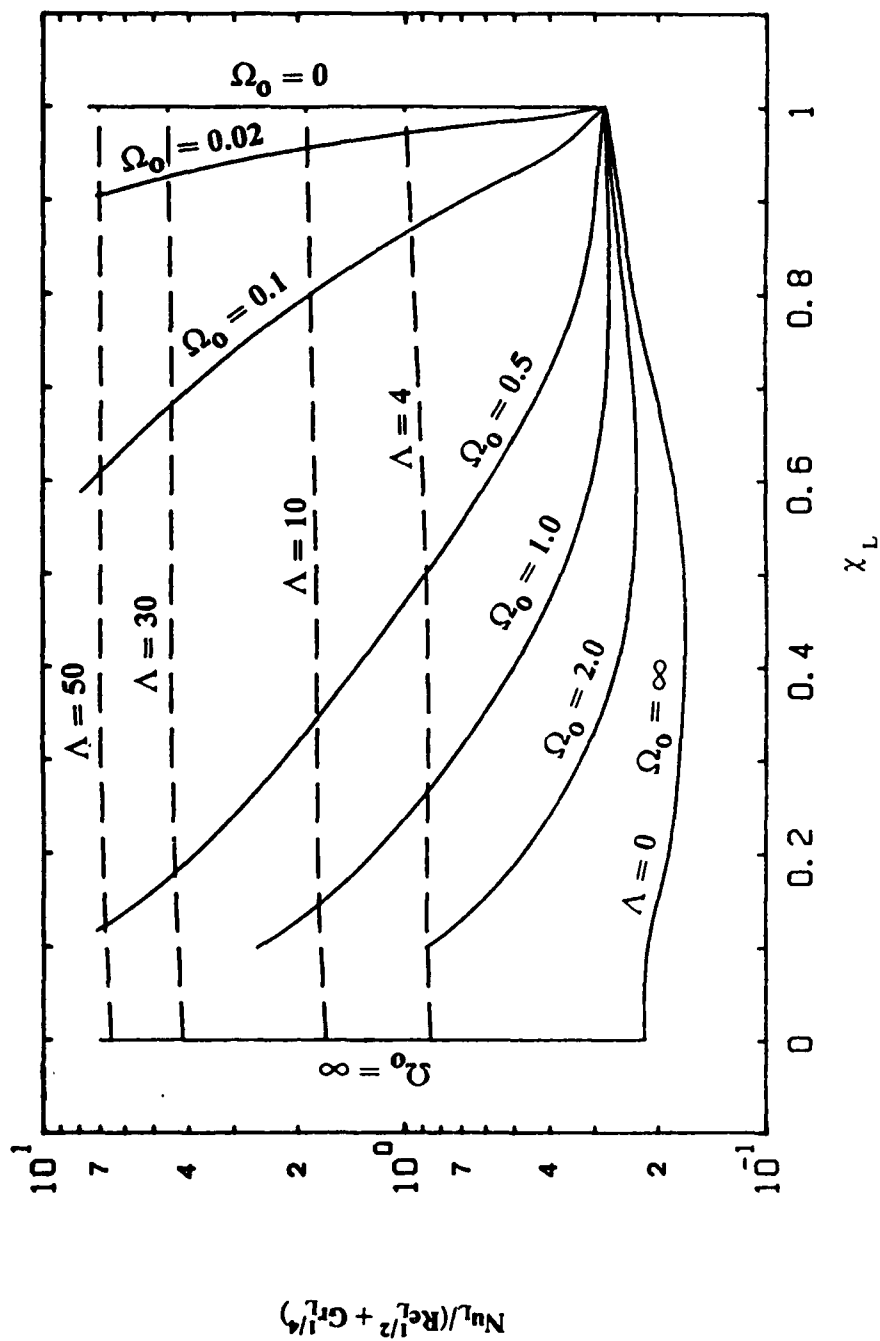


Figure 10. $Nu_L / (Re_L^{1/2} + Gr_L^{1/4})$ vs. χ_L for Mixed Convection, $Pr = 0.1$, UWT

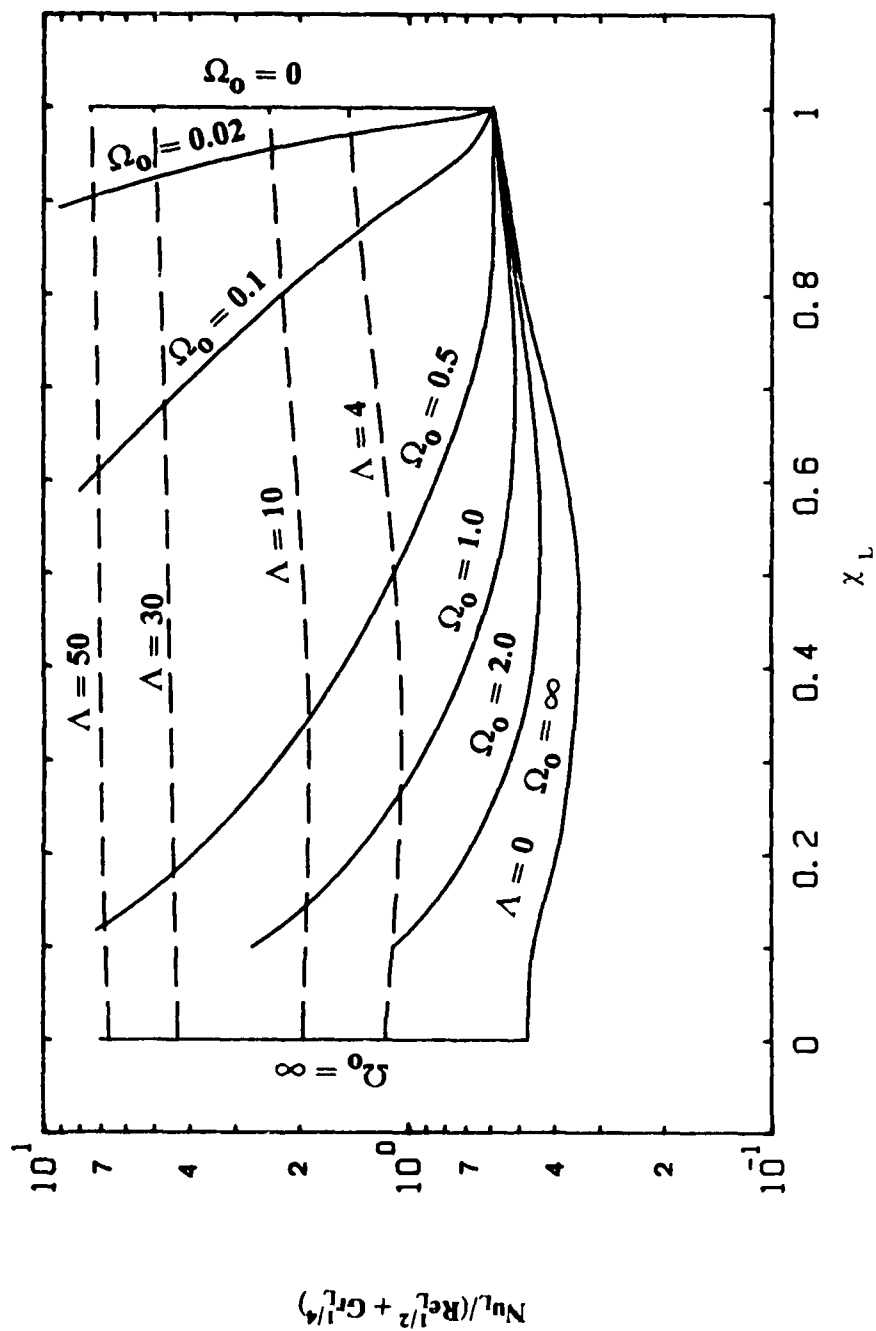


Figure 11. $Nu_L / (Re_L^{1/2} + Gr_L^{1/4})$ vs. χ_L for Mixed Convection, $Pr = 0.7$, UWT

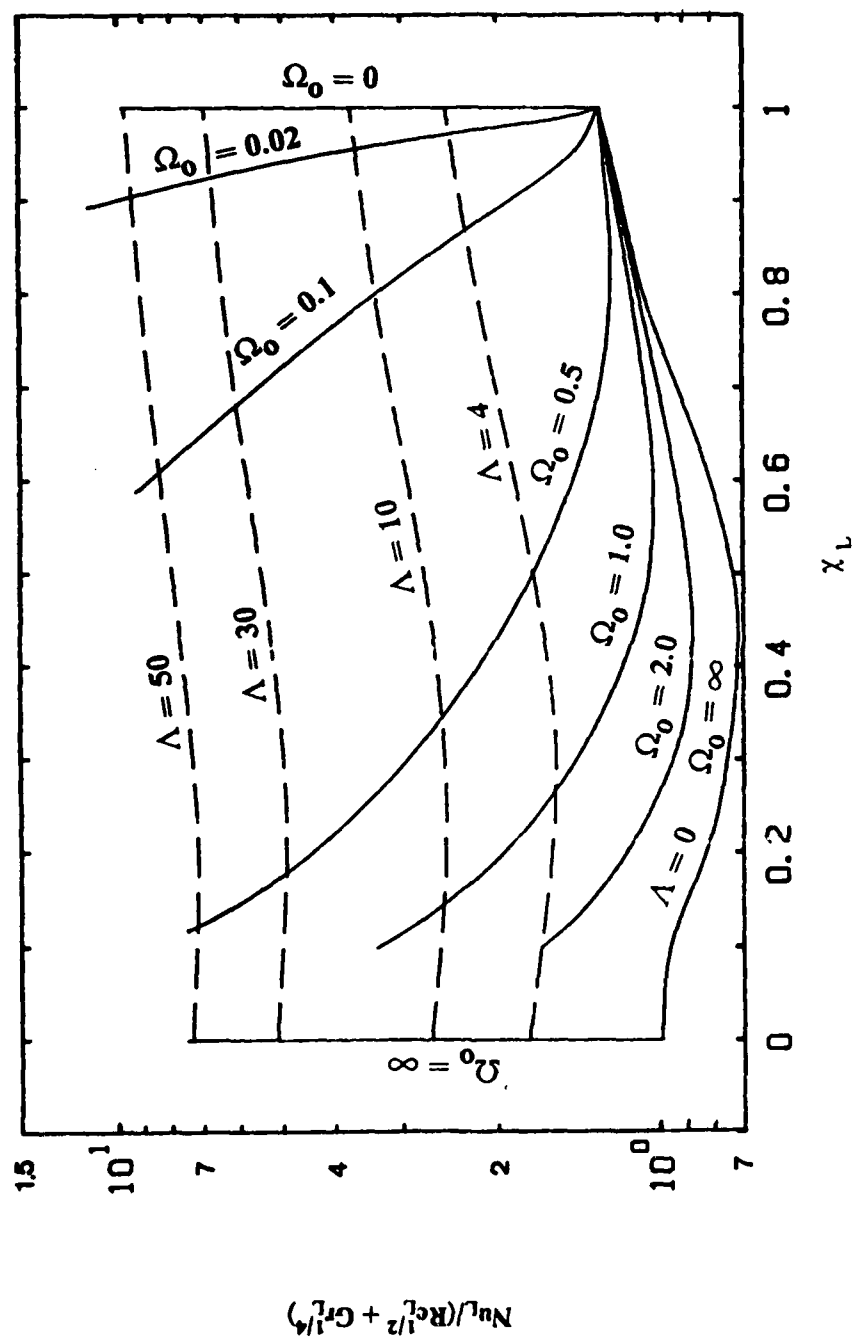


Figure 12. $Nu_L / (Re_L^{1/2} + Gr_L^{1/4})$ vs. x_L for Mixed Convection, $Pr = 7$, UWT

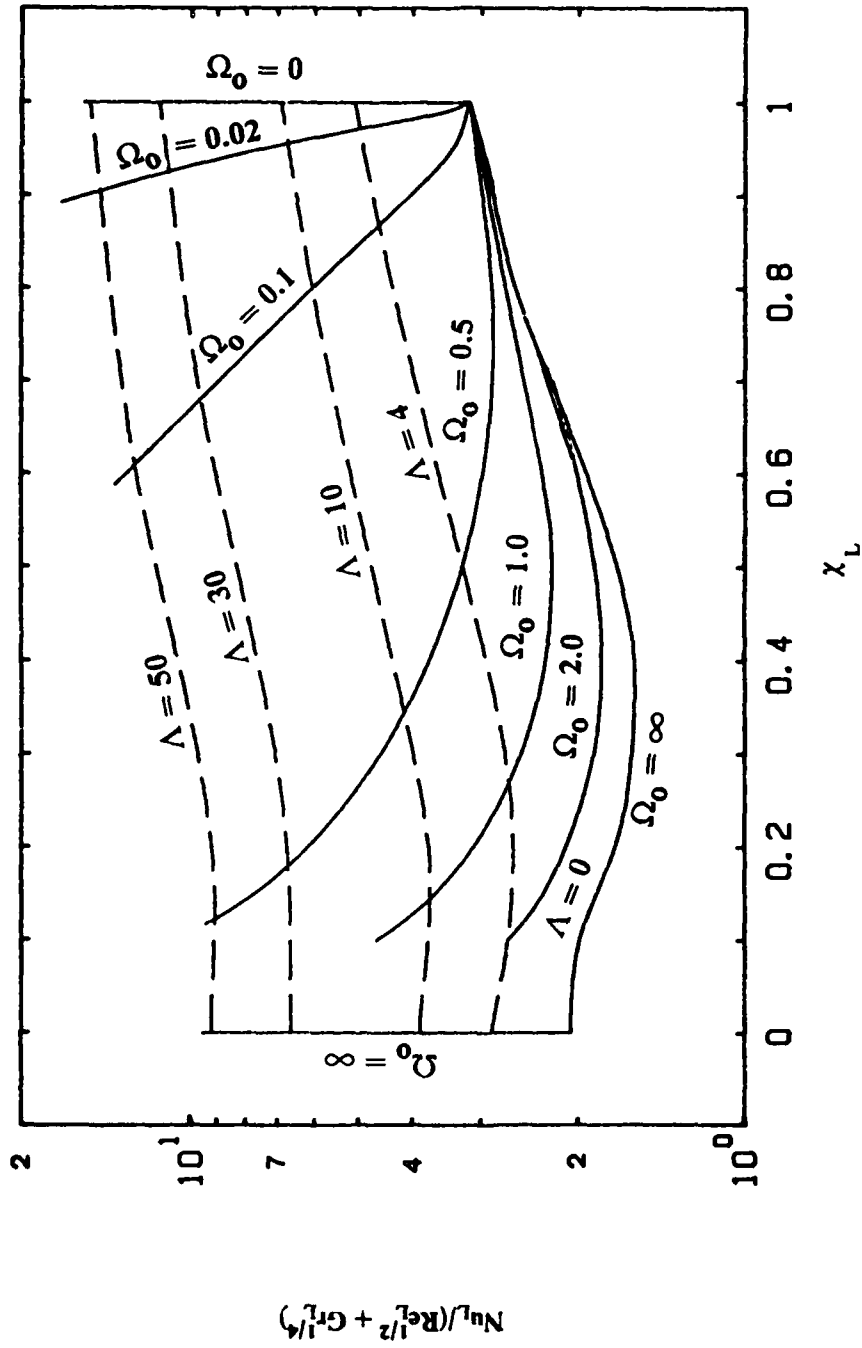


Figure 13. $Nu_L / (Re_L^{1/2} + Gr_L^{1/4})$ vs. x_L for Mixed Convection, $Pr = 100$, UWT

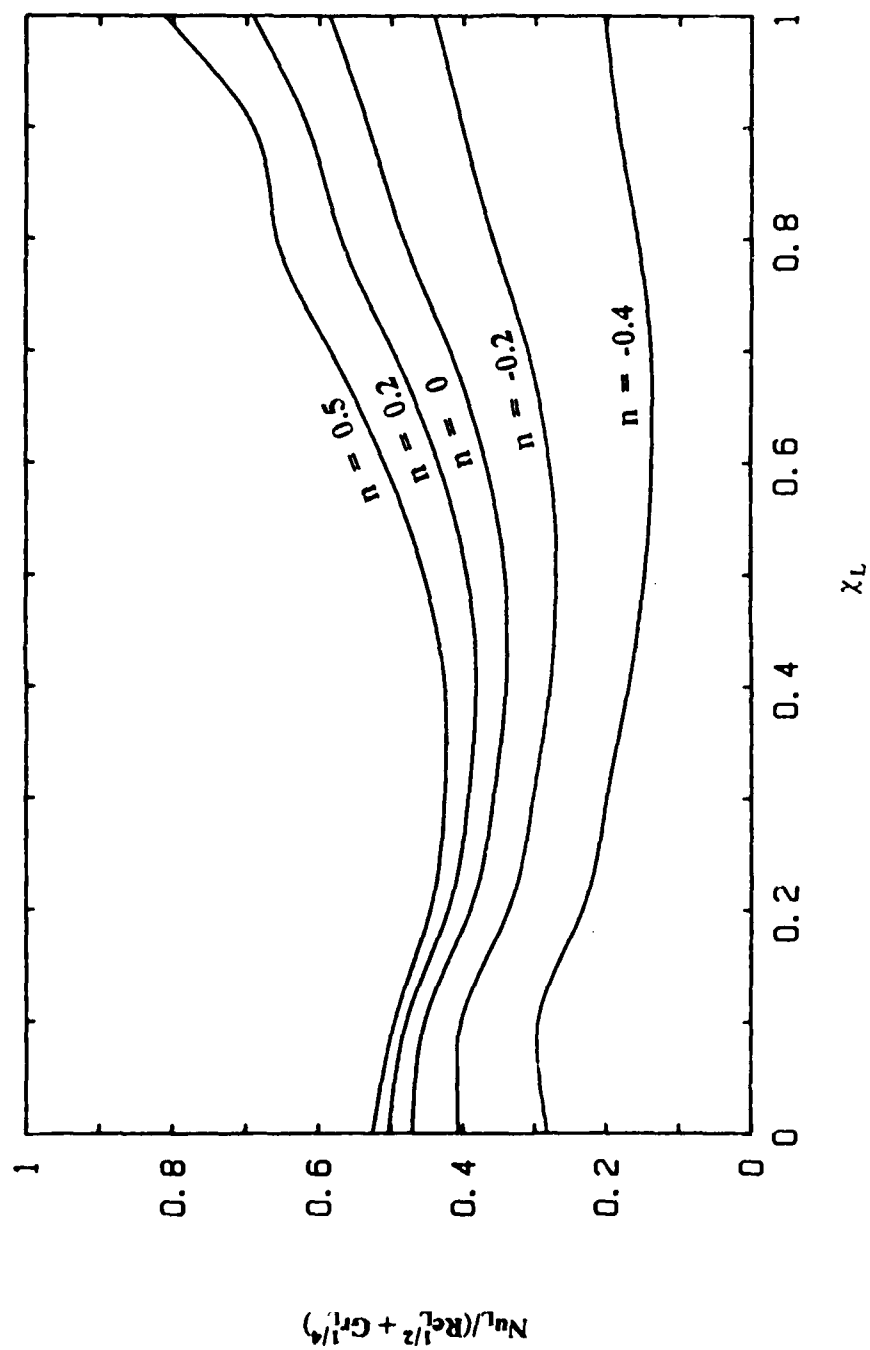


Figure 14: $Nu_L / (Re_L^{1/2} + Gr_L^{1/4})$ vs. x_L for Mixed Convection, $Pr = 0.7$, $\Lambda = 0$ (Flat Plate).

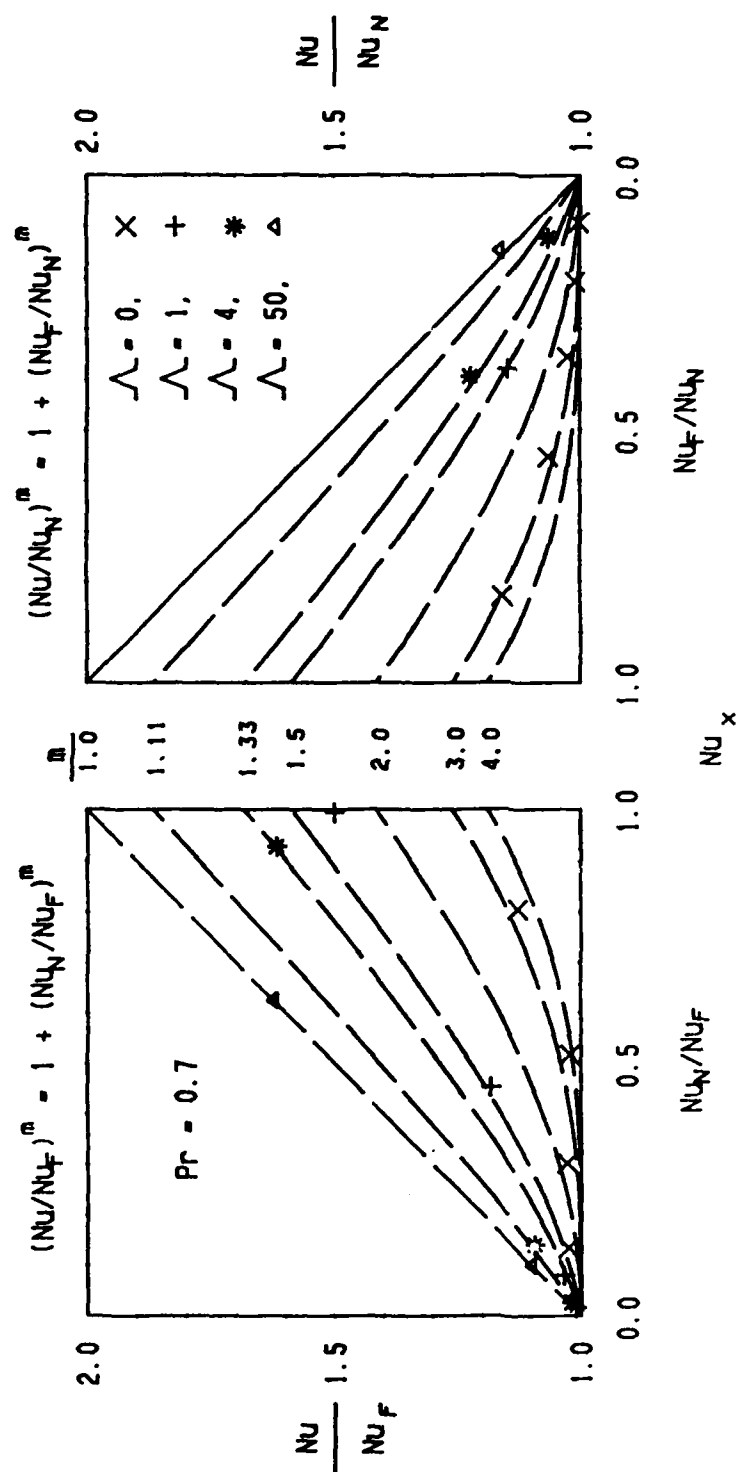


Figure 15. Development of a Correlation Equation For Buoyancy-Assisting, Mixed Convection.

IV. RECOMMENDATIONS FOR FURTHER STUDY

From the present study it was found that there exists a need to develop an accurate way of extending η_∞ in the numerical computations. Large values of η_∞ are required at high curvatures, but starting out at a large value is both numerically inefficient and can result in calculations beyond the precision capabilities of the computer. Therefore η_∞ must be increased gradually from its initial value of, say, 10. Secondly, the decision must be made as to when η_∞ is sufficient. This could be done by comparing both the boundary conditions and some select points on the velocity and temperature profiles for the solution at one value of η_∞ with the solution for an increased value of η_∞ while keeping the step size $\Delta\eta$ fixed. When there is no longer a change in these values, then the solution at that node is accepted and the problem advances to the next node in the ξ direction. Limitations to this might be the memory capability of the computer or precision difficulties if the thermal boundary layer is vastly different from the flow boundary layer. This can occur for both low and high Prandtl numbers. The memory problem can be helped by trying a step size initially of 0.05. With the increased value of η_∞ this may provide sufficient accuracy and should reduce the number of nodes in the radial direction.

Experimental results are needed for flow along vertical cylinders for the full range of mixed convection, ranging from pure forced convection to pure free convection, under various surface heating conditions. Experimental results are essential to determine the extent to which the imposed surface temperature variation in the analysis can be realized in the physical world. The singularity at $x=0$ for the case of $n < 0$ in the power law variation of the surface temperature, $T_w(x) - T_\infty = ax^n$, for example, must be accounted for and an experiment is the only real way this can be checked.

Variations of the problem to include transition to turbulence, or unsteady variations in wall temperature could be addressed. These should be done in conjunction with experiments when possible to prove their applicability or to provide information such as when and what type of transitions to turbulence occurs.

VITA

Jeffrey John Heckel [REDACTED] He received his Bachelor of Science degree from the United States Military Academy in June 1979. He has served as an officer in the Air Defense Artillery Branch of the United States Army since June 1979. He has served in assignments at Schofield Barracks, Hawaii and at Fort Leonard Wood, Missouri. While stationed at Fort Leonard Wood, he enrolled in the Graduate School of the University of Missouri-Rolla. In May 1986 he received his Master of Science degree in Engineering Management. Since June 1986 he has pursued a Master of Science degree in Mechanical Engineering. His next assignment will be as an instructor at the United States Military Academy.

APPENDIX A

TRANSFORMATION OF THE GOVERNING SYSTEM OF EQUATIONS IN

CHAPTER 2

In Chapter 2 the solution for the case of natural convection along a slender, vertical cylinder with variable surface heat flux is presented. Consider a semi-infinite, vertical cylinder with radius r_0 that is aligned in a quiescent ambient fluid at temperature T_∞ . The axial coordinate x is measured upward when $q_w > 0$ and downward when $q_w < 0$. The radial coordinate r is measured from the axis of the cylinder. The surface of the cylinder is subjected to an arbitrary heat flux $q_w(x)$ and the gravitational acceleration g is acting downward. The fluid properties are assumed to be constant except for variations in density which induce the buoyancy force. By employing the laminar boundary layer assumptions and making use of the Boussinesq approximation the governing conservation equations can be written as:

Continuity:

$$\frac{\partial}{\partial x}(ru) + \frac{\partial}{\partial r}(rv) = 0 \quad (A-1)$$

Momentum:

$$u \frac{\partial u}{\partial x} + v \frac{\partial u}{\partial r} = \frac{\nu}{r} \frac{\partial}{\partial r} \left(r \frac{\partial u}{\partial r} \right) + g\beta(T - T_\infty) \quad (A-2)$$

Energy:

$$u \frac{\partial T}{\partial x} + v \frac{\partial T}{\partial r} = \frac{\alpha}{r} \frac{\partial}{\partial r} \left(r \frac{\partial T}{\partial r} \right) \quad (A-3)$$

In these equations u and v are the velocity components in the x and r directions respectively; T is the fluid temperature; and ν , β and α are, respectively, the kinematic viscosity, the volumetric coefficient of thermal expansion and the thermal diffusivity of the fluid.

The boundary conditions are

$$u = v = 0, \quad \frac{\partial T}{\partial r} = -\frac{q_w(x)}{k} \quad \text{at } r = r_0 \quad (A-4)$$

$$u \rightarrow 0, \quad T \rightarrow T_\infty \quad \text{As } r \rightarrow \infty \quad (A-5)$$

$$u = 0, \quad T = T_\infty \quad \text{At } x = 0, r \geq r_0 \quad (A-6)$$

In writing the last boundary condition it is assumed that the flow and thermal boundary layer thicknesses are zero at the leading edge of the surface.

The conservation equations, along with the boundary conditions, are transformed into a dimensionless form by introducing the following dimensionless variables:

$$\eta = \frac{[r^2 - r_0^2]}{2r_0x} (Gr_x^*/5)^{1/5}, \quad \lambda = \frac{2x}{r_0} (Gr_x^*/5)^{-1/5} \quad (A-7)$$

$$f(\lambda, \eta) = \psi(x, r) / [5\nu r_0 (Gr_x^*/5)^{1/5}], \quad \theta(\lambda, \eta) = \frac{(T - T_\infty)(Gr_x^*/5)^{1/5}}{q_w(x) x/k} \quad (A-8)$$

$$Gr_x^* = g\beta q_w(x) x^4 / k\nu^2 \quad (A-9)$$

where η is the pseudo-similarity variable, $f(\lambda, \eta)$ is the reduced stream function, $\theta(\lambda, \eta)$ is the dimensionless temperature, λ is the curvature parameter, and $\psi(x, r)$ is the stream function that satisfies the continuity equation, with $u = (\partial\psi/\partial r)/r$ and $v = -(\partial\psi/\partial x)/r$. The transformation yields

$$u = 5\frac{\nu}{x} (Gr_x^*/5)^{2/5} f'(\lambda, \eta) \quad (A-10)$$

$$v = -5\nu \frac{r_o}{r} \left(\frac{g\beta}{5k\nu^2} \right)^{1/5} \left\{ \left(\frac{\partial f}{\partial \lambda} \frac{\partial \lambda}{\partial x} + f' \frac{\partial \eta}{\partial x} \right) (q_w^{1/5} x^{4/5}) + f \left[\frac{1}{5} q_w^{-4/5} \frac{\partial q_w}{\partial x} x^{4/5} + \frac{4}{5} x^{-1/5} q_w^{1/5} \right] \right\} \quad (A-11)$$

$$\frac{\partial u}{\partial x} = 5\nu \left(\frac{g\beta}{5k\nu^2} \right)^{2/5} \left\{ \left(\frac{\partial f'}{\partial \lambda} \frac{\partial \lambda}{\partial x} + f'' \frac{\partial \eta}{\partial x} \right) (q_w^{2/5} x^{3/5}) + f' \left[\frac{2}{5} q_w^{-3/5} \frac{\partial q_w}{\partial x} x^{3/5} + \frac{3}{5} x^{-2/5} q_w^{2/5} \right] \right\} \quad (A-12)$$

$$\frac{\partial u}{\partial r} = 5\nu (Gr_x^*/5)^{3/5} x^{-2} \frac{r}{r_o} f''(\lambda, \xi) \quad (A-13)$$

$$\frac{\partial}{\partial r} \left(r \frac{\partial u}{\partial r} \right) = 10\nu (Gr_x^*/5)^{3/5} x^{-2} \frac{r}{r_o} f' + 5\nu (Gr_x^*/5)^{4/5} x^{-3} \frac{r^3}{r_o^2} f'' \quad (A-14)$$

$$T - T_\infty = \frac{q_w x}{k} (Gr_x^*/5)^{-1/5} \theta(\lambda, \eta) \quad (A-15)$$

$$\frac{\partial T}{\partial x} = \frac{1}{k} \left(\frac{g\beta}{5k\nu^2} \right)^{-1/5} \left\{ \left(\frac{\partial \theta}{\partial \lambda} \frac{\partial \lambda}{\partial x} + \theta' \frac{\partial \eta}{\partial x} \right) (q_w^{4/5} x^{1/5}) + \theta \left[\frac{4}{5} q_w^{-1/5} \frac{\partial q_w}{\partial x} x^{1/5} + \frac{1}{5} x^{-4/5} q_w^{4/5} \right] \right\} \quad (A-16)$$

$$\frac{\partial T}{\partial r} = \frac{q_w}{k} \frac{r}{r_o} \theta'(\lambda, \xi) \quad (A-17)$$

$$\frac{\partial}{\partial r} \left(r \frac{\partial T}{\partial r} \right) = 2 \frac{q_w}{k} \frac{r}{r_o} \theta' + \frac{q_w}{k} x^{-1} (Gr_x^*/5)^{1/5} \frac{r^3}{r_o^2} \theta'' \quad (A-18)$$

in which the primes denote partial differentiation with respect to η .

Substitution of equations (A-10) through (A-18) into equations (A-1) through (A-6) results in

$$(1 + \eta\lambda)f''' + \lambda f'' + (\gamma + 4)ff'' - (2\gamma + 3)f^2 + \theta = \lambda(\gamma - 1)\left(f' \frac{\partial f}{\partial \lambda} - f \frac{\partial f'}{\partial \lambda}\right) \quad (A-19)$$

$$(1 + \eta\lambda)\theta'' + \lambda\theta' + \text{Pr}(\gamma + 4)f\theta' - \text{Pr}(4\gamma + 1)f'\theta = \text{Pr}\lambda(\gamma - 1)\left(\theta' \frac{\partial f}{\partial \lambda} - f \frac{\partial \theta}{\partial \lambda}\right) \quad (A-20)$$

$$\begin{aligned} f(\lambda, 0) = f'(\lambda, 0) = 0, \quad \theta'(\lambda, 0) = -1 \\ f'(\lambda, \infty) = 0, \quad \theta(\lambda, \infty) = 0 \end{aligned} \quad (A-21)$$

where

$$\gamma = \frac{x}{q_w} \frac{dq_w}{dx} \quad (A-22)$$

The system of equations (A-19) through (A-22) represents the general form of the transformed boundary layer equations for variable heat flux, $q_w(x)$, along vertical cylinders in natural convection. For the case of power law heat flux distribution $q_w(x) = ax^n$, one has from equation (A-22) that

$$\gamma = n \quad (A-23)$$

For long slender cylinders, the curvature parameter $\lambda = 2 \frac{x}{r_0} (\text{Gr}_x^*/5)^{-1/5}$ can be large. To lower the maximum value of calculations in the x or λ coordinate, one introduces a new $\xi(x)$ variable defined by

$$\lambda = C \xi^2 \quad (A-24)$$

with $C = 2 \cdot 5^{1/5}$.

Substituting equations (A-23) and (A-24) into equations (A-19) through (A-22) results in:

Momentum:

$$(1 + a_1\eta)f''' + a_1f'' + a_2ff'' + a_3f^2 + a_4\theta = a_5\left(f' \frac{\partial f}{\partial \xi} - f \frac{\partial f'}{\partial \xi}\right) \quad (A-25)$$

$$(1 + a_1 \eta) \theta'' + a_1 \theta' + \text{Pr } a_2 f \theta' + \text{Pr } a_6 f' \theta = \text{Pr } a_5 \left(\theta' \frac{\partial f}{\partial \xi} - f' \frac{\partial \theta}{\partial \xi} \right) \quad (26)$$

Boundary Conditions :

$$\begin{aligned} f(\xi, 0) = f'(\xi, 0) = 0, \quad \theta'(\xi, 0) = -1 \\ f'(\xi, \infty) = \theta(\xi, \infty) = 0 \end{aligned} \quad (27)$$

where

$$\begin{aligned} a_1 = C\xi^2, \quad a_2 = n + 4, \quad a_3 = -(2n + 3) \\ a_4 = 1, \quad a_5 = \xi(n - 1)/2, \quad a_6 = -(4n + 1) \end{aligned} \quad (28)$$

The proposed method of solution, developed by Lee et al. (1986b) requires boundary conditions in terms of f , f' and θ at $\eta = 0$. In equation (27) one has $\theta'(\lambda, 0) = -1$. This necessitates an additional transformation. Let

$$\phi(\xi, \eta) = \theta(\xi, \eta)/\theta(\xi, 0) \quad (29)$$

Then:

$$\theta(\xi, \eta) = \phi(\xi, \eta)\theta(\xi, 0) \quad (30)$$

$$\theta'(\xi, \eta) = \phi'(\xi, \eta)\theta(\xi, 0) \quad (31)$$

$$\theta''(\xi, \eta) = \phi''(\xi, \eta)\theta(\xi, 0) \quad (32)$$

Substituting $\theta'(\xi, 0) = -1$ from equation (27) into equation (31) for $\eta = 0$ results in

$$\theta(\xi, 0) = \frac{-1}{\phi'(\xi, 0)} \quad (33)$$

Substituting equation (33) into equations (30) through (32) leads to

$$\theta(\xi, \eta) = -\phi(\xi, \eta)/\phi'(\xi, 0) \quad (34)$$

$$\theta'(\xi, \eta) = -\phi'(\xi, \eta)/\phi'(\xi, 0) \quad (A-35)$$

$$\theta''(\xi, \eta) = -\phi''(\xi, \eta)/\phi'(\xi, 0) \quad (A-36)$$

$$\frac{\partial \theta}{\partial \xi} = -\frac{\partial}{\partial \xi} \left[\frac{\phi(\xi, \eta)}{\phi'(\xi, 0)} \right] \quad (A-37)$$

Substituting equations (A-29) through (A-37) into equations (A-25) through (A-28) results in :

$$(1 + a_1\eta)f''' + a_1f'' + a_2ff'' + a_3f^2 + a_7\phi = a_5 \left(f'' \frac{\partial f}{\partial \xi} + f' \frac{\partial f'}{\partial \xi} \right) \quad (A-38)$$

$$\begin{aligned} & (1 + a_1\eta)\phi'' + a_1\phi' + a_2Pr f\phi' + a_6Pr f'\phi \\ & = Pr a_5 \left\{ \phi' \frac{\partial f}{\partial \xi} - f' \left(\phi'(\xi, 0) \left[\frac{\partial}{\partial \xi} \left(\frac{\phi}{\phi'(\xi, 0)} \right) \right] \right) \right\} \end{aligned} \quad (A-39)$$

Boundary Conditions :

$$\begin{aligned} f(\xi, 0) = f'(\xi, 0) = 0 \quad \phi(\xi, 0) = 1 \\ f(\xi, \infty) = \phi(\xi, \infty) = 0 \end{aligned} \quad (A-40)$$

where a_1 through a_6 are as before and

$$a_7 = -\frac{a_4}{\phi'(\xi, 0)} \quad (A-41)$$

The boundary conditions are now in the proper form to be used in the finite difference solution method described in Appendix B.

The physical quantities of interest are the local Nusselt number Nu_x , the average Nusselt number \overline{Nu}_L , the local wall shear stress τ_w , the axial velocity distribution u , and the temperature profile $\phi(\xi, \eta)$. The local Nusselt number is defined by

$$Nu_x = \frac{hx}{k} \quad (A-42)$$

where $h = q_w / (T_w - T_\infty)$. Substituting q_w from equation (A-4) into equation (A-42), followed by the transformation, results in

$$Nu_x (Gr_x^*/5)^{-1/5} = \frac{1}{\theta(\xi, 0)} \quad (A-43)$$

Substituting equation (A-33) into equation (A-43) one obtains

$$Nu_x (Gr_x^*/5)^{-1/5} = -\phi'(\xi, 0) \quad (A-44)$$

The average Nusselt number is defined by $\overline{Nu}_L = \bar{h} \frac{L}{k}$ where the average heat transfer coefficient, \bar{h} , is obtained from

$$\bar{h} = \frac{1}{L} \int_0^L h dx \quad (A-45)$$

Substituting h into the definition of \bar{h} and carrying out the integration one obtains:

$$\overline{Nu}_L (Gr_L^*/5)^{-1/5} = -L^{-(4+n)/5} \int_0^L x^{(4+n)/5} \phi'(\xi, 0) x^{-1} dx \quad (A-46)$$

From equations (A-7) and (A-24) one can write

$$\xi = \left[\frac{(x/r_0)^{1-n}}{Gr_0^*} \right]^{1/10} \quad (A-47)$$

$$x = r_0 [Gr_0^* \xi^{10}]^{1/(1-n)} \quad (A-48)$$

$$x^{-1} dx = \frac{10}{1-n} \xi^{-1} d\xi \quad (A-49)$$

where $Gr_0^* = Gr_x^*$ at $x = r_0$; that is, $Gr_0^* = g\beta(a r_0^n) r_0^4 / kv^2$. Substituting equations (A-48) and (A-49) into equation (A-46), one gets

$$\overline{Nu}_L (Gr_L^*/5)^{-1/5} = -\frac{10}{1-n} \xi_L^N \int_0^{\xi_L} \xi^M \phi'(\xi, 0) d\xi \quad (A-50)$$

where

$$\begin{aligned} \xi_{1.} &= \xi \quad \text{at} \quad x = 1., \\ M &= (7 + 3n)/(1 - n), \quad N = (8 + 2n)/(n - 1) \end{aligned} \quad (A-51)$$

As $\xi \rightarrow 0$, equation (A-50) approaches

$$\overline{Nu}_L (Gr_{L*}/5)^{-1/5} \Big|_{\xi \rightarrow 0} = - \frac{5}{4+n} \phi'(0, 0) \quad (A-52)$$

Next, from the definition of local wall shear stress

$$\tau_w = \mu \frac{\partial u}{\partial r} \Big|_{r=r_o} \quad (A-53)$$

one obtains, by substituting equation (A-13) into equation (A-53),

$$\tau_w = 5 \frac{\mu v}{x^2} (Gr_{x*}/5)^{3/5} f'(\xi, 0) \quad (A-54)$$

From equation (A-10), the axial velocity distribution can be written as

$$\frac{ux}{v} = 5 (Gr_{x*}/5)^{2/5} f(\xi, \eta) \quad (A-55)$$

and the temperature profile $\phi(\xi, \eta)$ is given by equation (A-29).

APPENDIX B

METHOD OF SOLUTION FOR THE SYSTEM OF EQUATIONS IN CHAPTER 2

Equations (A-38) through (A-40) in Appendix A constitute a system of nonlinear partial differential equations in the (ξ, η) coordinates with parameters Pr and n . The method of Lee et al. (1986b) is employed to solve this system of equations for natural convection along a vertical cylinder with $q_w = ax^n$.

The first step is to convert the terms involving $\partial/\partial\xi$ in the following manner.

$$\frac{\partial H}{\partial \xi} = \frac{p}{\Delta \xi} (H - H_o) - q \left(\frac{\partial H}{\partial \xi} \right)_o = \frac{p}{\Delta \xi} (H - \bar{H}_o) \quad (B-1)$$

where H is a function of (ξ, η) , $\bar{H}_o = H_o + (q/p)\Delta\xi(\partial H/\partial\xi)_o$, and the subscript "o" denotes quantities at $\xi - \Delta\xi$. The values for p and q are $p=1$ and $q=0$ at $\xi=0$ and $\xi=\Delta\xi$, and $p=2$ and $q=1$ thereafter for $\xi \geq 2\Delta\xi$. Thus we have

$$\frac{\partial f}{\partial \xi} = \frac{p}{\Delta \xi} (f - \bar{f}_o) \quad (B-2)$$

$$\frac{\partial \Gamma}{\partial \xi} = \frac{p}{\Delta \xi} (\Gamma - \bar{\Gamma}_o) \quad (B-3)$$

$$\phi'(\xi, 0) \left[\frac{\partial}{\partial \xi} \left(\frac{\phi}{\phi'(\xi, 0)} \right) \right] = \frac{p}{\Delta \xi} \left(\frac{\bar{\phi}'(\xi, 0)_o}{\bar{\phi}'(\xi, 0)} - 1 \right) \phi + \frac{p}{\Delta \xi} (\phi - \bar{\phi}_o) \quad (B-4)$$

where

$$\bar{f}_o = f_o + \frac{q}{p} \Delta \xi \left(\frac{\partial f}{\partial \xi} \right)_o \quad (B-5)$$

$$\bar{\Gamma}_o = \Gamma_o + \frac{q}{p} \Delta \xi \left(\frac{\partial \Gamma}{\partial \xi} \right)_o \quad (B-6)$$

$$\bar{\phi}'(\xi, 0)_0 = \phi'(\xi, 0) + \frac{q}{p} \Delta \xi \left(\frac{\partial \phi'(\xi, 0)}{\partial \xi} \right)_0 \quad (B-7)$$

$$\bar{\phi}_0 = \phi_0 + \frac{q}{p} \Delta \xi \left(\frac{\partial \phi}{\partial \xi} \right)_0 \quad (B-8)$$

The f and ϕ equations are then linearized by using the simple technique for the product of two arbitrary functions F and G , defined as

$$FG = \tilde{F}G + \tilde{G}F - \tilde{F}\tilde{G} \quad (B-9)$$

where \tilde{F} and \tilde{G} indicate the values to be guessed. Applying equation (B-9) to the terms ff'' , f^2 , $f\phi'$, and $f'\phi$, one obtains

$$ff'' = \tilde{f}f'' + f'\tilde{f} - \tilde{f}'\tilde{f} \quad (B-10)$$

$$f^2 = 2\tilde{f}f' - \tilde{f}^2 \quad (B-11)$$

$$f\phi' = \tilde{f}\phi' + \tilde{\phi}'f - \tilde{f}\tilde{\phi}' \quad (B-12)$$

$$f'\phi = \tilde{f}'\phi + f'\tilde{\phi} - \tilde{f}'\tilde{\phi} \quad (B-13)$$

Substituting equations (B-2) through (B-13) into equations (A-38) through (A-40) results in:

Momentum equation:

$$\begin{aligned} & (1 + a_1\eta)f''' + [a_1 + (a_2 - a_5 p/\Delta\xi)\tilde{f} + a_5 p/\Delta\xi \tilde{f}_0]f'' \\ & + [2(a_3 + a_5 p/\Delta\xi)\tilde{f}' - a_5 p/\Delta\xi \tilde{f}'_0]f' + [(a_2 - a_5 p/\Delta\xi)\tilde{f}'']f + a_7\phi \\ & = [(a_2 - a_5 p/\Delta\xi)\tilde{f}\tilde{f}'' + (a_3 + a_5 p/\Delta\xi)\tilde{f}'^2] \end{aligned} \quad (B-14)$$

Energy equation:

$$\begin{aligned}
& (1 + a_1 \eta) \phi'' + [a_1 + \text{Pr}(a_2 - a_5 p / \Delta \xi) \tilde{f} + \text{Pr}(a_5 p / \Delta \xi) \tilde{f}_o] \phi' \\
& + [\text{Pr}(a_6 + a_8(a_5 p / \Delta \xi)) \tilde{f}'] \phi + [\text{Pr}\{(a_6 + a_8(a_5 p / \Delta \xi)) \tilde{\phi} - a_5 p / \Delta \xi \tilde{\phi}_o\}] f' \\
& + [\text{Pr}(a_2 - a_5 p / \Delta \xi) \tilde{\phi}'] f = [\text{Pr}\{(a_2 - a_5 p / \Delta \xi) \tilde{f} \tilde{\phi}' + (a_6 + a_8(a_5 p / \Delta \xi)) \tilde{f}' \tilde{\phi}\}]
\end{aligned} \quad (B-15)$$

Boundary conditions:

$$\begin{aligned}
f(\xi, 0) = f'(\xi, 0) = 0 \quad \phi(\xi, 0) = 1 \\
f(\xi, \infty) = \phi(\xi, \infty) = 0
\end{aligned} \quad (B-16)$$

where all terms have been defined except for

$$a_8 = \frac{\tilde{\phi}'(\xi, 0)_o}{\tilde{\phi}'(\xi, 0)} \quad (B-17)$$

Equations (B-14) and (B-15) can be rewritten in the following form.

$$A_0 f''' + (a_1 + \Lambda_1) f'' + \Lambda_2 f' + \Lambda_3 f + \Lambda_4 \phi = \Lambda_5 \quad (B-18)$$

$$B_0 \phi'' + (a_1 + B_1) \phi' + B_2 \phi + B_3 f' + B_4 f = B_5 \quad (B-19)$$

where

$$\begin{aligned}
\Lambda_0 &= 1 + a_1 \eta, \quad \Lambda_1 = a^* \tilde{f} + d^* \tilde{f}_o \\
\Lambda_2 &= 2b^* \tilde{f}' - d^* \tilde{f}_o', \quad \Lambda_3 = a^* \tilde{f}'' \\
\Lambda_4 &= a_7, \quad \Lambda_5 = a^* \tilde{f} \tilde{f}'' + b^* \tilde{f}'^2
\end{aligned} \quad (B-20)$$

$$\begin{aligned}
B_0 &= \Lambda_0, \quad B_1 = \text{Pr} \Lambda_1, \quad B_2 = \text{Pr} c^* \tilde{f}' \\
B_3 &= \text{Pr} (c^* \tilde{\phi} - d^* \tilde{\phi}_o), \quad B_4 = \text{Pr} a^* \tilde{\phi}' \\
B_5 &= \text{Pr} (a^* \tilde{f} \tilde{\phi}' + c^* \tilde{f}' \tilde{\phi})
\end{aligned} \quad (B-21)$$

$$\begin{aligned}
a^* &= a_2 - d^*, \quad b^* = a_3 + d^* \\
d^* &= a_5 p / \Delta \xi, \quad c^* = a_6 + a_8 d^*
\end{aligned} \quad (B-22)$$

and the other variables are as previously defined.

The system of equations has now been reduced to a system of quasi-linear ordinary differential equations. By defining $g = f'$ and applying the weighting factors [see Lee et al. (1986b)] one can write equations (18) and (19) in the finite-difference form as:

$$f_i - f_{i-1} - (\Delta\eta/2)(g_i + g_{i-1}) = 0 \quad (23)$$

$$\Lambda_0/(\Delta\eta)^2(\alpha_{-1}g_{i-1} + \alpha_0g_i + \alpha_{+1}g_{i+1}) + \Lambda_2g_i + \Lambda_3f_i + \Lambda_4\phi_i = \Lambda_5 \quad (24)$$

$$B_0/(\Delta\eta)^2(\beta_{-1}\phi_{i-1} + \beta_0\phi_i + \beta_{+1}\phi_{i+1}) + B_2\phi_i + B_3g_i + B_4f_i = B_5 \quad (25)$$

where $\Delta\eta$ is the step size in the η direction and the subscript "i" refers to values at the nodal point η_i .

In equations (24) and (25) the weighting factors are defined as:

$$\begin{aligned} \alpha_{-1} &= W_f(-z_{i-1/2}), \quad \alpha_{+1} = W_f(z_{i+1/2}), \quad \alpha_0 = -\alpha_{-1} - \alpha_{+1} \\ \beta_{-1} &= W_f(-z^*_{i-1/2}), \quad \beta_{+1} = W_f(z^*_{i+1/2}), \quad \beta_0 = -\beta_{-1} - \beta_{+1} \\ W_f(z) &= z/(1 - \exp(-z)) \\ z &= \Delta\eta(a_1 + \Lambda_1)/\Lambda_0, \quad z^* = \Delta\eta(a_1 + B_1)/B_0 \end{aligned} \quad (26)$$

Equations (23) through (25) are applied to the interior points. On the boundaries, equation (16) is written as

$$\begin{aligned} f_1 &= g_1 = 0, \quad \phi_1 = 1 \\ f_n - f_{n-1} - \frac{\Delta\eta}{2}(g_n + g_{n-1}) &= g_n = \phi_n = 0 \end{aligned} \quad (27)$$

where the subscript n is the number of nodes in the η direction.

Equations (23) through (27) constitute a system of algebraic equations that can be written in the matrix form

$$[A][X] = [B] \quad (28)$$

where $[A]$ is a band matrix of order $3n$ and bandwidth seven. The array $[X]$ which contains the solution in the form $(f_1, g_1, \phi_1, f_2, g_2, \phi_2, \dots, f_n, g_n, \phi_n)^T$ is a column matrix of order $3n$.

where $[A]$ is a band matrix of order $3n$ and bandwidth seven. The array $[X]$ which contains the solution in the form $(f_1, g_1, \phi_1, f_2, g_2, \phi_2, \dots, f_n, g_n, \phi_n)^T$ is a column matrix of order $3n$. The matrix $[B]$ is a column matrix of order $3n$ which contains the right hand sides of equations (B-23) through (B-25) and (B-27). The matrix $[A]$ is approximately diagonally dominant and equation (B-28) can be solved by the Gaussian elimination technique with high accuracy.

To obtain values for f'' and ϕ' , the results for f and ϕ along with the boundary conditions

$$f'''(\xi, 0) = -a_1 \tilde{f}''(\xi, 0) - a_4 \quad (B - 29)$$

$$\phi''(\xi, 0) = -a_1 \tilde{\phi}'(\xi, 0) \quad (B - 30)$$

$$f''(\xi, \infty) = \phi''(\xi, \infty) = 0 \quad (B - 31)$$

are used in a cubic spline interpolation routine [see, for example, Burden and Faires (1985)]. As the solution converges, the boundary conditions become exact and the values for f'' and ϕ' can be obtained with high accuracy.

The present method of solution employs a quasi-linearization of the original nonlinear system of equations and requires initial guesses for f , f' , f'' , ϕ , and ϕ' . The flat plate solution (i.e., $\xi = 0$) for the uniform surface heat flux case (UHF) for $Pr = 0.7$ was obtained and these results were used as the initial guesses for all other combinations of Pr and n at $\xi = 0$. For $\xi = \Delta\xi$, initial guesses were taken to be the results at $\xi = 0$. At $\xi = 2\Delta\xi$, a linear extrapolation of the results at $\xi = 0$ and $\xi = \Delta\xi$ was used. For $\xi \geq 3\Delta\xi$ a three point inverse polynomial extrapolation was used [see, for example, Traub (1964)]. This approach was found to improve the convergence of solutions up to 40% faster than simply using the previous node's values as the first guess.

To improve convergence of solutions it was found that the value for η_∞ needed to be taken larger as the value of the curvature parameter ξ increase. The value of η_∞ was initially set to 10 for $Pr \geq 0.7$ and to 15 for $Pr = 0.1$. It was increased by 5 when the value of f' or ϕ at

$\eta = 0.98\eta_\infty$ was greater than 0.001. Since $f'(\xi, \infty) = \phi(\xi, \infty) = 0$, the f' and ϕ values greater than 0.001 at $\eta = 0.98\eta_\infty$ indicate that the corresponding boundary layer thickness extends past η_∞ . To make this adjustment, all values past η_∞ were set to zero except for f which was taken to be the value at the old η_∞ extended out to the new η_∞ . This adjustment introduced less than 0.5 % difference in the values of the local Nusselt number when compared to a constant run at $\eta_\infty = 30$. This error was due primarily to η_∞ initially being less than 30 rather than to the adjustment itself.

The solution method is an iterative scheme and a solution was considered to be convergent when the calculated values for f , f' , and ϕ differed from the last guess of the respective values by less than 10^{-4} at all nodes (i.e., at all η values for a given ξ). When these criteria failed, new guesses for f , f' , and ϕ were found using a weighted average of the last guess and the resulting calculation. That is,

$$\tilde{f}_{\text{new}} = \omega f + (1 - \omega)\tilde{f}_{\text{old}} \quad (B - 32)$$

$$\tilde{f}'_{\text{new}} = \omega f' + (1 - \omega)\tilde{f}'_{\text{old}} \quad (B - 33)$$

$$\tilde{\phi}_{\text{new}} = \omega \phi + (1 - \omega)\tilde{\phi}_{\text{old}} \quad (B - 34)$$

where ω is a relaxation factor. Generally $\omega = 1$ resulted in quick convergence. However, if η_∞ was too small or for some small values of Pr and n it was sometimes necessary to use under-relaxation and set $\omega = 0.5$ to facilitate convergence.

It was found that as ξ was increased, errors resulted due to increasing boundary layer thicknesses. By using a step size of $\Delta\eta = 0.01$ errors were reduced for calculations at $\eta = 0$ at high values of the curvature parameter ξ . It was also found that the solution was not sensitive to the step size in ξ and $\Delta\xi = 0.1$ was used.

APPENDIX C

TRANSFORMATION OF THE GOVERNING SYSTEM OF EQUATIONS FOR THE
SPECIAL CASE OF NATURAL CONVECTION IN CHAPTER 3

In Chapter 3 the solution for the case of natural convection along a slender vertical cylinder with variable surface temperature is presented as a special case. Consider a semi-infinite, vertical cylinder with radius r_0 that is aligned in a quiescent ambient fluid at temperature T_∞ . The axial coordinate x is measured upward when $T_w > T_\infty$ and downward when $T_w < T_\infty$. The radial coordinate r is measured from the axis of the cylinder. The surface of the cylinder is subjected to an arbitrary variation in temperature $T_w(x)$, and the gravitational acceleration g is acting downward. Fluid properties are assumed to be constant except for variations in density which induce the buoyancy force. By employing the laminar boundary layer assumptions and making use of the Boussinesq approximation the governing conservation equations can be written as:

Continuity:

$$\frac{\partial}{\partial x}(ru) + \frac{\partial}{\partial r}(rv) = 0 \quad (C-1)$$

Momentum:

$$u \frac{\partial u}{\partial x} + v \frac{\partial u}{\partial r} = \frac{\nu}{r} \frac{\partial}{\partial r} \left(r \frac{\partial u}{\partial r} \right) + g\beta(T - T_\infty) \quad (C-2)$$

Energy:

$$u \frac{\partial T}{\partial x} + v \frac{\partial T}{\partial r} = \frac{\alpha}{r} \frac{\partial}{\partial r} \left(r \frac{\partial T}{\partial r} \right) \quad (C-3)$$

In these equations u and v are the velocity components in the x and r directions respectively; T is the fluid temperature; and ν , β and α are, respectively, the kinematic viscosity, the volumetric coefficient of thermal expansion and the thermal diffusivity of the fluid.

The boundary conditions are

$$u = v = 0, \quad T = T_w(x) \quad \text{at } r = r_0 \quad (C-4)$$

$$u \rightarrow 0, \quad T \rightarrow T_\infty \quad \text{As } r \rightarrow \infty \quad (C-5)$$

$$u = 0, \quad T = T_\infty \quad \text{At } x = 0, \quad r \geq r_0 \quad (C-6)$$

In writing equation (C-6) it is assumed that the flow and thermal boundary layer thicknesses are zero at the leading edge of the cylinder surface.

The conservation equations and the boundary conditions are then transformed into a dimensionless form by introducing the following dimensionless variables:

$$\eta = \frac{[r^2 - r_0^2]}{2r_0 x} (Gr_x/4)^{1/4}, \quad \lambda = \frac{2x}{r_0} (Gr_x/4)^{-1/4} \quad (C-7)$$

$$f(\lambda, \eta) = \psi(x, r) / [4\nu r_0 (Gr_x/4)^{1/4}], \quad \theta(\lambda, \eta) = (T - T_\infty) / [T_w(x) - T_\infty] \quad (C-8)$$

$$Gr_x = g\beta[T_w(x) - T_\infty] x^3 / \nu^2 \quad (C-9)$$

where η is the pseudo-similarity variable, $f(\lambda, \eta)$ is the reduced stream function, $\theta(\lambda, \eta)$ is the dimensionless temperature, λ is the curvature parameter, and $\psi(x, r)$ is the stream function that satisfies the continuity equation, with $u = (\partial\psi/\partial r)/r$ and $v = -(\partial\psi/\partial x)/r$. The transformation yields

$$u = 4 \frac{\nu}{x} (Gr_x/4)^{1/2} f'(\lambda, \eta) \quad (C-10)$$

$$v = -4 \frac{r_0}{r} \nu^{1/2} (g\beta/4)^{1/4} \left[\left(\frac{\partial f}{\partial \lambda} \frac{\partial \lambda}{\partial x} + f' \frac{\partial \eta}{\partial x} \right) \{ (T_w - T_\infty)^{1/4} x^{3/4} \} \right. \\ \left. + f \left\{ \frac{1}{4} (T_w - T_\infty)^{-3/4} \frac{\partial (T_w - T_\infty)}{\partial x} x^{3/4} + 3/4 x^{-1/4} (T_w - T_\infty)^{1/4} \right\} \right] \quad (C-11)$$

$$\begin{aligned} \frac{\partial u}{\partial x} = 4(g\beta/4)^{1/2} \left\{ \Gamma \left[x^{1/2} \left(\frac{1}{2}(\Gamma_w - \Gamma_\infty)^{-1/2} \frac{\partial(\Gamma_w - \Gamma_\infty)}{\partial x} \right) \right. \right. \\ \left. \left. + \frac{1}{2}x^{-1/2}(\Gamma_w - \Gamma_\infty)^{1/2} \right] + x^{1/2}(\Gamma_w - \Gamma_\infty)^{1/2} \left[\Gamma' \frac{\partial \eta}{\partial x} + \frac{\partial \Gamma}{\partial \lambda} \frac{\partial \lambda}{\partial x} \right] \right\} \end{aligned} \quad (C-12)$$

$$\frac{\partial u}{\partial r} = 4\nu(Gr_x/4)^{3/4}x^{-2}\frac{r}{r_o}\Gamma'(\lambda, \xi) \quad (C-13)$$

$$\frac{\partial}{\partial r} \left(r \frac{\partial u}{\partial r} \right) = 8\nu(Gr_x/4)^{3/4}x^{-2}\frac{r}{r_o}\Gamma'' + 4\nu(Gr_x/4)x^{-3}\frac{r^3}{r_o^2}\Gamma''' \quad (C-14)$$

$$T - T_\infty = (\Gamma_w(x) - \Gamma_\infty)\theta(\lambda, \eta) \quad (C-15)$$

$$\frac{\partial \Gamma}{\partial x} = \theta \frac{\partial(\Gamma_w - \Gamma_\infty)}{\partial x} + (\Gamma_w - \Gamma_\infty) \left(\frac{\partial \theta}{\partial \lambda} \frac{\partial \lambda}{\partial x} + \theta' \frac{\partial \eta}{\partial x} \right) \quad (C-16)$$

$$\frac{\partial \Gamma}{\partial r} = (\Gamma_w - \Gamma_\infty)\theta' \left(\frac{r}{r_o x} (Gr_x/4)^{1/4} \right) \quad (C-17)$$

$$\frac{\partial}{\partial r} \left(r \frac{\partial \Gamma}{\partial r} \right) = \frac{(\Gamma_w - \Gamma_\infty)}{r_o x} (Gr_x/4)^{1/4} \left\{ r^2 \theta'' \left(\frac{r}{r_o x} (Gr_x/4)^{1/4} \right) + 2r\theta' \right\} \quad (C-18)$$

in which the primes denote partial differentiation with respect to η .

Substitution of equations (C-10) through (C-18) into equations (C-1) through (C-6) results in

$$(1 + \eta\lambda)\Gamma'' + \lambda\Gamma' + (\gamma + 3)f\Gamma'' - 2(\gamma + 1)\Gamma^2 + \theta = \lambda(\gamma - 1) \left(\Gamma' \frac{\partial f}{\partial \lambda} - \Gamma \frac{\partial \Gamma'}{\partial \lambda} \right) \quad (C-19)$$

$$(1 + \eta\lambda)\theta'' + \lambda\theta' + \text{Pr}(\gamma + 3)f\theta' - \text{Pr}(4\gamma)\Gamma\theta = \text{Pr}\lambda(\gamma - 1) \left(\theta' \frac{\partial f}{\partial \lambda} - \Gamma \frac{\partial \theta}{\partial \lambda} \right) \quad (C-20)$$

$$\begin{aligned} f(\lambda, 0) = f'(\lambda, 0) = 0, \quad \theta(\lambda, 0) = 1 \\ f'(\lambda, \infty) = 0, \quad \theta(\lambda, \infty) = 0 \end{aligned} \quad (C-21)$$

where

$$\gamma = \frac{x}{T_w(x) - T_\infty} \frac{d}{dx} [T_w(x) - T_\infty] \quad (C-22)$$

The system of equations (C-19) through (C-22) represents the general form of the transformed boundary layer equations for variable wall temperature $T_w(x)$ along vertical cylinders in natural convection. For the case of power law variation in surface temperature, $T_w(x) = T_\infty + ax^n$, one obtains from equation (C-22) that

$$\gamma = n \quad (C-23)$$

For long slender cylinders, the curvature parameter $\lambda = 2 \frac{x}{r_0} (Gr_x/4)^{1/4}$ can be large. To lower the maximum value of calculations in the x or λ coordinate, one introduces a new $\xi(x)$ variable defined by

$$\lambda = C \xi^2 \quad (C-24)$$

with $C = 2 \cdot 4^{1/4}$.

Substituting equations (C-23) and (C-24) into equations (C-19) through (C-22) results in:

Momentum:

$$(1 + a_1 \eta) f''' + a_1 f'' + a_2 f f'' + a_3 f'^2 + a_4 \theta = a_5 \left(f'' \frac{\partial f}{\partial \xi} - f' \frac{\partial f'}{\partial \xi} \right) \quad (C-25)$$

Energy:

$$(1 + a_1 \eta) \theta'' + a_1 \theta' + Pr a_2 f \theta' + Pr a_6 f' \theta = Pr a_5 \left(\theta' \frac{\partial f}{\partial \xi} - f' \frac{\partial \theta}{\partial \xi} \right) \quad (C-26)$$

Boundary Conditions :

$$\begin{aligned} f(\xi, 0) = f'(\xi, 0) = 0, \quad \theta(\xi, 0) = 1 \\ f'(\xi, \infty) = \theta(\xi, \infty) = 0 \end{aligned} \quad (C-27)$$

where

$$\begin{aligned} a_1 = C\xi^2, \quad a_2 = n + 3, \quad a_3 = -2(n + 1) \\ a_4 = 1, \quad a_5 = \xi(n - 1)/2, \quad a_6 = -4n \end{aligned} \quad (C-28)$$

The physical quantities of interest are the local Nusselt number Nu_x , the average Nusselt number \overline{Nu}_L , the local wall shear stress τ_w , the axial velocity distribution u , and the temperature profile $\theta(\xi, \eta)$. From the definition of the local Nusselt number

$$Nu_x = \frac{hx}{k} = \frac{q_w}{T_w - T_\infty} \frac{x}{k} \quad (C-29)$$

along with $q_w = -k(\partial T/\partial r)_{r=r_0}$, one finds

$$Nu_x(Gr_x/4)^{-1/4} = -\theta'(\xi, 0) \quad (C-30)$$

The average Nusselt number is obtained from the expression

$$\overline{Nu}_L = \frac{\bar{h}L}{k} = \frac{1}{k} \int_0^L h dx \quad (C-31)$$

Substituting h into equation (C-31) and carrying out the integration, one finds:

$$\overline{Nu}_L(Gr_L/4)^{-1/4} = -L^{-(3+n)/4} \int_0^L x^{(3+n)/4} \theta'(\xi, 0) x^{-1} dx \quad (C-32)$$

From equations (C-7) and (C-24) one can write

$$\xi = \left[\frac{(x/r_0)^{1-n}}{Gr_0} \right]^{1/8} \quad (C-33)$$

$$x = r_0 [Gr_0 \xi^8]^{1/(1-n)} \quad (C-34)$$

$$x^{-1}dx = \frac{8}{1-n}\xi^{-1}d\xi \quad (C-35)$$

where $Gr_o = Gr_x$ at $x = r_o$; that is, $Gr_o = g\beta(a r_o^n) r_o^3/v^2$. Substituting equations (C-34) and (C-35) into equation (C-32), one gets

$$\overline{Nu}_L(Gr_L/4)^{-1/4} = -\frac{8}{1-n}\xi_L^N \int_0^{\xi_L} \xi^M \theta'(\xi, 0) d\xi \quad (C-36)$$

where

$$\begin{aligned} \xi_L &= \xi \text{ at } x = L, \\ M &= (5 + 3n)/(1 - n), \quad N = (6 + 2n)/(n - 1) \end{aligned} \quad (C-37)$$

As $\xi \rightarrow 0$, equation (C-36) approaches

$$\overline{Nu}_L(Gr_L/4)^{-1/4}_{\xi \rightarrow 0} = -\frac{4}{3+n}\theta'(0, 0) \quad (C-38)$$

Next, the local wall shear stress is found from

$$\tau_w = \mu \frac{\partial u}{\partial r} \Big|_{r=r_o} \quad (C-39)$$

Substituting equation (C-13) into equation (C-39) one obtains

$$\tau_w = 4 \frac{\mu v}{x^2} (Gr_x/4)^{3/4} f'(\xi, 0) \quad (C-40)$$

From equation (C-10), the axial velocity distribution can be written as

$$\frac{ux}{v} = 4(Gr_x/4)^{1/2} f(\xi, \eta) \quad (C-41)$$

and the temperature profile is given by $\theta(\xi, \eta) = (T - T_\infty)/(T_w - T_\infty)$.

APPENDIX D

TRANSFORMATION OF THE GOVERNING SYSTEM OF EQUATIONS FOR MIXED
CONVECTION IN CHAPTER 3

In Chapter 3 the solution for the case of mixed convection along a slender vertical cylinder with variable surface temperature is presented. Consider a semi-infinite, vertical cylinder with radius r_0 that is aligned parallel to a uniform, laminar free stream with velocity u_∞ and temperature T_∞ . The axial coordinate x is measured in the direction of the forced flow and the radial coordinate r is measured from the axis of the cylinder. The surface of the cylinder is subjected to an arbitrary variation in temperature $T_w(x)$, and the gravitational acceleration g is acting downward. Fluid properties are assumed to be constant except for variations in density which induce the buoyancy force. By employing the laminar boundary layer assumptions and making use of the Boussinesq approximation the governing conservation equations can be written as:

Continuity:

$$\frac{\partial}{\partial x}(ru) + \frac{\partial}{\partial r}(rv) = 0 \quad (D-1)$$

Momentum:

$$u \frac{\partial u}{\partial x} + v \frac{\partial u}{\partial r} = \frac{\nu}{r} \frac{\partial}{\partial r} \left(r \frac{\partial u}{\partial r} \right) \pm g\beta(T - T_\infty) \quad (D-2)$$

Energy:

$$u \frac{\partial T}{\partial x} + v \frac{\partial T}{\partial r} = \frac{\alpha}{r} \frac{\partial}{\partial r} \left(r \frac{\partial T}{\partial r} \right) \quad (D-3)$$

The positive sign in equation (D-2) applies to upward forced flow and the negative sign to downward forced flow. In these equations u and v are the velocity components in the x and r directions respectively; T is the fluid temperature; and ν , β and α are, respectively, the kinematic viscosity, the volumetric coefficient of thermal expansion and the thermal diffusivity of the fluid.

The boundary conditions are

$$u = v = 0, \quad T = T_w(x) \quad \text{at } r = r_0 \quad (D-4)$$

$$u \rightarrow 0, \quad T \rightarrow T_\infty \quad \text{As } r \rightarrow \infty \quad (D-5)$$

$$u = 0, \quad T = T_\infty \quad \text{At } x = 0, \quad r \geq r_0 \quad (D-6)$$

In writing equation (D-6) it is assumed that the flow and thermal boundary layer thicknesses are zero at the leading edge of the cylinder surface.

The conservation equations and the boundary conditions are then transformed into a dimensionless form by introducing the following dimensionless variables:

$$\eta = \frac{(r^2 - r_0^2)}{2r_0 x} (\text{Re}_x^{1/2} + \text{Gr}_x^{1/4}), \quad z = \frac{x}{r_0} \quad (D-7)$$

$$f(z, \eta) = \psi(x, r) / [v r_0 (\text{Re}_x^{1/2} + \text{Gr}_x^{1/4})], \quad \theta(z, \eta) = (T - T_\infty) / [T_w(x) - T_\infty] \quad (D-8)$$

$$\Omega_x = \frac{\text{Gr}_x}{\text{Re}_x^2}, \quad \chi = (1 + \Omega_x^{1/4})^{-1} \quad (D-9)$$

$$\text{Gr}_x = g\beta[T_w(x) - T_\infty] x^3 / \nu^2, \quad \text{Re}_x = u_\infty x / \nu \quad (D-10)$$

where η is the pseudo-similarity variable, z is the dimensionless axial coordinate, $f(z, \eta)$ is the reduced stream function, $\theta(z, \eta)$ is the dimensionless temperature, $\psi(x, r)$ is the stream function that satisfies the continuity equation, with $u = (\partial\psi/\partial r)/r$ and $v = -(\partial\psi/\partial x)/r$, Ω_x is the buoyancy parameter which varies from zero for pure forced convection to infinity for pure free convection, and χ is the mixed convection parameter which varies from zero for pure free convection to one for pure forced convection.

The transformation yields

$$u = u_\infty \chi^{-2} f'(z, r_0) \quad (D-11)$$

$$v = \frac{-r_0}{r} \sqrt{u_\infty v} \left\{ \left(\frac{\partial f}{\partial z} \left(\frac{1}{r_0} \right) + f' \frac{\partial \eta}{\partial x} \right) \chi^{1/2} \chi^{-1} + f' \left(\frac{1}{2} \chi^{-1/2} \chi^{-1} - \chi^{-2} \frac{\partial \chi}{\partial z} \frac{\chi^{1/2}}{r_0} \right) \right\} \quad (D-12)$$

$$\frac{\partial u}{\partial x} = u_\infty \left[\left(\frac{\partial f}{\partial z} \left(\frac{1}{r_0} \right) + f' \frac{\partial \eta}{\partial x} \right) \chi^{-2} + f' \left(-\frac{2\chi^{-3}}{r_0} \frac{\partial \chi}{\partial z} \right) \right] \quad (D-13)$$

$$\frac{\partial u}{\partial r} = u_\infty^{3/2} \chi^{-3} \frac{r}{r_0} (v\chi)^{-1/2} f''(z, \eta) \quad (D-14)$$

$$\frac{\partial}{\partial r} \left(r \frac{\partial u}{\partial r} \right) = 2 \frac{r}{r_0} u_\infty^{3/2} (v\chi)^{-1/2} \chi^{-3} f'' + \frac{u_\infty^2 \chi^{-4} r^3}{v\chi r_0^2} f''' \quad (D-15)$$

$$T - T_\infty = [T_w(x) - T_\infty] \theta(z, \eta) \quad (D-16)$$

$$\frac{\partial T}{\partial x} = \theta \frac{\partial (T_w - T_\infty)}{\partial x} + (T_w - T_\infty) \left(\frac{\partial \theta}{\partial z} \frac{1}{r_0} + \theta' \frac{\partial \eta}{\partial x} \right) \quad (D-17)$$

$$\frac{\partial T}{\partial r} = (T_w - T_\infty) \theta' \left(\frac{r}{r_0} \sqrt{\frac{u_\infty}{v\chi}} \chi^{-1} \right) \quad (D-18)$$

$$\frac{\partial}{\partial r} \left(r \frac{\partial T}{\partial r} \right) = \frac{(T_w - T_\infty)}{r_0 \chi} \sqrt{\frac{u_\infty}{v\chi}} \left\{ \frac{r^3}{r_0} \sqrt{\frac{u_\infty}{v\chi}} \chi^{-1} \theta'' + 2r\theta' \right\} \quad (D-19)$$

in which the primes denote partial differentiation with respect to η .

Substitution of equations (D-11) through (D-19) into equations (D-1) through (D-6) results in

$$(1 + \eta\Lambda)f''' + \Lambda f'' + \frac{1}{4}(2 + (1 - \chi)(\gamma + 1))ff'' - \frac{1}{2}(1 - \chi)(\gamma + 1)f^2 \pm (1 - \chi)^4\theta = -z \left(f'' \frac{\partial f}{\partial z} - f' \frac{\partial f'}{\partial z} \right) \quad (D - 20)$$

$$(1 + \eta\Lambda)\theta'' + \Lambda\theta' + \frac{\text{Pr}}{4}(2 + (1 - \chi)(\gamma + 1))f\theta' - \text{Pr}\gamma f'\theta = -\text{Pr}z \left(\theta' \frac{\partial f}{\partial z} - f' \frac{\partial \theta}{\partial z} \right) \quad (D - 21)$$

$$f(z, 0) = f'(z, 0) = 0, \quad \theta(z, 0) = 1 \\ f'(z, \infty) = \chi^2, \quad \theta(z, \infty) = 0 \quad (D - 22)$$

where

$$\Lambda = 2 \frac{x}{r_0} (\text{Re}_x^{1/2} + \text{Gr}_x^{1/4})^{-1} \quad (D - 23)$$

is the surface curvature parameter and

$$\gamma = \frac{x}{T_w(x) - T_\infty} \frac{d}{dx} [T_w(x) - T_\infty] \quad (D - 24)$$

The plus and minus signs in front of the term $(1 - \chi)^4\theta$ in equation (D-20) now represent buoyancy assisting flow and buoyancy opposing flow, respectively. For pure forced convection $\chi = 1$ and for pure free convection $\chi = 0$.

The system of equations (D-20) through (D-24) represents the general form of the transformed boundary layer equations for variable wall temperature $T_w(x)$ along vertical cylinders in mixed convection. For the case of power law variation in the surface temperature, $T_w(x) = T_\infty + ax^n$, one has from equation (D-24) that

$$\gamma = n \quad (D - 25)$$

Equations (D-20) through (D-22) contain three x -dependent parameters, $z(x)$, $\Lambda(x)$, and $\chi(x)$. These parameters can be related to a single x -dependent parameter $\xi(x)$ defined by

$$\xi = \left(\frac{z}{\text{Re}_0} \right)^{1/4}, \quad z = x/r_0 \quad (D-26)$$

Thus, one has

$$\Lambda = 2 \xi^2 \chi \quad (D-27)$$

$$\chi = [1 + \Omega_0 \xi^{1+n}]^{-1} \quad (D-28)$$

where

$$\Omega_0 = \left[\frac{\text{Gr}_0}{\text{Re}_0^{1-n}} \right]^{1/4} \quad (D-29)$$

with $\text{Gr}_0 = \text{Gr}_x$ and $\text{Re}_0 = \text{Re}_x$ for $x = r_0$. Also, the right-hand sides of equations (D-20) and (D-21) become, respectively

$$-\frac{1}{4} \xi \left(f'' \frac{\partial f}{\partial \xi} - f' \frac{\partial f}{\partial \xi} \right) \quad (D-30)$$

$$-\frac{\text{Pr}}{4} \xi \left(\theta' \frac{\partial f}{\partial \xi} - f' \frac{\partial \theta}{\partial \xi} \right) \quad (D-31)$$

Rewriting equations (D-20) and (D-21) one has:

Momentum:

$$(1 + a_1 \eta) f''' + a_1 f'' + a_2 f f'' + a_3 f^2 + a_4 \theta = a_5 \left(f' \frac{\partial f}{\partial \xi} - f \frac{\partial f'}{\partial \xi} \right) \quad (D-32)$$

Energy

$$(1 + a_1 \eta) \theta'' + a_1 \theta' + \text{Pr } a_2 f \theta' + \text{Pr } a_6 f \theta = \text{Pr } a_5 \left(\theta' \frac{\partial f}{\partial \xi} - f' \frac{\partial \theta}{\partial \xi} \right) \quad (D-33)$$

Boundary Conditions :

$$\begin{aligned} f(\xi, 0) = f'(\xi, 0) = 0, \quad \theta(\xi, 0) = 1 \\ f'(\xi, \infty) = a_7, \quad \theta(\xi, \infty) = 0 \end{aligned} \quad (D-34)$$

where

$$\begin{aligned} a_1 = \Lambda, \quad a_2 = \frac{1}{4}(2 + (1 - \chi)(n + 1)), \quad a_3 = \frac{1}{2}(\chi - 1)(n + 1) \\ a_4 = \pm (1 - \chi)^4, \quad a_5 = -\xi/4, \quad a_6 = -n, \quad a_7 = \chi^2 \end{aligned} \quad (D-35)$$

With Λ and χ related to ξ , the functions f and θ in equation (D-32) to (D-34) are functions of (ξ, η) and depend on three constant parameters n , Pr , and Ω_0 . These equations are now in the form that can be solved by the method proposed by Lee et al. [6]. See Appendix E for the solution method as applied to equations (D-32) through (D-34).

The physical quantities of interest include the local and average Nusselt numbers, the local and average friction factors, the axial velocity distribution, and the temperature profile. The local Nusselt number is defined by

$$Nu_x = \frac{hx}{k} \quad (D-36)$$

where $h = q_w/(T_w - T_\infty)$ and $q_w = -k(\partial T/\partial r)_{r=r_0}$. Thus, it can be shown that

$$Nu_x/(Re_x^{1/2} + Gr_x^{1/4}) = -\theta'(\xi, 0) \quad (D-37)$$

The average Nusselt number is obtained from the expression

$$\overline{Nu}_L = \frac{\bar{h}L}{k} \quad (D-38)$$

where

$$\bar{h} = \frac{1}{L} \int_0^L h dx \quad (D-39)$$

This results in

$$\overline{Nu}_L = - \int_0^L Re_x^{1/2} \chi^{-1} \theta'(\xi, 0) x^{-1} dx \quad (D-40)$$

or

$$\overline{Nu}_L / (Re_L^{1/2} + Gr_L^{1/4}) = - \chi_L L^{-1/2} \int_0^L x^{1/2} \frac{\theta'(\xi, 0)}{\chi} x^{-1} dx \quad (D-41)$$

where $\chi_L = \chi$ at $x = L$. From equation (D-26)

$$x = r_o Re_o \xi^4 \quad (D-42)$$

$$x^{-1} dx = 4 \xi^{-1} d\xi \quad (D-43)$$

Substituting equations (D-42) and (D-43) into equation (D-41), one arrives at

$$\overline{Nu}_L / (Re_L^{1/2} + Gr_L^{1/4}) = -4 \chi_L \xi_L^{-2} \int_0^{\xi_L} \frac{\theta'(\xi, 0)}{\chi} \xi d\xi \quad (D-44)$$

where $\xi_L = \xi$ at $x = L$. As $\xi \rightarrow 0$, equation (D-44) approaches

$$\overline{Nu}_L / (Re_L^{1/2} + Gr_L^{1/4})_{\xi \rightarrow 0} = -2\theta'(0, 0) \quad (D-45)$$

The friction factor is obtained from the definition

$$C_{f_x} = \frac{2\tau_w}{\rho u_\infty^2} = \frac{2}{\rho u_\infty^2} \mu \frac{\partial u}{\partial r} \Big|_{r=r_o} \quad (D-46)$$

Substituting equation (D-14) into equation (D-46) results in

$$C_{f_x} Re_x^{1/2} = 2\chi^{-3} f''(\xi, 0) \quad (D-47)$$

The expression for the average friction factor is derived from

$$C_{f_L} = \frac{2}{\rho u_\infty^2 L} \int_0^L \tau_w dx = \frac{2\nu}{u_\infty^2 L} \int_0^L \frac{\partial u}{\partial r} \Big|_{r=r_o} dx \quad (D-48)$$

Substituting equation (D-14) into equation (D-48), one obtains

$$C_{f_L} \text{Re}_L^{1/2} = 2L^{-1/2} \int_0^L x^{1/2} \chi^{-3} f'(\xi, 0) x^{-1} dx \quad (D-49)$$

Next, substituting equations (D-42) and (D-43) into equation (D-49), one obtains

$$C_{f_L} \text{Re}_L^{1/2} = 8\xi^{-2} \int_0^{\xi_L} \chi^{-3} f'(\xi, 0) \xi d\xi \quad (D-50)$$

As $\xi \rightarrow 0$, equation (D-50) approaches

$$C_{f_L} \text{Re}_L^{1/2} \xi \rightarrow 0 = 4f''(0, 0) \quad (D-51)$$

From equation (D-11), the axial velocity distribution can be written as

$$\frac{u}{u_\infty} = \frac{f'(\xi, \eta)}{\chi^2} \quad (D-52)$$

and the temperature profile is given by $\theta(\xi, \eta) = (T - T_\infty)/(T_w - T_\infty)$.

APPENDIX E

SOLUTIONS OF THE SYSTEM OF EQUATIONS (C-25)-(C-27) AND (D-32)-(D-34)

Equations (C-25) through (C-27) are identical in form to equations (D-32) through (D-34), with the coefficients a_1 through a_6 given by (C-28) for pure free convection and by equation (D-35) for mixed convection. The solution method of Lee et al. [6] was employed to solve the two systems of equations.

The first step is to convert the terms involving $\partial/\partial\xi$ in the following manner.

$$\frac{\partial H}{\partial \xi} = \frac{P}{\Delta \xi} (H - H_0) - q \left(\frac{\partial H}{\partial \xi} \right)_0 = \frac{P}{\Delta \xi} (H - \bar{H}_0) \quad (E-1)$$

where H is a function of (ξ, η) , $\bar{H}_0 = H_0 + (q/p)\Delta\xi(\partial H/\partial\xi)_0$, and the subscript "0" denotes quantities at $\xi = \Delta\xi$. The values for p and q are $p \approx 1$ and $q = 0$ at $\xi = 0$ and $\xi = \Delta\xi$,

and $p = 2$ and $q = 1$ thereafter for $\xi \geq 2\Delta\xi$. Thus we have

$$\frac{\partial f}{\partial \xi} = \frac{P}{\Delta \xi} (f - \bar{f}_0) \quad (E-2)$$

$$\frac{\partial f'}{\partial \xi} = \frac{P}{\Delta \xi} (f' - \bar{f}'_0) \quad (E-3)$$

$$\frac{\partial \theta}{\partial \xi} = \frac{P}{\Delta \xi} (\theta - \bar{\theta}_0) \quad (E-4)$$

where

$$\bar{f}_0 = f_0 + \frac{q}{P} \Delta \xi \left(\frac{\partial f}{\partial \xi} \right)_0 \quad (E-5)$$

$$\bar{f}'_0 = f'_0 + \frac{q}{P} \Delta \xi \left(\frac{\partial f'}{\partial \xi} \right)_0 \quad (E-6)$$

$$\bar{\theta}_o = \theta_o + \frac{q}{p} \Delta \xi \left(\frac{\partial \theta}{\partial \xi} \right)_o \quad (E-7)$$

The f and θ equations are then linearized by using the simple technique for the product of two arbitrary functions F and G , defined as

$$FG = \tilde{F}G + \tilde{G}F - \tilde{F}\tilde{G} \quad (E-8)$$

where \tilde{F} and \tilde{G} indicate the values to be guessed. Applying equation (E-8) to the terms ff'' , f^2 , $f\theta'$, and $f\theta$, one obtains

$$ff'' = \tilde{f}f'' + \tilde{f}''f - \tilde{f}''\tilde{f} \quad (E-9)$$

$$f^2 = 2\tilde{f}f' - \tilde{f}^2 \quad (E-10)$$

$$f\theta' = \tilde{f}\theta' + \tilde{\theta}'f - \tilde{f}\tilde{\theta}' \quad (E-11)$$

$$f\theta = \tilde{f}\theta + \tilde{f}\tilde{\theta} - \tilde{f}\tilde{\theta} \quad (E-12)$$

Substituting equations (E-2) through (E-12) into equations (C-25) and (C-26) (or D-32 and D-33) results in:

Momentum equation:

$$\begin{aligned} & (1 + a_1\eta)f'' + [a_1 + (a_2 - a_5 p/\Delta\xi)\tilde{f} + a_5 p/\Delta\xi \tilde{f}_o]f'' \\ & + [2(a_3 + a_5 p/\Delta\xi)\tilde{f} - a_5 p/\Delta\xi \tilde{f}_o]f' + [(a_2 - a_5 p/\Delta\xi)\tilde{f}'']f + a_4\theta \\ & = [(a_2 - a_5 p/\Delta\xi)\tilde{f}f'' + (a_3 + a_5 p/\Delta\xi)\tilde{f}'^2] \end{aligned} \quad (E-13)$$

Energy equation:

$$\begin{aligned} & (1 + a_1\eta)\phi'' + [a_1 + \text{Pr}(a_2 - a_5 p/\Delta\xi)\tilde{f} + \text{Pr}(a_5 p/\Delta\xi)\tilde{f}_o]\theta'' \\ & + [\text{Pr}(a_6 + a_5 p/\Delta\xi)\tilde{f}'']\theta + [\text{Pr}\{(a_6 + a_5 p/\Delta\xi)\tilde{\theta} - a_5 p/\Delta\xi \tilde{\theta}_o\}]f' \\ & + [\text{Pr}(a_2 - a_5 p/\Delta\xi)\tilde{\theta}']f = [\text{Pr}\{(a_2 - a_5 p/\Delta\xi)\tilde{f}\tilde{\theta}' + (a_6 + a_5 p/\Delta\xi)\tilde{f}'\tilde{\theta}\}] \end{aligned} \quad (E-14)$$

Equations (E-13) and (E-14) can be rewritten in the following form.

$$A_0 f''' + (a_1 + A_1) f'' + A_2 f' + A_3 f + A_4 \theta = A_5 \quad (E-15)$$

$$B_0 \theta'' + (a_1 + B_1) \theta' + B_2 \theta + B_3 f' + B_4 f = B_5 \quad (E-16)$$

where

$$\begin{aligned} A_0 &= 1 + a_1 \eta, & A_1 &= a^* \tilde{f} + d^* \tilde{f}_0 \\ A_2 &= 2b^* \tilde{f}' - d^* \tilde{f}_0', & A_3 &= a^* \tilde{f}'' \\ A_4 &= a_4, & A_5 &= a^* \tilde{f} \tilde{f}' + b^* \tilde{f}'^2 \end{aligned} \quad (E-17)$$

$$\begin{aligned} B_0 &= A_0, & B_1 &= \text{Pr } A_1, & B_2 &= \text{Pr } e^* \tilde{f}' \\ B_3 &= \text{Pr } (c^* \tilde{\theta} - d^* \tilde{\theta}_0'), & B_4 &= \text{Pr } a^* \tilde{\theta}' \\ B_5 &= \text{Pr} (a^* \tilde{f} \tilde{\theta}' + e^* \tilde{f}' \tilde{\theta}) \end{aligned} \quad (E-18)$$

$$\begin{aligned} a^* &= a_2 - d^*, & b^* &= a_3 + d^* \\ d^* &= a_5 \text{ p}/\Delta \xi, & e^* &= a_6 + d^* \end{aligned} \quad (E-19)$$

The coefficients a_1 through a_6 and the functions \tilde{f}_0 , \tilde{f}_0' , and $\tilde{\theta}_0$ are as previously defined.

The f and θ equations have now been reduced to a system of quasi-linear ordinary differential equations. By defining $g = f'$ and applying the weighting factors (see Lee et al. [6]), one can write equations (E-15) and (E-16) in the finite-difference form as:

$$f_i - f_{i-1} - (\Delta \eta / 2)(g_i + g_{i-1}) = 0 \quad (E-20)$$

$$A_0 / (\Delta \eta)^2 (\alpha_{-1} g_{i-1} + \alpha_0 g_i + \alpha_{+1} g_{i+1}) + A_2 g_i + A_3 f_i + A_4 \theta_i = A_5 \quad (E-21)$$

$$B_0 / (\Delta \eta)^2 (\beta_{-1} \theta_{i-1} + \beta_0 \theta_i + \beta_{+1} \theta_{i+1}) + B_2 \theta_i + B_3 g_i + B_4 f_i = B_5 \quad (E-22)$$

where $\Delta \eta$ is the step size in the η direction and the subscript "i" refers to values at the nodal point η_i .

In equations (E-21) and (E-22) the weighting factors are defined as:

$$\begin{aligned}\alpha_{-1} &= W_f(-z_{i-1/2}), & \alpha_{+1} &= W_f(z_{i+1/2}), & \alpha_0 &= -\alpha_{-1} - \alpha_{+1} \\ \beta_{-1} &= W_f(-z^*_{i-1/2}), & \beta_{+1} &= W_f(z^*_{i+1/2}), & \beta_0 &= -\beta_{-1} - \beta_{+1} \\ W_f(z) &= z/(1 - \exp(-z)) \\ z &= \Delta\eta(a_i + A_i)/A_0, & z^* &= \Delta\eta(a_i + B_i)/B_0\end{aligned}\quad (E-23)$$

Equations (E-20) through (E-23) are applied to the interior points. On the boundaries, equation (C-27) or (D-34) applies such that

$$\begin{aligned}f_1 &= g_1 = 0, & \theta_1 &= 1 \\ f_n - f_{n-1} - \frac{\Delta\eta}{2}(g_n + g_{n-1}) &= \theta_n = 0, & g_n &= a_7\end{aligned}\quad (E-24)$$

where the subscript n is the number of nodes in the η direction, and $a_7 = 0$ for natural convection and $a_7 = \chi^2$ for mixed convection.

Equations (E-20) through (E-24) constitute a system of algebraic equations that can be written in the matrix form

$$[A][X] = [B] \quad (E-25)$$

where $[A]$ is a band matrix of order $3n$ and bandwidth seven. The array $[X]$ which contains the solution in the form $(f_1, g_1, \theta_1, f_2, g_2, \theta_2, \dots, f_n, g_n, \theta_n)^T$ is a column matrix of order $3n$. The matrix $[B]$ is a column matrix of order $3n$ which contains the right hand sides of equations (E-20) through (E-22) and (E-24). The matrix $[A]$ is approximately diagonally dominant and equation (E-25) can be solved by the Gaussian elimination technique with high accuracy.

To obtain values for f' and θ' , the results for f and θ along with the boundary conditions

$$f'''(\xi, 0) = -a_1 \tilde{f}''(\xi, 0) - a_4 \quad (E-26)$$

$$\theta''(\xi, 0) = -a_1 \tilde{\theta}'(\xi, 0) \quad (E-27)$$

$$f'''(\xi, \infty) = \theta'''(\xi, \infty) = 0 \quad (E-28)$$

are used in a cubic spline interpolation routine (see, for example, Burden and Faires [7]). As the solution converges, the boundary conditions become exact and the values for f'' and θ' can be obtained with high accuracy.

The present method of solution employs a quasi-linearization of the original nonlinear system of equations and requires initial guesses for f , f' , f'' , θ , and θ' . The flat plate solution (i.e., $\xi = 0$) for the uniform wall temperature case (UWT) for $Pr = 0.7$ was obtained and these results were used as the initial guesses for all other combinations of Pr , n , and Ω_0 at $\xi = 0$. For $\xi \geq \Delta\xi$, good convergence was obtained by simply letting the solution at the previous node be the guesses for the next node.

The solution method is an iterative scheme. A solution was considered to be convergent when the calculated values for f , f' , and θ differed from the last guess of the respective values by less than 10^{-4} at all nodes. When these criteria failed to be met, new guesses for f , f' , and θ were found using a weighted average of the last guess and the resulting calculation. That is

$$\tilde{f}_{\text{new}} = \omega f + (1 - \omega)\tilde{f}_{\text{old}} \quad (E - 29)$$

$$\tilde{f}'_{\text{new}} = \omega f' + (1 - \omega)\tilde{f}'_{\text{old}} \quad (E - 30)$$

$$\tilde{\theta}_{\text{new}} = \omega \theta + (1 - \omega)\tilde{\theta}_{\text{old}} \quad (E - 31)$$

Generally $\omega = 1$ resulted in quick convergence. However, for $\Omega_0 = 2$ it was often necessary to use under-relaxation with $\omega = 0.5$ to facilitate convergence.

It was found that numerical results depended upon the choice of η_∞ . As ξ was increased, it was necessary to increase η_∞ . The value of η_∞ was initially set to 15 and was increased by 5 when the value of $|f' - a_7|$ or θ was greater than 0.001 at $\eta = 0.98\eta_\infty$. Since $f'(\xi, \infty) - a_7 = \theta(\xi, \infty) = 0$, the $|f' - a_7|$ and θ values greater than 0.001 at $0.98\eta_\infty$ indicate that the corresponding boundary layer thickness extends past η_∞ . To make this adjustment for natural convection, all values of f and θ and their derivatives past η_∞ were set to zero except for f which was taken to be the value at the old η_∞ extended out to the new η_∞ .

The adjustment for mixed convection is slightly more complicated. Again all values were set to zero except the values for \tilde{f} , \tilde{f}' , $(\partial f / \partial \xi)_o$, $(\partial f' / \partial \xi)_o$, \tilde{f}_o and \tilde{f}'_o . They were adjusted as follows.

$$\tilde{f}_i = \tilde{f}_{i-1} + \Delta \eta \tilde{f}'_{i-1} \quad (E-32)$$

$$\tilde{f}'_i = \tilde{f}'_{i-1} \quad (E-33)$$

$$\left(\frac{\partial f}{\partial \xi} \right)_{oi} = (\tilde{f}_i - f_{oi}) / \Delta \xi \quad (E-34)$$

$$\left(\frac{\partial f'}{\partial \xi} \right)_{oi} = -2\chi_o^3 \Omega_o (n+1) \xi_o^n \quad (E-35)$$

$$\tilde{f}_{oi} = f_{oi} + \frac{q}{p} \Delta \xi \left(\frac{\partial f}{\partial \xi} \right)_{oi} \quad (E-36)$$

$$\tilde{f}'_{oi} = \frac{q}{p} \Delta \xi \left(\frac{\partial f'}{\partial \xi} \right)_{oi} \quad (E-37)$$

This adjustment introduced less than 1.0 % difference in the local Nusselt number for $Pr = 0.7$ as compared to a constant run at $\eta = 30$. This error was due primarily to η_∞ being less than 30 initially rather than to the adjustment itself.

It was found that as ξ was increased, errors resulted due to the growing boundary layer thicknesses. By using $\Delta \eta = 0.01$ numerical errors were reduced for calculations at high values of the curvature parameter ξ . It was found that the step size $\Delta \xi$ did not affect the solution appreciably and $\Delta \xi = 0.1$ was used.